Approaches to Pyranose Carbohybrids

By

Rakesh A. Akula

Submitted in Partial Fulfillment of the Requirements

for the Degree of

Master of Science

in the Chemistry Program

YOUNGSTOWN STATE UNIVERSITY

December, 2004

Approaches to Pyranose Carbohybrids

Rakesh A. Akula

I hereby release this thesis to the public. I understand that this thesis will be made available from the Ohio LINK ETD Center and the Maag Library Circulation Desk for public access. I also authorize the University or other individuals to make copies of this thesis as needed for scholarly research.

Signature: Rakesh A. Akula 12/1/04

Rakesh A. Akula — Date

Approvals:

Dr. Peter Norris — 12/01/04 — Date
Thesis Advisor

Dr. John A. Jackson — 12-1-04 — Date
Committee Member

Dr. Timothy R. Wagner — 12/1/04 — Date
Committee Member

Dr. Peter J. Kasvinsky — 12/3/04 — Date
Dean of Graduate Studies

Thesis Abstract

The following work describes new pathways towards synthesis of sugar analogs that may act as glycomimetics for the sugars present in bacteria that make capsular polysaccharide. Two main approaches were investigated in the synthesis of *N*-glycosides. Staudinger and aza-Wittig reactions provided an approach towards synthesis of glucosyl imines. Another approach towards synthesis of *N*-glycosides involved Huisgen's 1,3-dipolar cycloaddition of azides with alkynes in the presence of Cu(I) as catalyst. These reactions were carried out in water as solvent to afford, regiospecifically, 1,4-disubsituted 1,2,3-triazoles in high yields.

Acknowledgements

I would like to convey my thanks to Youngstown State University Chemistry Department and School of Graduate Studies for giving me an opportunity to pursue masters program. I would like to express my gratitude to Dr. John Jackson and Dr. Timothy Wagner for being my committee members and for giving suggestions when I needed.

My special thanks to my family (Mom, Dad, Aparna and Ajay) for their support, which encouraged me to continue my studies. I am grateful to you all for the inspiration and wisdom you have imparted to me. Thanks for supporting me financially, mentally and morally, whatever I am today it is because of your efforts and dedication.

I am thankful to Dan Kibler and Penny Miner for helping me start my research. I am also thankful to many friends and colleagues at Youngstown State University, I would like to thank to Matt, Dave, Travis, Craig, Monica, Dobosh for all the fun filled days in lab.

I am also grateful to Dr. Peter Norris for his guidance, feedback and encouragement. Thank you for your efforts in all of my research work and for your patience that helped to complete my thesis and graduate program. I would like to thank you Doc for providing me research experience and publishing my research work and I am sure this will be instrumental in achieving my professional goals.

Table of Contents

List of Schemes

List of Tables

List of Figures

Introduction

General carbohydrate structure

Carbohydrates are essential biopolymers of life and the main sources of energy supply in most cells. Furthermore, saccharides such as cellulose, pectin and xylan determine the structure of plants and they are also involved in complex biological processes such as catalysis and highly selective molecular recognition. Carbohydrates are now implicated in a wide range of processes such as cell-cell recognition, fertilization, embryogenesis, neuronal development, hormone activities, the proliferation of cells and their organization into specific tissues, and bacterial infection. Apart from these structural and energy storage roles, saccharides also comprise the major blood group antigens, providing the ability to distinguish between native and foreign cells. Additionally, carbohydrates serve as building blocks of protective cell walls and some antibiotics produced by microorganisms are a rich source of branched chain sugars.[1]

Among the major classes of biomolecules carbohydrates constitute the most abundant group of natural products and allow almost limitless structural variations due to their chiral diversity and numerous functional groups. The molecular diversity of carbohydrates offers a valuable tool for drug discovery in the areas of biologically important oligosaccharides, glycoconjugates and molecular scaffolds by investigating their structural and functional impact.

The increased appreciation of the roles of carbohydrates in the biological and pharmaceutical sciences has resulted in a revival of interest in carbohydrate chemistry.[1] In the first 50 years of the 20th century, the chemistry, biochemistry, and biology of carbohydrates were prominent subjects of interest. However, during the initial phase of the modern

revolution in molecular biology, studies of glycans and glycomimetics lagged far behind those of other major classes of molecules. This was in large due to their inherent structural complexity. The development of a variety of new technologies for exploring the structures of these sugar chains has opened up a new frontier of molecular biology, which has been called glycobiology. This word was coined in 1988 by Rademacher, Parekh, and Dwek to recognize the coming together of the traditional disciplines of carbohydrate chemistry and biochemistry with modern understanding of the cellular and molecular biology of glycans.[2] During the last decade, reliable glycosylation methods and strategies to construct complex oligosaccharides have become available. Further, steps have been made to assemble oligosaccharides on solid supports and to construct oligosaccharide libraries.

The history of carbohydrate chemistry can be traced back to the late 1800's, first investigated extensively by Emil Fischer. In 1884 Fischer began his work on the sugars; he studied the chemistry of sugars and determined their structures using a synthetic strategy. Fischer also discovered D-L isomerism in sugars. His work led him to study the fermentation of sugars and the enzymes that cause it. He established the stereochemical nature and isomerization of the sugars, and between 1891 and 1894 he worked out the stereochemical configuration of all the aldohexoses. His greatest success was his synthesis of glucose, fructose and mannose in 1890, starting from glycerol. In 1902 Fischer was awarded the Nobel Prize in Chemistry for his work on sugar and purine synthesis. His studies have paved the way for many researchers to discover the important biological roles of sugars and his investigation of enzymes in fermentation of sugars laid a strong foundation for enzyme biochemistry.[3]

Carbohydrate is a general name referring to monosaccharides, disaccharides, trisaccharides, oligiosaccharides, and polysaccharides. The simplest members of the carbohydrate family are usually referred to as "saccharides" because of their sweet taste. Literally, carbohydrate means, "hydrate of carbon." There are indeed some carbohydrates that can be broken down into hydrates of carbon but not all of them can. For example, glucose (blood sugar) has the molecular formula $C_6H_{12}O_6$, which can also be written as $C_6(H_2O)_6$. Similarly, sucrose (table sugar) has a molecular formula $C_{12}H_{22}O_{11}$, which can be broken down into $C_{12}(H_2O)_{11}$. Even though many carbohydrates cannot be accurately described simply as hydrates of carbon, they still are considered members of the carbohydrate family. A more accurate description of all carbohydrates would be polyhydroxyaldehydes or polyhydroxyketones. The chemistry of simple carbohydrates is essentially the chemistry of hydroxyl groups (alcohols) and that of the carbonyl group (aldehydes and ketones).[4] Monosaccharides are monomers of the more complex carbohydrates. The general formula is $C_nH_{2n}O_n$, where n = 3 – 8. The number of carbons in the monosaccharide is indicated by the prefix tri-, tetra-, pent-, hex-, etc; and the name of a monosaccharide ends in –ose; carbohydrates derived from aldehydes are called aldoses and those derived from ketones are called ketoses (Figure 1).

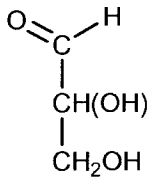

glyceraldehyde

(an aldotriose)

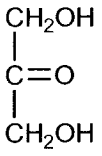

dihydroxyacetone

(a ketotriose)

Figure 1: Structures of a simple aldose and ketose

Most carbohydrates have at least one stereocenter. For example, the simplest carbohydrate, glyceraldehyde, has one stereocenter, which means that there are two enantiomers.[5] The stereochemistry of carbohydrates is usually indicated by "D" and "L" rather than "*R*" and "*S*." Representations of the two enantiomers of glyceraldehyde are shown in Figure 2.

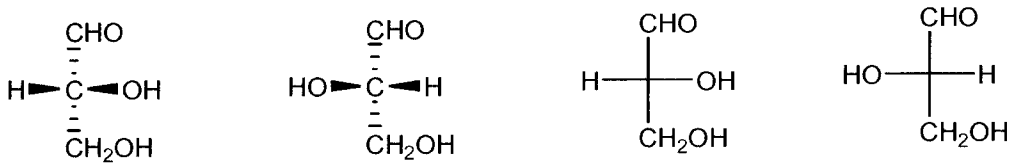

(*R*)-glyceraldehyde (*S*)-glyceraldehyde D-glyceraldehyde L-glyceraldehyde

$[\alpha]_D^{25} = +13.5^\circ$ $[\alpha]_D^{25} = -13.5^\circ$

Figure 2: Structures of enantiomers of glyceraldehyde.

In a Fischer projection "D" is used when the hydroxyl group on the first chiral carbon from the bottom is on the right side, and "L" is used when the hydroxyl group on the first chiral carbon is on the left side (Figure 3).

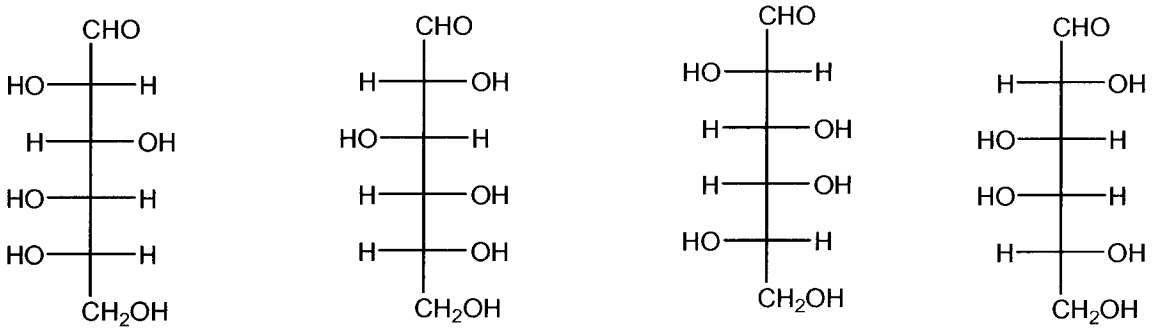

L-Glucose D-Glucose L-Galactose D-Galactose

Figure 3: Structures of D and L isomers of glucose and galactose.

Monosaccharides exist as acyclic, furanose (five-membered ring) and pyranose (six-membered) forms in solution. For example, in Figure 4 **1b** is an alpha-pyranose sugar, **1c** is an beta-pyranose sugar, **1d** is an alpha-furanose sugar, **1e** is a beta-furanose sugar and **1a** is the open ring form.

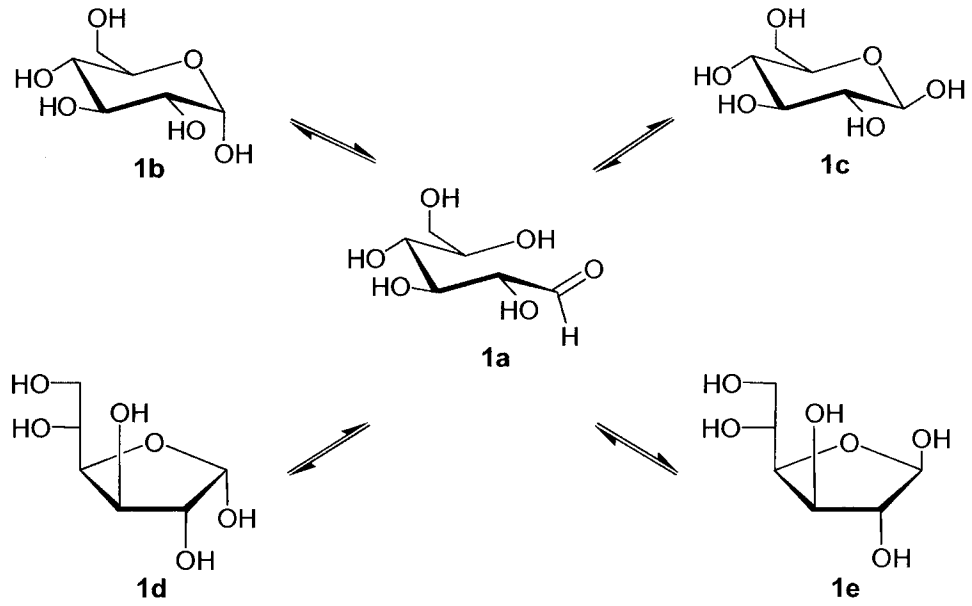

Figure 4: Configurations of D-glucose in solution.

It is a known fact that aldehydes (and ketones) react with alcohols to form hemiacetals (and hemiketals) and monosaccharides have both the alcohol and the carbonyl functional groups, which can react to give a cyclic hemiacetal (hemiketal) (Figure 5).

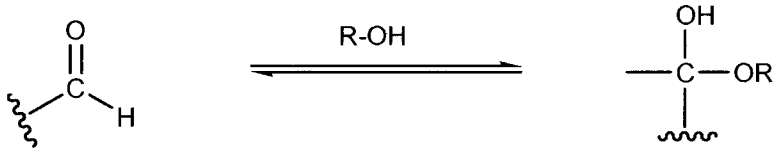

Figure 5: Structure of a simple hemiacetal.

The formation of a ring in glucose results from attack of an oxygen atom attached to C4 or C5 onto the carbonyl carbon of the aldehyde. Upon closing the ring two different structures can be drawn, one with the hydroxyl group pointing up (β) and one with the hydroxyl group pointing down (α) (Figure 6).

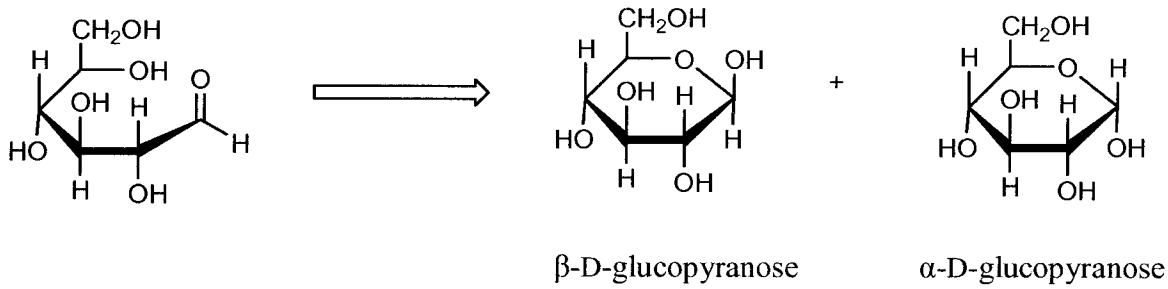

β-D-glucopyranose α-D-glucopyranose

Figure 6: Structures of β-D-glucopyranose and α-D-glucopyranose.

The α and β designations are used to refer to the orientation of the hydroxyl group at carbon 1 (the *anomeric* carbon) relative to that of the -CH_2OH group on carbon 5. If both groups are pointing in the same direction (up), the designation is β, if they point in opposite directions, the designation is α.[5]

Carbohydrate synthesis

Based on biological significance carbohydrates can be divided into several subdivisions, three of the most significant being amino sugars, glycals and glycosides. Amino sugars are a class of compounds in which one hydroxyl group has been replaced with an amino group commonly but not necessarily at the anomeric carbon. The synthesis of amino sugars has been investigated in great detail because they are an important component of naturally occurring polysaccharides. Some of the naturally occurring amino sugars are shown (Figure 7).

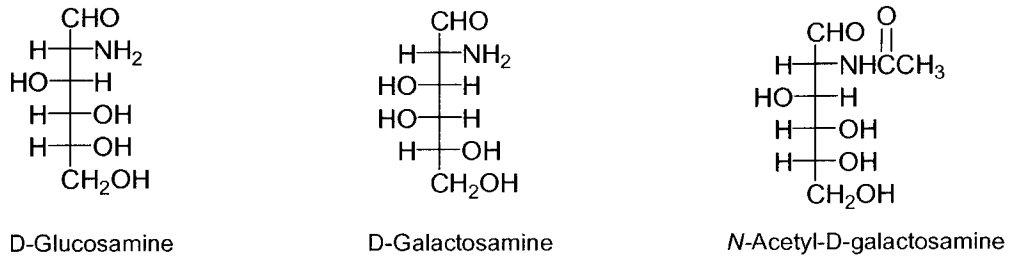

Figure 7: Structures of common amino sugars.

In an example of amino sugar synthesis, Schmidt and Das have introduced a reaction in which a tri-*O*-benzyl-D-galactal was transformed into a 2-deoxy-2-nitrogalactopyranoside. Addition of an alcohol to 3,4,6-tri-*O*-benzyl-2-nitro-D-galactal (**2**, prepared from **1**, Scheme 1) under conditions of base catalysis afforded 2-deoxy-2-nitrogalactopyranosides in high yields. High α-selectivity was obtained with strong bases, whereas weaker bases furnished mainly the corresponding β-galactopyranosides. In the presence of a strong base like NaOMe the free alkoxide attacks the anomeric carbon atom from the α side yielding the α isomer **3** whereas in the presence of a weak base like an amine, addition from the β side is kinetically favored yielding β isomer **4**.[6]

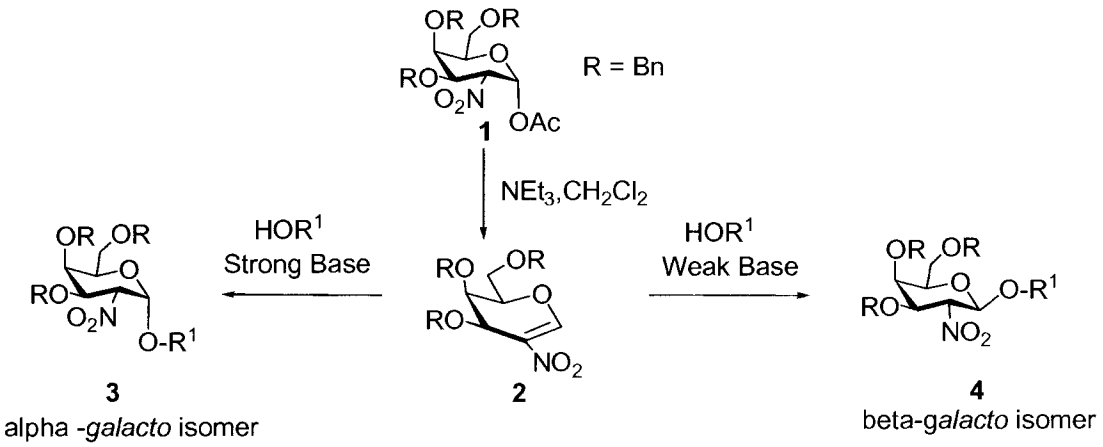

Scheme 1: Schmidt's synthesis of amino sugars.

Glycals are sugar derivatives with a highly reactive double bond between carbons 1 and 2 and glycals have proved to be useful starting points in the stereoselective synthesis of *O*-glycosides. Zinc-catalyzed reductive elimination from acetobromoglucose (**6**, prepared from pentaacetate **5**, Scheme 2) to give triacetyl D-glucal (**7**) is the most usual entry into glycal chemistry. This reaction leads to formation of the acetylated glycal, which can then be de-acetylated and further functionalized. A variety of reducing conditions have been reported; zinc/acetic acid with or without platinic chloride has been most commonly used, but higher yields have been reported for the reactions involving titanium(III). This method is applicable to all cases where further functionalization is carried out in neutral or basic conditions but reactions requiring acidic catalysis are incompatible due to the acid-sensitive enol ether present in the molecule.[7] Glycals produced by this method have been employed in the synthesis of 1,2-anhydrosugars.[8]

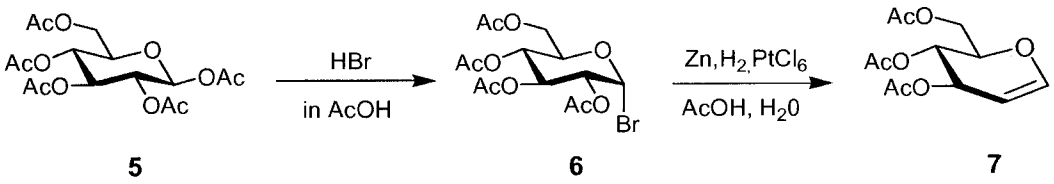

5 **6** **7**

Scheme 2: Synthesis of 3,4,6-tri-*O*-acetyl-D-glucal.

Glycosides have been found to be abundant in nature, which makes them potential targets for synthesis. A glycoside is a sugar in which the hydroxyl group at the anomeric position is substituted with other functionality like –*O*R, –*C*R, –*N*R, or –*S*R, resulting in *O*-glycosides, *C*-glycosides, *N*-glycosides, and *S*-glycosides respectively. Glycosides comprise several important classes such as hormones, sweeteners, alkaloids, flavonoids, antibiotics, etc. Although the history of some glycosides dates back more than a century, they have come

to the forefront of scientific investigation only during the last half a century. *O*-Glycosides comprise by far the most extensive group of plant glycosides. Formation of glycosides usually involves the linking of the hydroxyl group of the aglycone to the anomeric center of a suitable sugar moiety.[9]

In a synthesis of an *O*-glycoside, a glycosyl donor (so called since it donates a glycosyl moiety) is reacted with a free hydroxyl group in a glycosyl acceptor, generally in the presence of some promoter, to give a glycoside (Scheme 3).[5] In the formation of *O*-glycosides, the glycosyl donors that create an intermediate with a cationic charge at the anomeric center of the glycosyl donor are widely used. This cationic intermediate, stabilized by resonance with the ring oxygen, is then attacked by the nucleophilic hydroxyl group of the acceptor to form the glycosidic linkage.

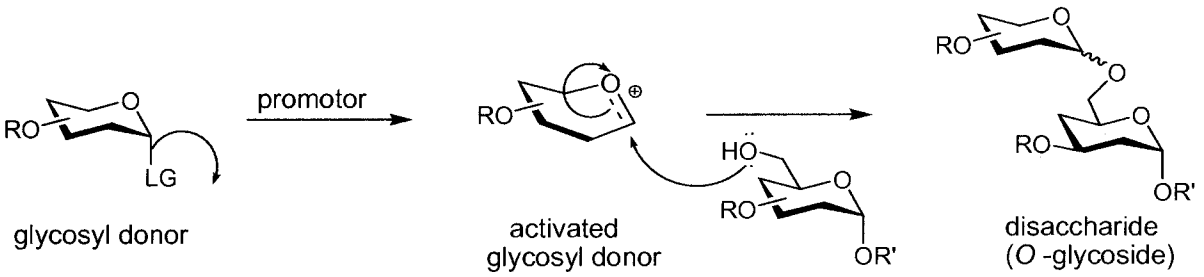

Scheme 3: General glycosylation reaction.

A number of *C*-linked nucleosides with potent pharmacological properties have been isolated. Synthetically prepared *C*-glycosides have also been shown to prevent viral and bacterial infections by inhibiting glycosidase enzymes, which are involved in growth and development of certain bacteria and viruses.[10] The reductive lithiation method developed by Lancelin and group allows generation of *C*-glycosides in good yields with good stereocontrol. Hydrochlorination of tri-*O*-benzyl-D-glucal (**8**, Scheme 4) with HCl produced

the 2-deoxy-D-glucopyranosyl chloride **9**. Reductive lithiation *via* a two-step single electron transfer mechanism with lithium naphthalide generates the α-organolithium species **10** in good yield, and subsequent reaction of this species with an electrophile (e.g. *p*-$MeOC_6H_4CHO$) produces the α-*C*-linked glycoside **11** with excellent stereoselectivity.[11] The stereoselectivity can be explained by the preference of the anomeric anion to adopt the more stable axial orientation.

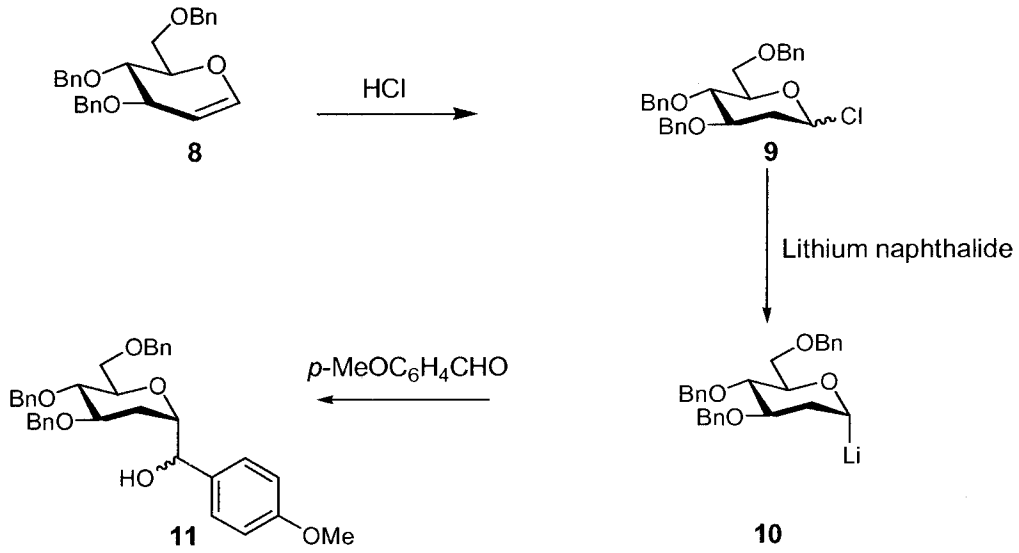

Scheme 4: Synthesis of a *C*-glycoside.

N-Glycoside chemistry

Another type of glycoside that is commonly observed in biological systems are the *N*-glycosides.[12] Especially important are the *N*-glycosides formed *via* reaction of D-ribose and 2-deoxy-D-ribose with the purine and pyrimidine bases in the construction of nucleosides and nucleoside analogues. For example, reaction of cytosine (**13**) with D-ribofuranose (**12**) yields the ribonucleoside (**14**, Equation 1). The new bond that is formed between the nitrogen of the base and the anomeric carbon of the carbohydrate is referred to as an *N*-glycoside bond.

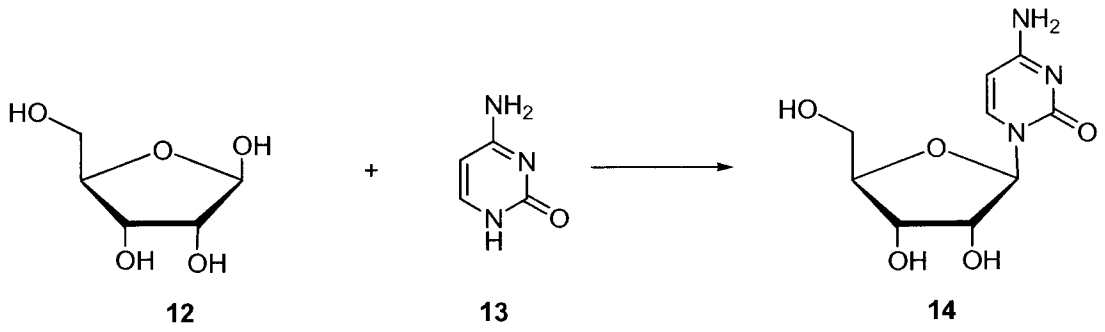

D-Ribofuranose Cytosine Ribonucleoside

Equation 1: Synthesis of ribonucleoside from ribose sugar.

Interest in the synthesis of glycosyl amides as *N*-glycosides has been driven by the presence of similar types of compounds in naturally occurring biomolecules such as glycoproteins and nucleic acids. Glycosyl amides have been suggested as potential glycomimetics for the inhibition of glycosyl hydrolases and as useful precursors in the synthesis of glycosylated materials such as detergents.[13]

Schmidt has presented a versatile and efficient approach to synthesis of nucleosides of 2-deoxy-2-nitro-D-galactose and *N*-acetyl-D-galactosamine, and this approach widened the scope of the strategy of addition reactions on 2-nitro-D-galactal to the formation of *N*-glycosides (Equation 2).

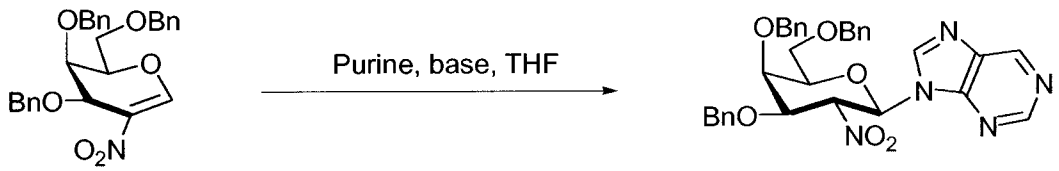

Equation 2: Nucleoside formation by Michael addition reaction.

Experimental conditions that were used favored β-glycoside formation with nitrogen heterocycles acting as nucleophiles. The β-selectivity could be due to kinetically favored β-

side addition of nucleophile on C1 and also due to hydrogen bond interaction of the nucleophile with H-1 of the starting material. [14]

Azide chemistry

Hemming *et. al.* reported the conversion of aldehydes and ketones into imines and the subsequent synthesis of α-unsubstituted and α-branched secondary amines by the reduction of the imine. The synthesis utilizes a tandem process, which begins with an aza-Wittig reaction between the aldehyde and an iminophosphorane that was produced by a Staudinger reaction between the azide starting material and a phosphine (Scheme 5).

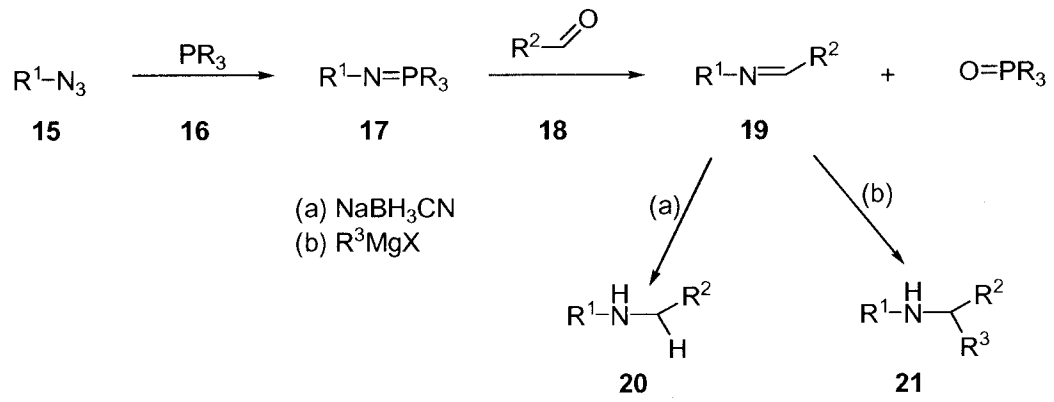

Scheme 5: Synthesis of imines and subsequent reduction to amines.

Thus, the Staudinger reaction between the phosphine **16** and the azide **15** gave the iminophosphoranes **17**, which were made to undergo aza-Wittig reaction with aldehydes to give the imines (**19**). The reduction of imines with sodium borohydride gave the α-unsubstituted amines (**20**) in high yields. Reaction of the imines with an organometallic reagent like RMgX gave α-branched secondary amines (**21**) again in high yields. They also reported that polymer-supported cyanoborohydride brought about the reduction of the

intermediate imines **19** in good yields. Chromatographic separation of the phosphine oxide was not required; the polymer supported phosphine oxide was removed by filtration.[15]

O'Neil and his group reported that triphenylphosphine in Staudinger and Mitsunobu reactions can be replaced with DPPE [1,2-bis(diphenylphosphino)ethane]. When triphenylphosphine is used in these reactions, the only by-product that is formed is triphenylphosphine oxide. However, it has always been difficult to separate triphenylphosphine oxide from the product on column chromatography, as the by-product has a tendency to co-elute with reaction products. This has been attributed to the strong hydrogen bond forming ability of triphenylphosphine oxide and also hydrophobic effects. However, the by-product that is formed with DPPE gives rise to a bis(phosphine oxide) by-product and this by-product being more polar than triphenylphosphine oxide, it was easily removed from the reaction mixture by simple filtration allowing for rapid and simple purification of the reaction mixture.[16]

Click chemistry is a modular approach that uses only the most practical and reliable chemical transformations. Despite many successes in synthesis of new drugs, drug discovery approaches that are based on nature's secondary metabolites are often hampered by slow and complex syntheses. Click chemistry simplifies compound synthesis, through the use of only the most simple and selective chemical transformations, thus providing the means for faster lead discovery and optimization. A reaction can be termed as a "click reaction" when a reaction has wide scope, gives high yields consistently, the reaction is easy to perform, insensitive to oxygen or water and reaction work-up and product isolation must be simple, without requiring chromatographic purification.[17]

Huisgen's 1,3-dipolar cycloaddition of alkynes and azides yielding triazoles is an example of a click reaction. Triazole derivatives have found use in synthesis of various agrochemicals and pharmaceuticals and are useful as intermediates in synthesis of other heterocycles such as oxazole analogs or as intermediates in the synthesis of oxazole-containing natural products.[18] The design and synthesis of triazoles which possess therapeutic value and have applications in the chemical industry is presently in the initial stages of development.[19] In recent years, efforts have been made to explore cycloaddition on carbohydrate-derived alkenes and alkynes and this has led to well-designed methodologies for the synthesis of chiral triazoles, tetrazoles and various imino sugars which can be further used to synthesize inhibitors of glycosidases and glycosyl transferases.[20]

Azides serve as one of the most reliable means to introduce nitrogen substituents through substitution reactions and moreover azides are unique for click chemistry purposes due to their extraordinary stability towards H_2O, O_2 and the majority of organic synthesis conditions. Sharpless has reported the use of copper(I) sources as a catalyst, which unite azides (**23**) and terminal alkynes (**22**) to give only 1,4-disubstituted 1,2,3-triazoles (**24**, Equation 3).[21]

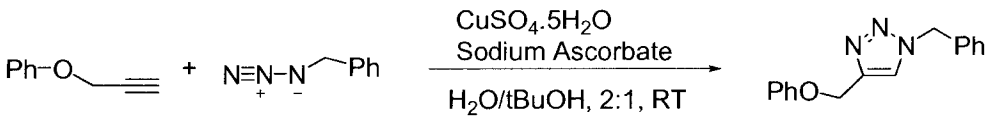

22 **23** **24**

Equation 3: Synthesis of 1,4-disubstituted 1,2,3-triazoles.

Meldal and coworkers reported the use of Cu(I)-catalyzed 1,3-dipolar cycloaddition of terminal alkynes to azides on solid phase. The resin-bound copper acetylide was reacted with primary, secondary, and tertiary alkyl azides, aryl azides and an azido sugar at 25 °C,

affording 1,4-disubstituted 1*H*-[1,2,3]-triazoles *regiospecifically* with high yields and high purity.[22]

Ju *et. al.* reported a simple synthetic protocol for the 1,3-dipolar cycloaddition of azides with electron-deficient alkynes. An alkyne with at least one neighboring electron-withdrawing group undergoes the cycloaddition successfully without any catalysts at room temperature in water. In the case of the terminal alkynes, the cycloaddition reaction proceeded much faster in the presence of a Cu(I) catalyst. They determined the regiochemsitry of the products by X-ray crystallography, which indicated formation of 1,4-regioisomer selectively (Equation 4).[23]

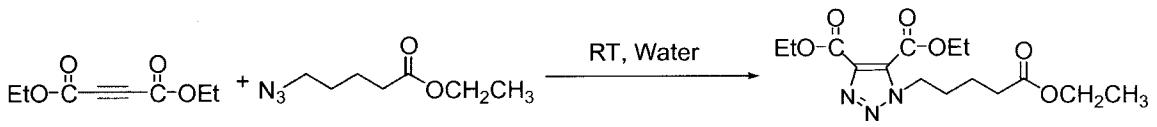

Equation 4: 1,3-dipolar cycloaddition of azides with electron deficient alkynes.

We are currently working towards synthesis of sugars that may act as glycomimetics for the sugars present in bacteria that make capsular polysaccharides. Microorganisms that cause invasive disease commonly produce extra-cellular capsular polysaccharides. Capsules enhance microbial virulence by rendering the bacterium resistant to phagocytosis.[24] *Staphylococcus aureus* is one of the bacteria that produce a capsular polysaccharide around itself and is becoming increasingly resistant to antibiotic treatment. Many strains of this microbe have developed that do not respond to the most powerful antibiotics, which are currently available in the market. *S. aureus* is an important bacterial pathogen responsible for a broad spectrum of human and animal diseases including cutaneous as well as wound infections and more life-threatening infections such as endocarditis and bacteremia.

Moreover, *S. aureus* produces numerous exotoxins, some of which cause diseases such as toxic shock syndrome and food poisoning. The majority of clinical *S. aureus* isolates produce either a type 5 or type 8 capsule, which renders the organisms resistant to phagocytic uptake.[25] *S. aureus* is highly efficient at acquiring resistance to antibiotics; the first documented case of a vancomycin-resistant *S. aureus* infection in a United States patient was recently reported by the Centers for Disease Control.[26]

S. aureus produces a capsular polysaccharide, which is made up of three amino sugars, *N*-acetyl-D-mannose uronic acid, *N*-acetyl-D-fucosamine and *N*-acetyl-L-fucosamine. The goal of this research is to develop methods for the synthesis of glycomimetics or compounds with structures similar to those found in the capsular polysaccharide of *S. aureus*. Our initial investigation in this area will be focused on the synthesis of *N*-glycosides of D-glucose and L-rhamnose derivatives.

Statement of problem

Disease causing microbes that have become resistant to drug therapy are an increasing public health problem. There is a growing need for new and more effective treatments. *Staphylococcus aureus* is one of these bacteria, which is responsible for infectious diseases found in hospitals and communities. Many strains of this microbe have become resistant to most powerful antibiotics because of the presence of the protecting coat called "capsule" or capsular polysaccharide, which provides protection to the microbe against phagocytosis. The goal of this research is to develop glycomimetics or compounds with structures similar to those found in the capsular polysaccharide of *S. aureus*.

The following work describes synthesis of glycosyl imines based on Staudinger and aza-Wittig type reactions. Peracetylated sugar derived from D-glucose was chosen as starting material, which upon simple S_N1 reaction results in the formation of the α-glycosyl bromide, which further undergoes S_N2 reaction to give, the stereospecifically β-glycosyl azide. DPPE [1,2-bis(diphenylphosphino)ethane] was used to produce intermediate phosphinimine in a Staudinger reaction that would further react with aldehydes in an aza-Wittig type process to give glycosyl imines. 1,3-Dipolar cycloaddition reactions between β-glycosyl azide and alkynes was also investigated. Reactions afforded regiospecifically 1,4-disubstituted 1,2,3-triazoles. Synthesis of *N*-glycosides through these approaches may lead to sugar analogs, which could potentially inhibit the appropriate enzymes produced by *S. aureus*.

Results and Discussion:

1. Synthesis of D-glucosyl azide from D-glucose pentaacetate

The main goal of this research was to construct new synthetic *N*-glycosides from inexpensive starting materials that are easy to work with. We investigated methods to develop glycomimetic compounds for which the precursor is a D-glucosyl azide (**25**) and for synthesis of this azide, we chose peracetylated D-glucose as our starting material (Scheme 6).

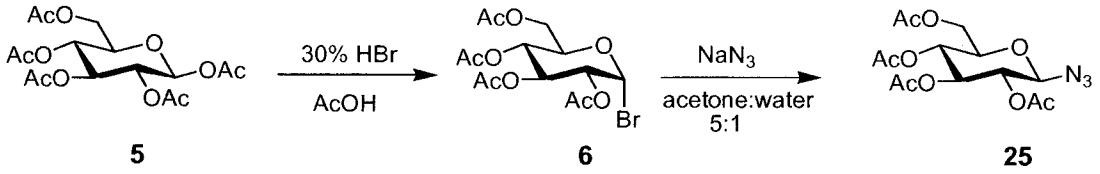

5 **6** **25**

Scheme 6: Synthesis of glucosyl azide.

The initial step in the synthesis of glucose azide **25** involves the treatment of β-D-glucose pentaacetate **5** with 30% HBr in acetic acid, which undergoes simple S_N1 reaction and gives rise to α-glucosyl bromide **6**, which is the thermodynamically favored product with the bromine atom in the axial position. Electronegative bromine prefers the axial position due to the anomeric effect, which in this case can be explained by overlap of one of the lone pairs of electrons on oxygen with the antibonding σ*-orbital of the C-Br bond. TLC indicated complete consumption of the starting material and formation of a new spot burning at a higher R_f value than that of the starting material. ^{1}H NMR data showed disappearance of the doublet signal for the anomeric proton signal at 5.70 ppm in the peracetate and the appearance of a doublet at 6.60 ppm with a coupling constant of 4.02 Hz.

α-Glucosyl bromide **6** was then reacted with sodium azide in acetone/water, which resulted in sterospecific formation of β-glucosyl azide **25** by S_N2 reaction. Aqueous work up

on the reaction mixture yielded a white solid, which was subjected to recrystallization using ethanol to afford colorless crystals in 93% yield. TLC again showed complete consumption of starting material and appearance of a new spot burning at an R_f value lower than that of the staring material. ^{1}H NMR data showed the disappearance of the doublet at 6.60 ppm, which corresponds to the anomeric proton of the α-glycosyl bromide and appearance of a new doublet signal at 4.61 ppm. The replacement of Br with N_3 causes shielding of the anomeric proton and moves the signal upfield in the glucosyl azide. Investigation of the ^{13}C NMR spectrum indicated the signals for the methyl carbons of the acetyl protecting groups between 21.0-22.6 ppm.

The conversion of α-glucosyl bromide **6** to β-glucosyl azide **25** can also be confirmed by a change in the coupling constant values for the protons on C1 and C2. The coupling constant for the anomeric proton in the β-glucosyl azide is higher in comparison to α-glucosyl bromide (8.78 Hz versus 4.02 Hz). This can be attributed to the fact that the protons on C1 and C2 are gauche to each other in the α-glucosyl bromide and therefore have a lower coupling constant value, whereas in the β-glycosyl azide they are anti-periplanar and have a higher coupling constant value (Figure 8).

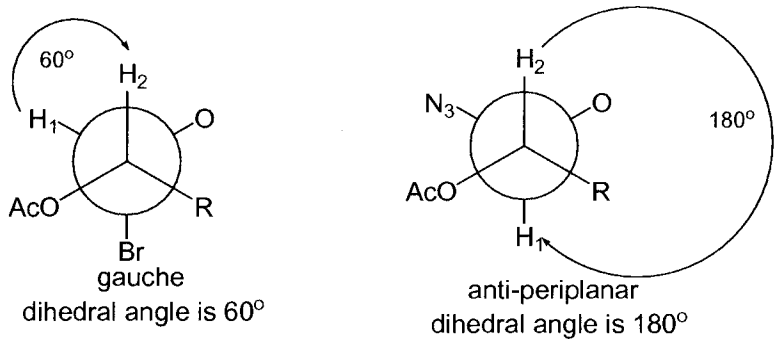

Figure 8: Structures of gauche and anti situations in **6** and **25**.

2. Conversion of glycosyl azides into imines

Synthesis of glycosyl imines was investigated by using the Staudinger reaction and aza-Wittig type reaction. Glucosyl azide **25** was reacted with DPPE [1,2-bis(diphenylphosphino)ethane] *via* Staudinger reaction, then the intermediate that is formed in the reaction reacts with an aldehyde in a aza-Wittig type process to give glycosyl imines. The reaction sequence first involves the formation of an intermediate (**26**) followed by the loss of nitrogen to afford a phosphinimine ylide (**27**). The phosphinimine ylide formed is then reacted with an aldehyde to afford *N*-glucosyl imines (**28**, Scheme 7).

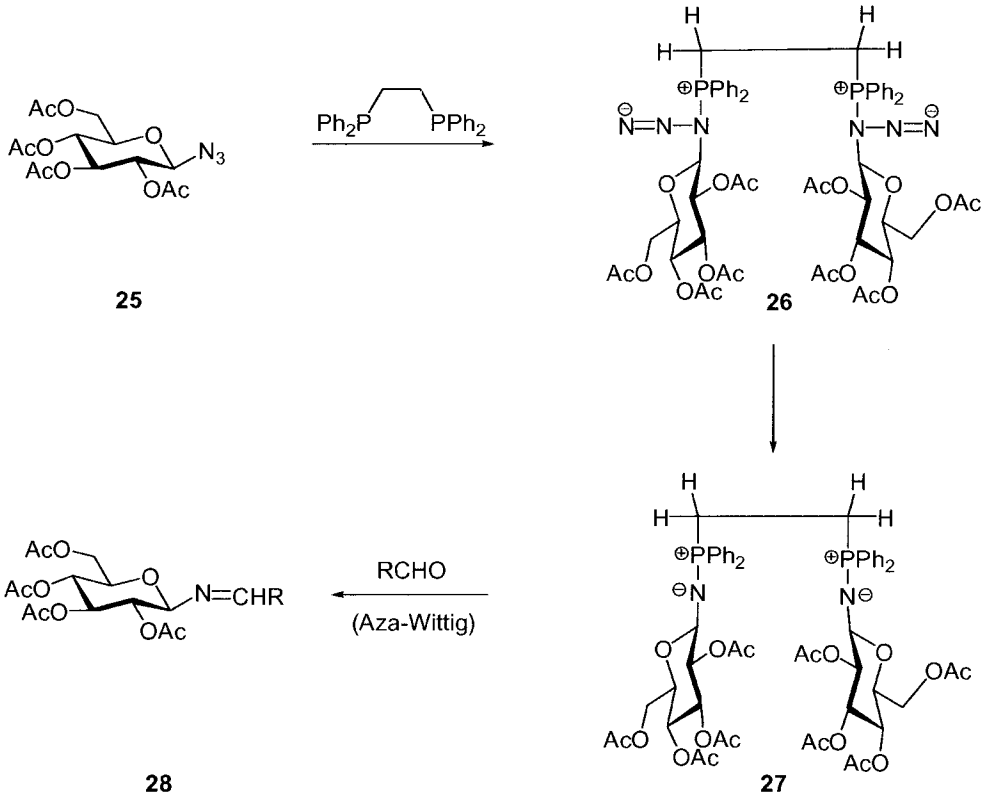

Scheme 7: Conversion of glycosyl azides into imines.

Previously Staudinger/aza-Wittig reactions have been carried out using triphenyl phosphine as a reagent. The reactions with this reagent are simple and high yielding, the only by-product being triphenylphosphine oxide. However, it has been difficult to separate the

triphenylphosphine oxide from the crude reaction mixture on column chromatography. This can be attributed to the strong hydrogen bonding ability of triphenylphosphine oxide and also due to hydrophobic effects. Others have also reported the tendency of triphenylphosphine oxide to co-elute with reaction products, and to overcome this problem the use of several modified phosphines has been reported.

We tried to use DPPE [1,2-bis(diphenylphosphino)ethane] as a replacement for triphenylphosphine under the hypothesis that the phosphine oxide, which is a byproduct, may precipitate in methylene chloride. We have used half an equivalent of DPPE anticipating that the bisphosphine oxide would precipitate from the reaction. The reaction worked with the DPPE according to our plans to give the desired imine, however the DPPE oxide did not precipitate from methylene chloride. The bisphosphine oxide by-product is much more polar than triphenylphosphine oxide and this by-product was easily removed by filtration through a short column of silica gel.

Glucosyl azide **25** was reacted with eight different aldehydes (Table 1), however only five aldehydes afforded the desired imine product. The reaction vessel containing the benzaldehyde provided the highest yield, however, no products were isolated from reactions with isovaleraldehyde, isobutyraldehyde, and phenylacetaldehyde. Both isobutyraldehyde and phenylacetaldehyde were reacted for 48-72 hr periods with glucosyl azide, however only azide starting material was seen by ^{1}H NMR analysis of the crude residue after evaporation. Interestingly in the reaction with isovaleraldehyde TLC showed a UV-active spot burning at a lower R_f value than that of starting material, however ^{1}H NMR of product showed multiple products indicating formation of by-products or incompleteness of the reaction.

Starting material	Aldehyde	Product	% Yield	R_f value*
25	*p*-Nitro benzaldehyde	**29**	85	0.51
	Benzaldehyde	**30**	87	0.45
	4-Bromo benzaldehyde	**31**	47	0.38
	4-Ethyl benzaldehyde	**32**	55	0.56
	Phenyl acetaldehyde	N/R	-	-
	Isovaleraldehyde	N/R	-	-
	Isobutyraldehyde	N/R	-	-
	Napthaldehyde	**33**	60	0.41

* Solvent system – 1:1 hexanes/ethyl acetate.

Table 1: Synthesis of Imines *via* Staudinger reactions using glucosyl azide **25**.

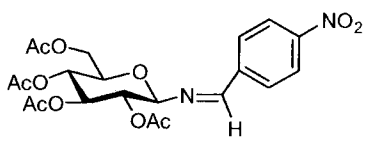

29

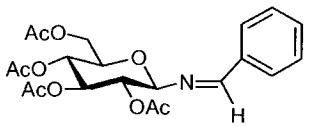

30

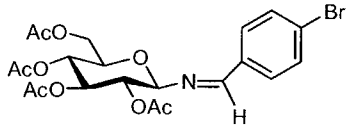

31

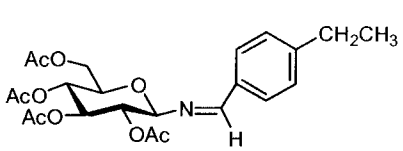

32

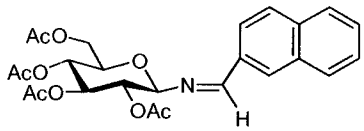

33

Figure 9: D-Glucosyl imine compounds **29-33**.

The general method of adding a glycosyl azide to an aldehyde and DPPE was investigated in the synthesis of imine compounds. One of the first aldehydes to be reacted with the azide was *p*-nitro benzaldehyde (Equation 5).

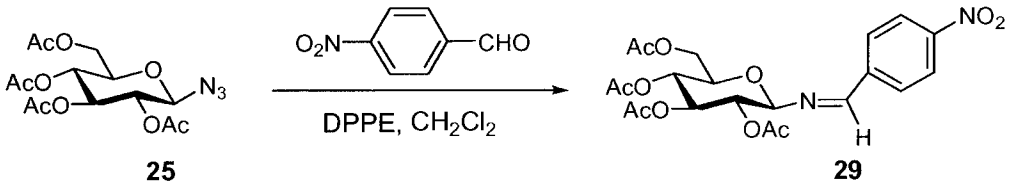

25 **29**

Equation 5: Synthesis of imine **29** from azide **25** using DPPE.

Mechanistically, the initial step involves the attack of a phosphorous atom of DPPE on the azide, which results in the formation of an intermediate, which then loses nitrogen gas to produce an ylide. This ylide then attacks the carbonyl carbon of *p*-nitro benzaldehyde *via* aza-Wittig reaction with loss of bis(phosphine oxide) to produce the desired imine product. The reaction afforded a high yield (85%) of **29** as a yellow crystalline solid. TLC indicated a UV-active spot that burned at a lower R_f value than the starting material.

^{1}H NMR showed the appearance of a singlet at 8.51 ppm indicating the single proton on the carbon atom between nitrogen and the aromatic ring. The signal at 7.88 ppm has a coupling constant of 8.78 Hz, which is same value for the H-1 at 4.61 in the starting material azide, thus indicating the downfield movement of the signal for H-1 in the product, which indicates the formation of the imine compound. Analysis of the ^{13}C NMR spectrum also provided evidence for the formation of **29** by presenting four signals in the region 170.2-171.6 ppm, which correspond to the carbonyl carbons of acetyl protecting groups. The aryl ring carbon signals are also found between 124.9-159.2 ppm. The same reaction between glucosyl azide **25** and *p*-nitro benzaldehyde was also carried out using triphenylphosphine

instead of DPPE to compare the yields and purity of the product (Equation 6). TLC showed consumption of starting material and formation of a new spot with R_f value lower than that of starting material. The reaction afforded a crude product in the yield of 55%, however after purification of product on column, the ^1H spectrum of the product was not clean showing multiple products or by-products.

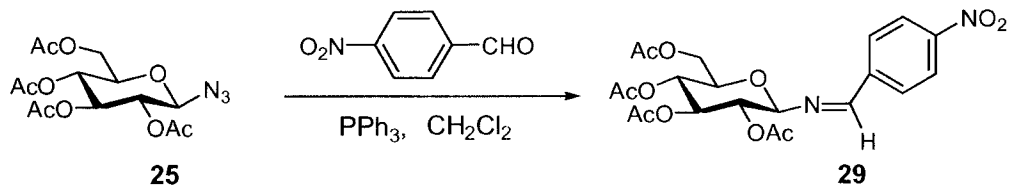

25 **29**

Equation 6: Synthesis of imine **29** from azide **25** using triphenyl phosphine.

The reaction of glucosyl azide **25** with benzaldehyde afforded the imine product (**30**, Equation 7) in the highest yield (87%). The reaction progress was monitored by TLC, which showed a UV-active spot that burned at a higher R_f value than that of starting material after a six-hour reaction time. The ^1H NMR spectrum showed evidence of the product by indicating a singlet signal at 8.4 ppm corresponding to the proton attached to carbon atom present between nitrogen and the aromatic ring. The signals corresponding to carbons in the aromatic ring were seen around 129.6-136.1 ppm in the ^{13}C NMR spectrum.

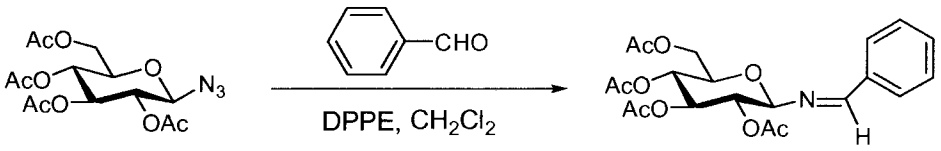

25 **30**

Equation 7: Synthesis of imine **30** from azide **25**.

As for D-glucosyl imine products **29-33**, yields of the products in the 47-87% range were observed. The ^1H NMR spectra of all the products showed similar patterns, particularly

the signal corresponding to the imine proton, which was observed in the region of 8.40-9.10 ppm for all the products. Comparing the yields obtained from compounds **29-33**, the presence of the more electron-withdrawing group on the aromatic ring of the aldehyde possibly explains a higher product yield than the aldehyde that has an electron-donating group on aromatic ring. For example, compound **29** has an electron-withdrawing NO_2- group on it making it more electrophilic and thus giving higher yields and in comparison, compound **31** has an electron-donating Br- group making it less electrophilic and thus giving lower yields.

3. Attempted conversion of glucosyl imines to glucosyl amines

Hemming *et. al.* reported a method to convert imines into amines by reduction. They reported that polymer-supported cyanoborohydride could be used to bring about the reduction of the imines to amines in good yields.[15]

Upon successful synthesis of imines, the amine synthesis was attempted by reduction of imines to amines with sodium cyanoborohydride (Equation 8). Based on the results obtained from the reaction between glucosyl azide **25** and *p*-nitro benzaldehyde and benzaldehyde, which afforded a high yield of products **29** and **30**, these imines were chosen as the starting materials for the possible reduction of the imine.

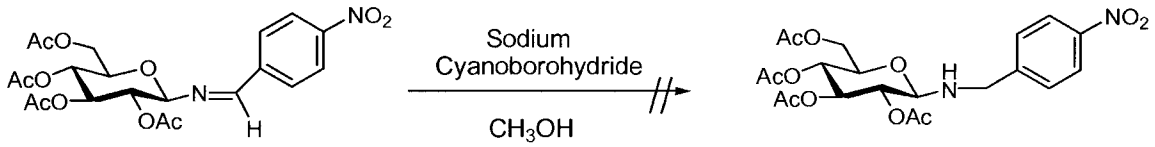

29 **34**

Equation 8: Attempted reduction of imine to amine.

Imine product **29** was dissolved in CH_3OH, followed by addition of sodium cyanoborohydride, and the mixture was stirred for overnight. The reaction was analyzed by TLC, which showed consumption of starting material and formation of a new spot with an R_f value lower than that of starting material. However, ^1H NMR spectrum of product showed multiple products suggesting that amine product **34** may decompose under the reaction conditions. Reduction of the imine was also attempted using polymer-supported sodium cyanoborohydride with extended reaction time and the reaction mixture being subjected to reflux, but the expected product **34** could not be obtained.

4. Synthesis of glucopyranosyl-1,2,3-triazoles

In the search for new methods for constructing glycomimetics related to sugars present in the capsular polysaccharides of *S. aureus.*, we thought that 1,3-dipolar cycloaddition reactions (Equation 9) could be used as an efficient tool allowing for the building of glycomimetics starting from inexpensive materials and reactions that are simple to work with.

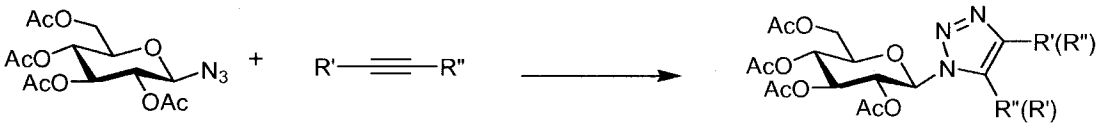

25 **35**

Equation 9: 1,3-dipolar cycloaddition of glucosyl azides to give 1,2,3-triazoles.

1,2,3-Triazoles (e.g. **35** in Equation 9) are in general prepared through a coupling reaction between alkynes and azides and it is usually required that these reactions are conducted at high temperature and run for long periods of time. The thermal cycloaddition reaction between terminal alkyne and azide causes another problem with regard to the

regioselectivity of the derived triazoles, giving rise to a mixture of 1,4-disubstituted and 1,5-disubstituted 1,2,3-triazoles.[27]

Yuriko Root earlier accomplished the construction of 1,2,3-triazoles by using toluene as solvent and reaction mixtures were refluxed at 110 °C for six hours. A glucuronosyl azide and a glucosyl azide were reacted with different types of alkynes, which afforded 1,2,3-triazoles without regioselectivity (Equation 10).[28]

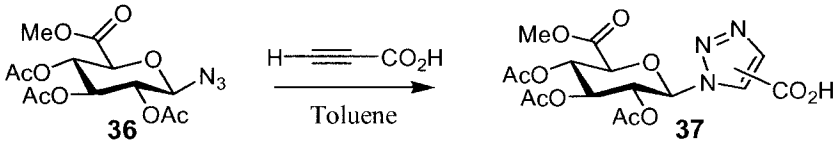

Equation 10: Synthesis of 1,2,3-triazoles from glucuronosyl azide.

The groups of Sharpless and Meldal have independently reported that catalytic amounts of Cu(I) salts would considerably increase the reaction rates and also enhance the regioselectivity to generate exclusively the 1,4-disubstituted product (Scheme 8).[29]

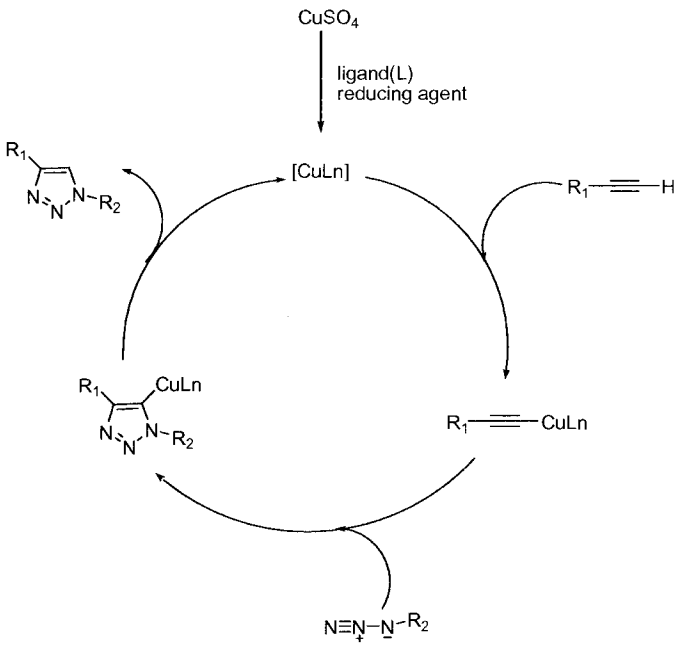

Scheme 8: Catalytic cycle of the Cu(I)-catalyzed azide-alkyne coupling.

Starting material	Alkyne	Product	% Yield	R_f value*
25	Heptyne	**38**	89	0.21
	Nonyne	**39**	81	0.27
	Decyne	**40**	78	0.28
	Dodecyne	**41**	94	0.30
	Phenyl acetylene	**42**	85	0.21
	Trimethylsilyl acetylene	N/R	-	-
	Propiolic acid	N/R	-	-
	Ethyl propiolate	**43**	92	0.17
	Diethyl acetylenedicarboxylate	**44**	92	0.50
	Diphenyl acetylene	N/R	-	-
	4-Ethynyltoluene	**45**	82	0.21
	1-Ethynyl-3-fluorobenzene	**46**	61	0.48
	4-Ethynyl anisole	**47**	80	0.47
	3-Cyclopentyl-1-propyne	**48**	80	0.56

* Solvent system – 1:1 hexanes/ethyl acetate.

Table 2: Cycloaddition reactions with glucosyl azide **25**.

In the present work triazole synthesis using glucosyl azide **25** with alkynes was first investigated using toluene as solvent system, which afforded products for some alkynes, but

reaction time was very long and mixtures of 1,4- and 1,5-triazoles were isolated. The reactions were then carried out using the $CuSO_4$/ascorbic acid system in aqueous medium. Glucosyl azide **25** was reacted with different types of alkynes, which afforded a rapid, regiospecific synthesis of various glucosyl 1,4-disubstituted-1,2,3-triazoles, without use of any cosolvent and the reaction afforded products in high yields, which were easily isolated by simple filtration (Table 2).

Glucosyl azide **25** was reacted with fourteen different types of alkynes to afford a variety of compounds (Figure 10), however no triazole products were isolated from reactions with trimethylsilyl acetylene, propiolic acid, and diphenyl acetylene. Reactions with these three alkynes were monitored by TLC, which showed consumption of starting material but analysis of ^{1}H NMR spectra did not reveal formation of a triazole product.

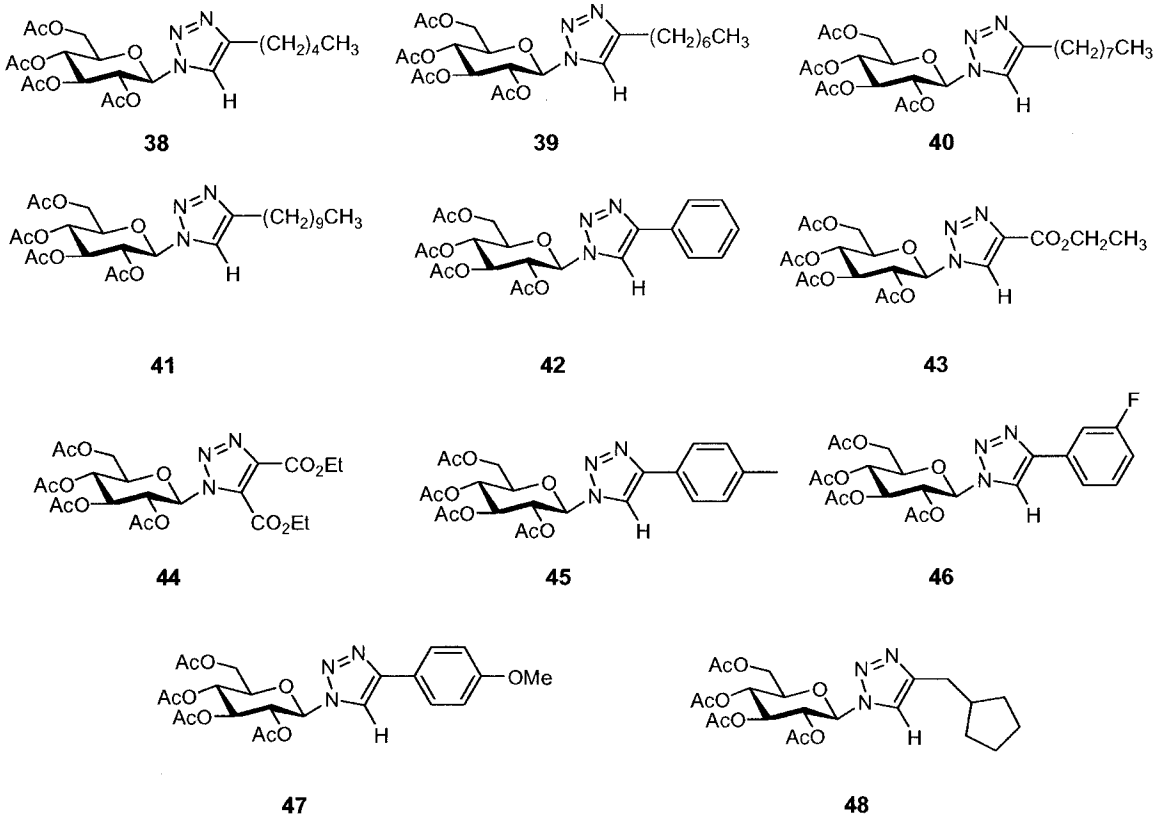

Figure 10: Glucosyl triazole products.

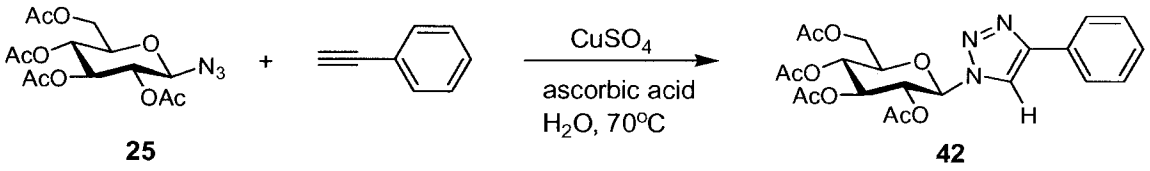

Equation 11: Synthesis of triazole **42** from azide **25**.

Some of the typical results from these experiments are presented here. One of the first alkynes to be reacted with azide **25** was phenyl acetylene (Equation 11). This reaction was refluxed for eight hours and progression of reaction was monitored by TLC, which showed total consumption of starting material and formation of a new spot with an R_f value lower than that of starting material. The reaction mixture was cooled and filtered and the crude product was subjected to recrystallization with 95% ethanol, which afforded product as a pure white fluffy solid. The ^{1}H NMR spectrum of the product (**42**) revealed a singlet signal at 8.00 ppm that corresponds to the triazole proton and the signals that correspond to protons of the aromatic ring were present in the range of 7.25-7.84 ppm. The ^{13}C NMR spectrum also showed signals in the range of 126.9-130.8 ppm that correspond to carbons of the aromatic ring. The high-resolution mass spectral analysis also provided confirming data for the product formation; mass for $C_{22}H_{25}N_3O_9$(+Na) was found to be 498.1451, which was close to the calculated mass of 498.1488. The formation of the 1,4-isomer was confirmed by nOe experiments on the product, which showed interaction between H-1 of the pyranose ring and the proton attached to the triazole ring, which would not be the case if the 1,5-isomer were formed.

The reaction of diethylacetylene dicarboxylate with glucosyl azide **25** was carried out in water without use of any copper catalyst and the reaction afforded a single isomer (**44**, Equation 12).

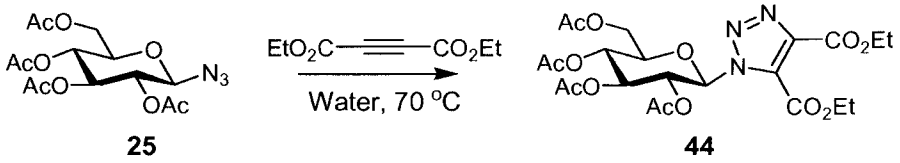

25 **44**

Equation 12: Synthesis of triazole **44** from azide **25**.

The TLC of the reaction showed a UV-active spot that burned at an R_f value lower than that of starting material. Analysis of the ^{1}H NMR spectrum showed the appearance of a new doublet signal at 6.11 ppm indicating the formation of a triazole product and disappearance of a doublet at 4.61 ppm, which corresponds to starting material. The evidence for the formation of the triazole was obtained from the triplet signal observed at 1.41 ppm for ($CO_2CH_2C\underline{H}_3$) and quartet signal at 4.41 ppm for ($CO_2C\underline{H}_2CH_3$) with coupling constant of 7.2 Hz. The ^{13}C NMR spectrum also provided the signals at 131.8 ppm and 141.3 ppm that correspond to the triazole carbons and the signals at 15.1 ppm and 15.4 ppm that correspond to the methyl group carbons ($CO_2CH_2\underline{C}H_3$).

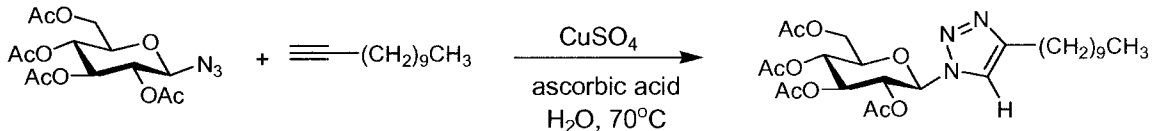

25 **41**

Equation 13: Synthesis of triazole **41** from azide **25**.

The reaction of glucosyl azide **25** with dodecyne afforded the triazole product (**41**, Equation 13) in highest yield (94%). The reaction progress was monitored by TLC, which showed a UV-active spot that burned at a lower R_f value than that of starting material after a six hour reaction time. The ^{1}H NMR spectrum showed evidence of the product by indicating a singlet signal at 7.48 ppm corresponding to the triazole proton. Also shown on ^{1}H NMR is

the triplet signal with coupling constant of 7.04 Hz that corresponds to the terminal methyl group of dodecyne. Analysis of the ^{13}C NMR spectrum also provided evidence for the formation of product by indicating five signals in the region 150.2-171.4 ppm, which indicates the carbonyl carbons of the acetyl protecting groups. The dodecyne carbon chain signals are found between 7.07-33.1 ppm and the signal at 7.07 ppm represents the methyl group of the dodecyne carbon chain.

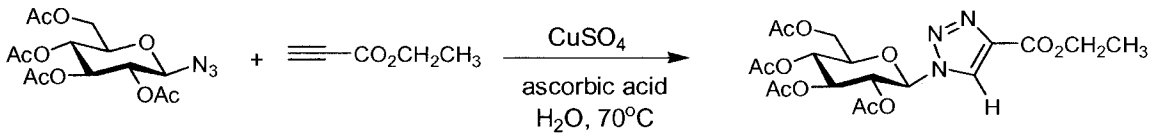

25 **43**

Equation 14: Synthesis of triazole **43** from azide **25**.

Compound **25** was reacted with ethyl propiolate to afford triazole product **43** in 92% yield (Equation 14). The investigation of TLC showed a UV-active spot that burned at a lower R_f value than that of starting material. The ^1H NMR spectrum showed the presence of $CO_2CH_2C\underline{H}_3$ by presenting a triplet at 1.39 ppm and the quartet signal for $CO_2C\underline{H}_2CH_3$ was observed at 4.40 ppm. The singlet signal for the triazole proton was observed at 8.34 ppm indicating the formation of product **43**. Investigation of ^{13}C spectra also gave evidence for product formation by presenting a signal at 161.1 ppm, which corresponds to the carbonyl carbon of the carboxylic acid ester.

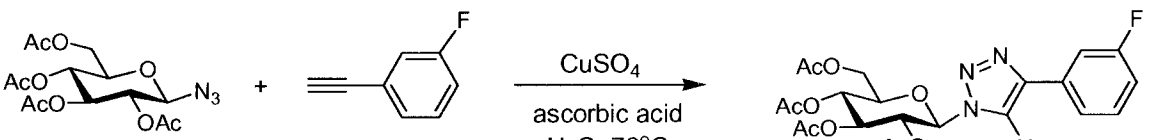

25 **46**

Equation 15: Synthesis of triazole **46** from azide **25**.

Another alkyne that was reacted with the glucosyl azide **25** was 1-ethynyl-3-fluorobenzene (Equation 15). TLC showed the appearance of a new spot, which had an R_f value lower than that of starting material. Formation of the product is evidenced by ^{1}H NMR, which showed a singlet at 8.01 ppm, which corresponds to the triazole proton, and signals for protons of the aromatic ring were observed in the range of 7.36-7.60 ppm. The ^{13}C NMR spectrum also indicated the formation of product by presenting signals for triazole carbons at 119.3 and 122.5 and signals for carbons on the aromatic ring were observed in the range of 169.9-171.6 ppm. Investigation of the high-resolution mass spectral data afforded an M^+ for $C_{22}H_{25}N_3O_9F$ (+Na) of 516.1385, which corresponds to calculated molecular weight of 516.1394 with the addition of a sodium atom. This reaction was refluxed for 12 hrs, which was longer in comparison to reactions with other alkynes and the reaction after filtration afforded a brown powder in 61% yield, which was also less in comparison with other alkynes. The decrease in yield and long reaction time might be explained by the presence of the electron-withdrawing fluorine atom on the aromatic benzene ring of the alkyne, which makes it less reactive, thus decreasing reaction rate and yield.

For all the reaction products **38-48**, yields of the products in the 61-94% range were observed. All the products afforded clean ^{1}H and ^{13}C spectra that were easy to interpret. The ^{1}H NMR spectra of the products showed similar patterns, the important one being the triazole proton, which was observed as a singlet in the region of 7.48-8.34 ppm. In summary, it can be concluded that the use of $CuSO_4$/ascorbic acid as catalyst not only increased reaction rates but also improved product yields. The use of $CuSO_4$/ascorbic acid as catalyst also gave the 1,4-regioisomer instead of mixtures of isomers, which was confirmed by an nOe experiment on product **42**.[30]

5. An approach to synthesis of L-fucosamine derivatives from L-rhamnose.

As a part of a project with the aim of finding new methods to produce glycomimetics related to the capsular polysaccharide of *S. aureus*, synthesis of L-fucosamine derivatives from L-rhamnose has been undertaken. L-Rhamnose was selected as starting material because it is cheap, easily available, and safe to work with. The following sequence of reactions is proposed to synthesize the target L-fucosamine derivative (Scheme 9).

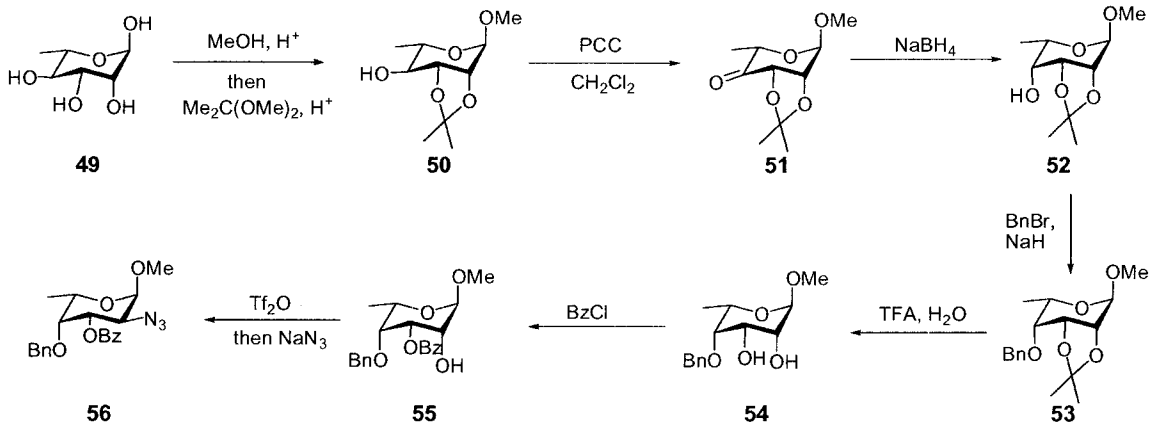

Scheme 9: Synthesis of L-fucosamine derivative from L-rhamnose.

The initial step involves the treatment of L-rhamnose (**49**) with HCl gas in anhydrous methanol, which leads to attack of H^+ on the hydroxyl group present on C1. Loss of H_2O produces a carbocation, which is stabilized by the ring oxygen atom. Then methyl alcohol attacks the carbocation and results in the formation of an acetal (Equation 16).

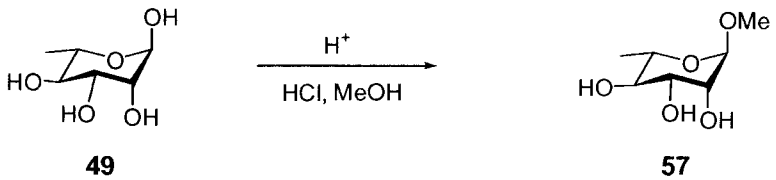

Equation 16: Synthesis of methyl α-L-rhamnopyranoside.

Formation of **57** was indicated by TLC, which showed formation of a new spot with higher R_f value than starting material. Crude ^1H NMR presented a singlet signal at 3.45 ppm,

which corresponds to three hydrogens of the methoxy group on C1. Mass spectral data also indicated formation of product; mass for $C_7H_{12}O_5$ was found to be 143.0 (-2OH), which corresponds to the calculated mass of 218.24.

The second step involves the protection of hydroxyl groups and in this step dimethoxypropane reacts with the hydroxyl groups present on C2 and C3 because they are *cis* and projecting out of the plane of molecule (Equation 17). Progress of reaction was monitored by TLC, which showed total consumption of starting material after 3 hours of reaction and also showed formation of a new spot with an R_f value higher than that of starting material. Formation of product **50** was confirmed by ^1H NMR, which presented two new signals as singlets at 1.26 and 1.44 ppm, corresponding to two methyl groups. ^1H NMR also presented a singlet signal at 3.35 ppm corresponding to the $-OCH_3$ group on C1. ^{13}C NMR also indicated formation of product by presenting a signal at 18.7 ppm corresponding to C-6 and signals at 27.4 and 29.2 ppm corresponding to two methyl groups of the isopropylidene protecting group.

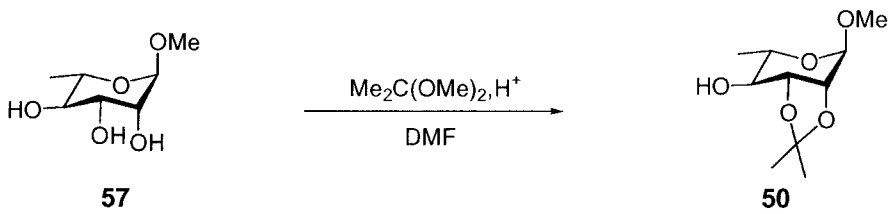

57 **50**

Equation 17: Synthesis of methyl 2,3-*O*-isopropylidene-α-L-rhamnopyranoside

The next sequence of reactions involved oxidation of **50** with pyridinium chlorochromate in dichloromethane, which afforded a ketone at C4, which upon stereoselective reduction with sodium borohydride afforded the inverted alcohol **52** in 83% yield (Scheme 10).

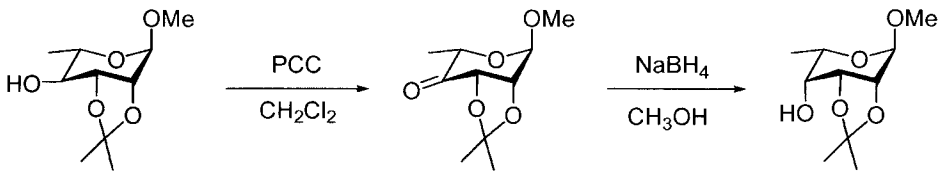

50 **51** **52**

Scheme 10: Inversion of stereochemistry at C4 of **50**.

Formation of **51** was monitored by TLC, which showed a new spot with higher R_f value than that of starting material. Formation of the ketone on C4 was confirmed by ^1H NMR, which indicated disappearance of the doublet signal at 2.83 ppm that represented the hydroxyl group on C4 of product **51**. All other signals presented were similar to that of product **50**.

The reduction of **51** was carried out using sodium borohydride in methyl alcohol and progress of reaction was monitored by TLC, which indicated formation of product by presenting a new spot that burned at a lower R_f value than that of starting material. ^1H NMR showed the appearance of a doublet signal at 2.2 ppm that corresponds to formation of the hydroxyl group on C4. Mass spectral analysis proved formation of the product; mass for $C_{10}H_{16}O_5$ was found to be 187 ($-OCH_3$), which corresponds to calculated mass of 218.24.

All the above reactions gave decent yields in the range of 63-83% on large scale, without use of column chromatography for purification. The further reactions in the scheme are based on efficient stereoselective reactions and it can be carried further to produce analogs of L-fucosamine. These analogs might act as glycomimetics that may disrupt the biosynthetic pathway by which the capsular polysaccharide of *S. aureus* is generated.

Experimental:

General Procedures

The reaction rates were investigated by thin layer chromatography (TLC) on Whatman aluminum-backed plates coated with silica gel. UV light was used to detect spots since most of the reaction materials are UV-active. TLC plates were treated with 5% sulfuric acid/95% ethanol solution to burn the reaction spots to indicate the carbohydrate product. The products from the reaction were purified *via* flash column chromatography using 60-Å silica gel with hexane/ethyl acetate solvent mixtures. The products obtained were identified from Nuclear Magnetic Resonance spectra on samples dissolved in either $CDCl_3$ or D_6-DMSO, using a Varian Gemini 2000 system, at a frequency of 400 MHz for ^1H spectra and 100 MHz for ^{13}C spectra. All chemical shifts were recorded in parts per million (ppm). Splitting patterns of multiplets are labeled as follows: s (singlet), d (doublet), dd (doublet of doublets), ddd (doublet of doublet of doublets), q (quartet), m (multiplet) and coupling constants (*J*) are measured in Hertz. A Bruker Esquire-HP 1100 mass spectrometer was used for low-resolution MS. A Perkin-Elmer polarimeter was used to measure optical rotation of compounds produced herein.

Preparation of glucosyl azide (25) from 1,2,3,4,6-penta-*O*-acetyl-β-D-glucose (5).

In a 250 mL round-bottom flask equipped with a septum and magnetic stir bar, 1,2,3, 4,6-penta-*O*-acetyl-β-glucose (**5**) (25 g, 64.1 mmol) was dissolved in 30% HBr in acetic acid (100 mL). The solution was allowed to react for six hours. The reaction was monitored by TLC (1:1, hexane: ethyl acetate), which showed consumption of starting material. The reaction mixture was reduced and the residue left after evaporation was dissolved in methylene chloride (400 mL) and washed with cold saturated sodium bicarbonate (200 mL) and water (200 mL). The aqueous layers were extracted with methylene chloride (2 x 100 mL) and the organic extracts were dried over anhydrous $MgSO_4$ and concentrated to afford the bromide (**6**) as brown syrup. Then **6** was placed in 250 mL round bottom flask and was dissolved in 100 mL of acetone. Sodium azide (12 g, 188.3 mmol) was added to flask and 20 mL of water was added to dissolve sodium azide. The reaction mixture was allowed to run for six hours until TLC (1:1, hexane: ethyl acetate, R_f= 0.45) showed consumption of starting material. The mixture was washed with water (100 mL) and extracted with methylene chloride (3 x 100 mL). The organic extracts were dried over $MgSO_4$ and reduced to give a white solid, which was further subjected to recrystallization from methanol, which afforded **25** as pure colorless crystals in 93% yield.

^{1}H NMR ($CDCl_3$): δ 2.00, 2.03, 2.04, 2.05 (4s, 12H total, 4 x $COC\underline{H}_3$), 3.76 (ddd, 1H, H-5, *J* = 2.38, 4.76, 10.06 Hz) 4.12 (dd, 1H, H-6, *J* = 2.24, 12.53 Hz), 4.23 (dd, 1H, H-6', *J* = 4.83, 12.53 Hz), 4.61 (d, 1H, H-1, *J* = 8.78 Hz), 4.91 (dd, 1H, H-2, *J* = 8.97, 9.52 Hz), 5.06 (dd, 1H, H-3, *J* = 9.80, 9.52 Hz), 5.17 (dd, 1H, H-4, *J* = 9.52, 9.52 Hz).

^{13}C NMR ($CDCl_3$): δ 21.7, 21.7, 21.8, 21.9, 62.8, 68.9, 71.7, 73.7, 75.1, 88.9, 170.1, 170.2, 170.9, 171.4.

m/z calculated : 373.11 *m/z* found : 391.2 ($+H_2O$).

R_f = 0.45 (hexanes / ethyl acetate 1:1)

Melting point: 105-110 °C

$[\alpha]_D$ –30.8 (*c* 1.0, CH_2Cl_2).

Synthesis of glycosyl imines

Typical procedure for synthesis of glucopyranosyl imines.

In an oven-dried 100 mL round bottom flask equipped with magnetic stir bar and septum inlet was placed D-glucosyl azide **25** (1 mmol) dissolved in methylene chloride (5 mL). To the solution was added aldehyde (2 mmol). DPPE (0.55 mmol) was dissolved in 5 mL of methylene chloride and was slowly added to the reaction mixture dropwise. The solution was allowed to stir at room temperature for 8-12 hours. Progress of reaction was monitored by TLC using 1:1 and 3:1 hexanes/ethyl acetate as solvent systems. Upon completion of the reaction, phosphine oxide, which is a byproduct, was removed by filtration through dry silica in a short column using 3:1 hexanes/ethyl acetate as solvent system. The filtrate obtained was reduced and the product was isolated *via* flash column using 3:1 hexanes/ethyl acetate as solvent system. The column afforded products **28-32** as crystals with yields in the range of 47-87%.

Aldehyde	**Aldehyde**
p-Nitro benzaldehyde	4-Ethyl benzaldeyde
Benzaldehyde	Napthaldehyde
4-Bromo benzaldeyde	

Table 3: Aldehyde reagents.

***p*-Nitro benzaldehyde derivative 29.**

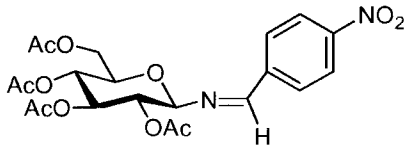

29

^{1}H NMR ($CDCl_3$): δ 2.01, 2.04, 2.05, 2.06, (4s, 12H total, 4 x COC<u>H</u>$_3$), 3.91 (ddd, 1H, H-5, *J* = 2.38, 4.76, 6.95 Hz) 4.22 (dd, 1H, H-6, *J* = 2.11, 12.44 Hz), 4.31 (dd, 1H, H-6', *J* = 4.66, 12.35 Hz), 4.91–5.10 (m, 1H, H-2), 5.13 (dd, 1H, H-3, *J* = 9.70, 9.88 Hz), 5.39 (dd, 1H, H-4, *J* = 9.33, 9.52 Hz), 7.88 (d, 1H, H-1, *J* = 8.78 Hz), 8.05 – 8.51 (m, 4H, Ar-H), 8.50 (s, 1H, R-N=C-<u>H</u>-R).

^{13}C NMR ($CDCl_3$): δ 21.9, 21.9, 22.0, 22.1, 74.4,75.0, 92.4, 124.9, 130.4, 141.6, 150.4, 159.2, 170.2, 170.4, 171.2, 171.6.

m/z calculated : 480.13 *m/z* found : 481.1 (+ H^+).

R_f = 0.51 (hexanes / ethyl acetate 1:1)

Melting point: 115-120 °C

$[\alpha]_D$ –18.4 (*c* 1.0, CH_2Cl_2)

Benzaldehyde derivative 30.

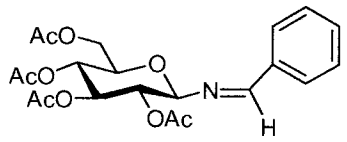

30

^{1}H NMR ($CDCl_3$): δ 1.99, 2.00, 2.04, 2.08 (4s, 12H total, 4 x $COC\underline{H}_3$), 3.87 (ddd, 1H, H-5, *J* = 2.10, 4.76, 9.88 Hz) 4.20 (dd, 1H, H-6, *J* = 2.01, 12.26 Hz), 4.30 (dd, 1H, H-6', *J* = 4.85, 12.35 Hz), 4.83 (d, 1H, H-1, *J* = 8.78 Hz), 5.01 (dd, 1H, H-2, *J* = 9.33, 9.33 Hz), 5.17 (dd, 1H, H-3, *J* = 9.70, 9.70 Hz), 5.35 (dd, 1H, H-4, *J* = 9.52, 9.51 Hz), 7.39 – 7.50 (m, 3H, Ar-H), 7.70 – 7.74 (m, 2H, Ar-H), 8.40 (s, 1H, R-N=C-$\underline{H}$-R').

^{13}C NMR ($CDCl_3$): δ 22.7, 21.8, 21.9, 22.0, 63.3, 69.6, 73.1, 74.5, 74.8, 94.3, 129.6, 129.8, 132.7, 136.1, 162.7, 169.9, 170.3, 171.2, 171.5.

m/z calculated : 435.15 *m/z* found : 436.2 (+ H^+).

R_f = 0.45 (hexanes / ethyl acetate 1:1)

Melting point: 110-115 °C

$[\alpha]_D$ –34.39 (*c* 2.0, CH_2Cl_2)

4-Bromo benzaldehyde derivative 31.

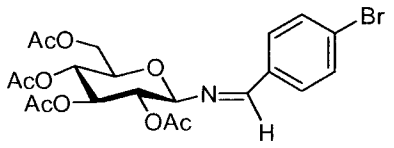

31

^{1}H NMR ($CDCl_3$): δ 2.02, 2.04, 2.06, 2.10 (4s, 12H total, 4 x $COC\underline{H}_3$), 3.89–3.92 (m, 1H, H-5), 4.23 (dd, 1H, H-6, J = 1.09, 12.08 Hz), 4.32 (dd, 1H, H-6', J = 4.66, 12.35 Hz), 4.87 (d, 1H, H-1, J = 8.78 Hz), 4.99 (dd, 1H, H-2, J = 9.15, 9.33 Hz), 5.17 (dd, 1H, H-3, J = 9.80, 9.52 Hz), 5.38 (dd, 1H, H-4, J = 9.33, 9.52 Hz), 7.55 (d, 2H, Ar-H_a, J = 8.42 Hz), 7.58 (d, 2H, Ar-H_b, J = 8.42 Hz), 8.38 (s, 1H, R-N=C-$\underline{H}$-R').

^{13}C NMR ($CDCl_3$): δ 21.8, 21.9, 22.0 22.1, 63.2, 69.6, 73.0, 74.4, 74.9, 93.7, 127.3, 131.1, 132.9, 135.0, 161.1, 170.1, 170.4, 171.2, 171.6.

m/z calculated : 513.06 *m/z* found : 514.1 (+ H^+).

R_f = 0.38 (hexanes / ethyl acetate 1:1)

Melting point: 135-140 °C

$[\alpha]_D$ –37.2 (*c* 2.0, CH_2Cl_2)

4-Ethyl benzaldehyde derivative 32.

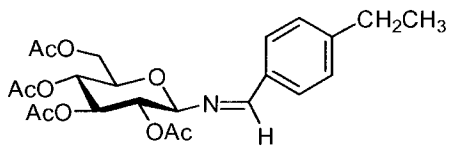

32

^{1}H NMR ($CDCl_3$): δ 1.23 (t, 3H, Ar-$CH_2C\underline{H}_3$, J = 7.37 Hz) 1.97, 2.01, 2.04, 2.08 (4s, 12H total, 4 x $COC\underline{H}_3$), 2.66 (q, 2H, Ar-$C\underline{H}_2CH_3$, J = 7.56 Hz) 3.87 (ddd, 1H, H-5, J = 2.19, 4.76, 10.06 Hz) 4.20 (dd, 1H, H-6, J = 2.28, 12.35 Hz), 4.30 (dd, 1H, H-6', J = 4.76, 12.26 Hz), 4.80 (d, 1H, H-1, J = 8.78 Hz), 5.02 (dd, 1H, H-2, J = 9.36, 9.15 Hz), 5.18 (dd, 1H, H-3, J = 9.82, 9.70 Hz), 5.34 (dd, 1H, H-4, J = 9.52, 9.52 Hz), 7.22 (d, 2H, Ar-H_a, J = 8.05 Hz), 7.65 (d, 2H, Ar-H_b, J = 8.05 Hz), 8.40 (s, 1H, R-N=C-$\underline{H}$-R').

^{13}C NMR ($CDCl_3$): δ 1.3, 16.6, 21.9, 21.9, 22.1, 30.2, 63.3, 69.6, 73.1, 74.5, 74.9, 94.9, 129.2, 129.9, 133.6, 149.4, 163.0, 170.0, 170.3, 171.3, 171.7.

m/z calculated : 463.18 *m/z* found : 464.2 (+ H^+).

R_f = 0.56 (hexanes / ethyl acetate 1:1)

Melting point: 135-140 °C

$[\alpha]_D$ –34.9 (*c* 2.0, CH_2Cl_2)

Naphthaldehyde derivative 33.

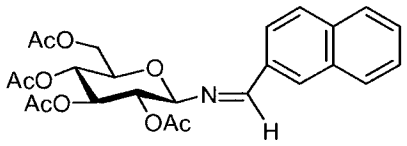

33

^{1}H NMR ($CDCl_3$): δ 2.02, 2.03, 2.06, 2.10 (4s, 12H total, 4 x $COCH_3$) 3.93 (ddd, 1H, H-5, *J* = 2.38, 4.76, 10.06 Hz), 4.26 (dd, 1H, H-6, *J* = 2.28, 12.35 Hz), 4.35 (dd, 1H, H-6', *J* = 4.76, 12.44 Hz), 4.96 (d, 1H, H-1, *J* = 8.84 Hz), 5.14 (dd, 1H, H-2, *J* = 9.15, 9.52 Hz), 5.22 (dd, 1H, H-3, *J* = 9.86, 9.52 Hz), 5.41 (dd, 1H, H-4, *J* = 9.51, 9.52 Hz), 7.48–8.70 (m, 7H, Ar-H), 9.07 (s, 1H, R-N=C-H-R').

^{13}C NMR ($CDCl_3$): δ 21.8, 21.9, 22.0, 22.1, 63.3, 69.7, 73.2, 74.6, 94.7, 124.9, 126.2, 127.2, 128.4, 129.7, 130.9, 131.4, 132.4, 133.2, 134.7, 162.3, 170.2, 170.4, 171.3, 171.7.

m/z calculated : 485.16 *m/z* found: 486.2 (+ H^+).

R_f = 0.41 (hexanes / ethyl acetate 1:1)

Melting point: 145-150 °C

$[\alpha]_D$ –38.31 (*c* 2.0, CH_2Cl_2)

Typical procedure for synthesis of glucopyranosyl-1,2,3-triazoles *via* Cu(I)-catalyzed reactions.

D-glucosyl azide **25** (1 mmol), $CuSO_4$ (0.01g, 0.04 mmol), ascorbic acid (0.1 g, 0.56 mmol) and alkyne (1.1 mmol) were placed in 100 mL two neck round bottom flask equipped with condenser and thermometer. Reactants were heated together in water (15 mL) at 60-70 ^{o}C for 8-12 hours. The reaction mixture was cooled to room temperature and then in an ice bath. The solid was filtered using a glass frit and washed with water (10 mL) and methanol (10 mL) to leave a fluffy powder. The crude product was further subjected to recrystallization using 95% ethanol to afford product as a pure solid.

Alkyne	**Alkyne**
Heptyne	Diethyl acetylene dicarboxylate
Nonyne	4-Ethynyl toluene
Decyne	1-Ethynyl-3-fluorobenzene
Dodecyne	4-Ethynyl anisole
Phenyl acetylene	3-Cyclopentyl-1-propyne
Ethyl propiolate	

Table 4: Alkyne reagents

Heptyne derivative 38.

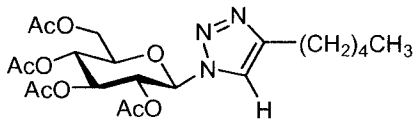

38

^{1}H NMR ($CDCl_3$): δ 0.86 (t, 3H, C_4H_8-C<u>H</u>$_3$, J = 6.95 Hz), 1.22 –1.24 (m,4H) 1.67–1.69 (m, 2H) 1.83, 2.00, 2.04, 2.05 (4s, 12H total, 4 x COC<u>H</u>$_3$), 2.68 (t, 2H, R–C<u>H</u>$_2$$C_3H_6CH_3$, J = 7.5 Hz), 3.97 (ddd, 1H, H-5, J = 2.19, 4.94, 7.14 Hz), 4.11 (dd, 1H, H-6, J = 2.1, 12.5 Hz), 4.27 (dd, 1H, H-6', J = 4.9, 12.6 Hz), 5.21 (dd, 1H, H-2, J = 9.3, 10.1 Hz), 5.36–5.44 (m, 2H, H-3, H-4), 5.83 (d, 1H, H-1, J = 8.9 Hz), 7.49 (s, 1H,Triazole-H).

^{13}C NMR ($CDCl_3$): δ 1.3, 7.1, 15.3, 21.4, 21.8, 22.00, 23.6, 26.8, 30.0, 32.5, 62.7, 68.9, 71.3, 73.8, 76.1, 77.9, 86.7, 119.8, 169.8, 170.3, 170.8, 171.4.

m/z calculated : 469.206 *m/z* found : 470.0 (+ H^+).

R_f = 0.21 (hexanes / ethyl acetate 1:1)

Melting point: 155-160 °C

$[\alpha]_D$ –30.6 (*c*, 0.5, $CHCl_3$)

Nonyne derivative 39.

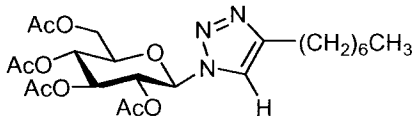

39

^{1}H NMR ($CDCl_3$): δ 0.86 (t, 3H, R-C_6H_{12}-C<u>H</u>$_3$, J = 6.74 Hz), 1.26–1.40 (m, 8H), 1.51–1.65 (m, 2H) 1.86, 2.02, 2.06, 2.08 (4s, 12H total, 4 x COC<u>H</u>$_3$), 2.69 (t, 2H, R–C<u>H</u>$_2$$C_6H_{12}CH_3$, J = 7.68 Hz), 3.99 (m, 1H, H-5), 4.12 (dd, 1H, H-6, J = 1.8, 12.44 Hz), 4.29 (dd, 1H, H-6', J = 5.03, 12.53 Hz), 5.22 (dd, 1H, H-2, J = 9.52, 9.52 Hz), 5.37–5.45 (m, 2H, H-3,H-4), 5.84 (d, 1H, H-1, J = 8.78), 7.49 (s, 1H,Triazole-H).

^{13}C NMR ($CDCl_3$): δ 1.3, 15.4, 21.4, 21.8, 22.0, 23.9, 26.8, 30.2, 30.3, 33.0, 33.3, 62.7, 68.9, 71.3, 73.8, 76.1, 86.7, 119.8, 150.2, 169.8, 170.3, 170.8, 171.4.

m/z calculated : 497.237 *m/z* found : 498.1 (+ H^+).

R_f = 0.27 (hexanes / ethyl acetate 1:1)

Melting point: 135-140 °C

$[\alpha]_D$ –28.2 (*c*, 0.5, $CHCl_3$)

Decyne derivative 40.

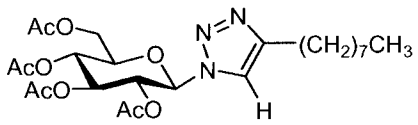

40

^{1}H NMR ($CDCl_3$): δ 0.84 (t, 3H, R-C_7H_{14}-C<u>H</u>$_3$, J = 6.58 Hz), 1.24–1.40 (m, 10H) 1.51–1.65 (m, 2H) 1.84, 2.01, 2.04, 2.06 (4s, 12H total, 4 x COC<u>H</u>$_3$), 2.68 (t, 2H, R– C<u>H</u>$_2$$C_7H_{14}CH_3$, J = 7.59 Hz), 3.96–3.99 (m, 1H, H-5), 4.10–4.30 (m, 2H, H-6, H-6'), 5.21 (dd, 1H, H-2, J = 8.78, 9.33 Hz), 5.36–5.44 (m, 2H, H-3, H-4), 5.83 (d, 1H, H-1, J = 7.88 Hz), 7.48 (s, 1H, Triazole-H).

^{13}C NMR ($CDCl_3$): δ 1.3, 15.4, 21.4, 21.8, 21.8, 21.9, 23.9, 26.8, 30.1, 30.4, 30.4, 30.5, 62.7, 68.8, 71.3, 73.9, 76.1, 86.7, 119.7, 150.2, 166.1, 169.8, 170.3, 170.8, 171.4.

m/z calculated : 511.253 *m/z* found : 512.1 (+ H^+).

R_f = 0.28 (hexanes / ethyl acetate 1:1)

Melting point: 130-135 °C

$[\alpha]_D$ –92.4 (*c*, 0.5, $CHCl_3$)

Dodecyne derivative 41.

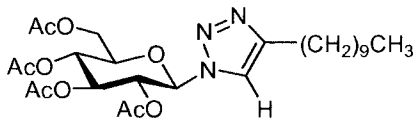

41

^{1}H NMR ($CDCl_3$): δ 0.86 (t, 3H, R-C_9H_{18}-C<u>H</u>$_3$, J = 7.04 Hz), 1.24–1.40 (m,14H), 1.75– 1.85 (m, 2H), 2.05, 2.05, 2.07, 2.07 (4s, 12H total, 4 x COC<u>H</u>$_3$), 2.69 (t, 2H, R– C<u>H</u>$_2$$C_{11}H_{22}CH_3$, J = 7.60 Hz), 3.97 (m, 1H, H-5), 4.11–4.31 (m, 2H, H-6, H-6'), 5.22 (dd, 1H, H-2, J = 8.60, 9.15 Hz), 5.36–5.45 (m, 2H, H-3, H-4), 5.84 (d, 1H, H-1, J = 7.87), 7.48 (s, 1H,Triazole-H).

^{13}C NMR ($CDCl_3$): δ 7.1, 15.4, 21.4, 21.8, 21.8, 21.8, 23.9, 26.9, 30.4, 30.6, 30.8, 33.1, 62.7, 68.9, 71.3, 73.9, 76.2, 86.7, 119.8, 150.2, 169.8, 170.3, 170.8, 171.4.

m/z calculated : 539.284 *m/z* found : 540.1 (+ H^+).

R_f = 0.30 (hexanes / ethyl acetate 1:1)

Melting point: 135-140 °C

$[\alpha]_D$ –108.4 (*c*, 0.5, $CHCl_3$)

Phenyl acetylene derivative 42.

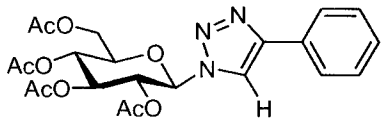

42

^{1}H NMR ($CDCl_3$): δ 1.65, 1.88, 2.03, 2.08 (4s, 12H total, 4 x $COC\underline{H}_3$), 4.03 (ddd, 1H, H-5, *J* = 1.83, 4.76, 10.07 Hz), 4.15 (dd, 1H, H-6, *J* = 1.83, 12.53 Hz), 4.32 (dd, 1H, H-6', *J* = 5.12, 12.63 Hz), 5.27 (dd, 1H, H-2, *J* = 9.52, 9.88 Hz), 5.44 (dd, 1H, H-3, *J* = 9.33, 9.33 Hz), 5.52 (dd, 1H, H-4, *J* = 9.52, 9.33), 5.93 (d, 1H, H-1, *J* = 9.15 Hz) 7.25–7.84 (m, 5H, Ar –H), 8.00 (s, 1H, Triazole- H).

^{13}C NMR ($CDCl_3$): δ 21.5, 21.8, 22.0, 62.7, 68.9, 71.3, 73.9, 76.3, 86.9, 118.8, 126.9, 129.6, 129.9, 130.8, 149.1, 169.9, 170.8, 171.4.

HRMS calculated for $C_{22}H_{25}N_3O_9$ (+Na): 498.1488, found 498.1451.

m/z calculated : 475.15 *m/z* found : 476.1 (+ H^+).

R_f = 0.21 (hexanes / ethyl acetate 1:1)

Melting point: 200-205 °C

$[\alpha]_D$ –85.8 (*c*, 1.0, CH_2Cl_2)

Ethyl propiolate derivative 43.

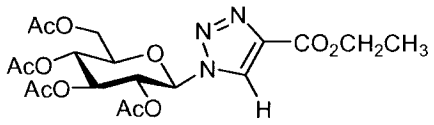

43

^{1}H NMR ($CDCl_3$): δ 1.39 (t, 3H, J = 7.14 Hz, R-COO-CH_2-C$\underline{H}_3$) 1.87, 2.01, 2.05, 2.07 (4s, 12H total, 4 x CO$C\underline{H}_3$), 4.01 (m, 1H, H-5), 4.13 (dd, 1H, H-6, J = 2.10, 12.72 Hz), 4.29 (dd, 1H, H-6', J = 5.03, 12.63 Hz), 4.40 (m, 2H, R-COO-C$\underline{H}_2$-CH_3) 5.23 (dd, 1H, H-2, J = 9.33, 9.88 Hz), 5.40 (m, 2H, H-3, H-4), 5.92 (d, 1H, H-1, J = 8.97 Hz), 8.34 (s, 1H, Triazole-H).

^{13}C NMR ($CDCl_3$): δ 1.3, 15.5, 21.4, 21.7, 21.8, 21.9, 62.6, 62.7, 68.7, 71.6, 73.5, 87.0, 127.1, 141.9, 161.1, 169.8, 170.2, 170.7, 171.3.

m/z calculated : 471.148 *m/z* found : 471.9 (+ H^+).

R_f = 0.17 (hexanes / ethyl acetate 1:1)

Melting point: 165-170 °C

$[\alpha]_D$ –66.4 (*c*, 0.5, $CHCl_3$)

Diethyl acetylene dicarboxylate derivative 44.

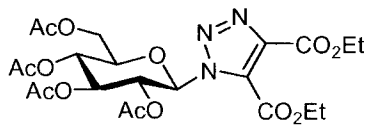

44

^{1}H NMR ($CDCl_3$): δ 1.41 (t, 3H, $CO_2CH_2C\underline{H}_3$, J = 7.2 Hz), 1.39 (t, 3H, $CO_2CH_2C\underline{H}_3$, J = 7.1 Hz) 1.88, 2.02, 2.04, 2.06 (4s, 12H total, 4 x $COC\underline{H}_3$), 3.95 (ddd, 1H, H-5, J = 2.1, 4.85, 10.06 Hz), 4.10 (dd, 1H, H-6, J = 2.3, 12.63 Hz), 4.26 (dd, 1H, H-6', J = 4.94, 12.63 Hz), 4.41 (q, 2H, $CO_2C\underline{H}_2CH_3$, J = 7.04, 7.14 Hz) 4.46 (q, 2H, $CO_2C\underline{H}_2CH_3$, J = 7.14, 7.06 Hz) 5.23 (dd, 1H, H-2, J = 9.70, 9.88 Hz), 5.38 (m, 2H, H-3, J = 9.33, 9.51 Hz) 5.96 (dd, 1H, H-4, J = 9.33, 9.51 Hz), 6.11 (d, 1H, H-1, J = 9.33 Hz).

^{13}C NMR ($CDCl_3$): δ 15.1, 15.4, 21.6, 22.8, 21.8, 21.9, 62.5, 63.2, 64.4, 68.4, 70.7, 74.0, 76.2, 86.5, 131.8, 141.3, 158.9, 160.5, 169.4, 170.1, 171.1, 171.3.

m/z calculated : 543.17 *m/z* found : 561.1 (+ H_2O).

R_f = 0.50 (hexanes / ethyl acetate 1:1)

Melting point: 110-115 °C

$[\alpha]_D$ –33.4 (*c*, 0.5, $CHCl_3$)

4-Ethynyl toluene derivative 45.

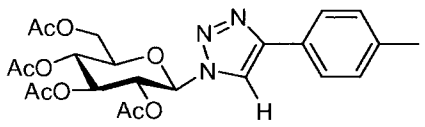

45

^{1}H NMR ($CDCl_3$): δ 1.87, 2.03, 2.07, 2.08 (4s, 12H total, 4 x $COC\underline{H}_3$), 2.37 (s, 3H, Ar- $C\underline{H}_3$), 4.02 (ddd, 1H, H-5, J = 2.10, 5.12, 7.14 Hz), 4.14 (dd, 1H, H-6, J = 2.01, 12.63 Hz), 4.32 (dd, 1H, H-6', J = 5.03, 12.72 Hz), 5.26 (dd, 1H, H-2, J = 9.33, 10.06 Hz), 5.43 (dd, 1H, H-3, J = 9.33, 9.33 Hz), 5.52 (dd, 1H, H-4, J = 9.52, 9.52 Hz), 5.92 (d, 1H, H-1, J = 9.33 Hz), 7.22–7.72 (m, 4H, Ar –H), 7.95 (s, 1H, Triazole-H).

^{13}C NMR ($CDCl_3$): δ 21.5, 21.8, 22.0, 22.6, 62.7, 68.8, 71.3, 73.9, 76.2, 86.8, 118.4, 126.8, 127.8, 130.5, 139.5, 149.5, 166.1, 167.5, 169.9, 170.3, 170.8, 171.4, 183.3.

m/z calculated: 489.174 *m/z* found : 490.0 (+ H^+).

R_f = 0.21 (hexanes / ethyl acetate 1:1)

Melting point: 220-225 °C

$[\alpha]_D$ –34.6 (*c*, 0.5, $CHCl_3$)

1-Ethynyl-3-fluorobenzene derivative 46.

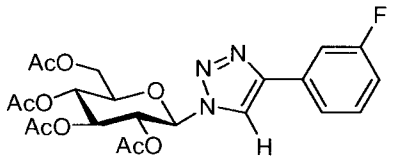

46

^{1}H NMR ($CDCl_3$): δ 1.88, 2.03, 2.07, 2.08 (4s, 12H total, 4 x $COC\underline{H}_3$), 4.02 (ddd, 1H, H-5, *J* = 2.19, 5.10, 10.25 Hz), 4.15 (dd, 1H, H-6, *J* = 2.01, 12.63 Hz), 4.33 (dd, 1H, H-6', *J* = 5.12, 12.63 Hz), 5.26 (dd, 1H, H-2, *J* = 9.15, 10.06 Hz), 5.47 (m, 2H, H-3, H-4), 5.92 (d, 1H, H-1, *J* = 8.97 Hz) 7.36–7.60 (m, 4H, Ar –H), 8.01 (s, 1H, Triazole- H).

^{13}C NMR ($CDCl_3$): δ 21.5, 21.8, 22.0, 62.7, 68.8, 71.3, 73.7, 76.3, 86.9, 113.8, 114.0, 116.6, 119.3, 122.5, 122.5, 131.5, 131.5, 170.0, 170.3, 170.8, 171.4.

HRMS calculated for $C_{22}H_{25}N_3O_9F$ (+Na): 516.1394, found 516.1385.

m/z calculated : 493.149 *m/z* found : 494.0 (+ H^+).

R_f = 0.48 (hexanes / ethyl acetate 1:1)

Melting point: 210-215 °C

$[\alpha]_D$ –68.6 (*c*, 0.5, $CHCl_3$)

4-Ethynyl anisole derivative 47.

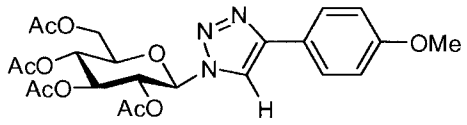

47

^{1}H NMR ($CDCl_3$): δ 1.87, 2.03, 2.07, 2.08 (4s, 12H total, 4 x $COC\underline{H}_3$), 3.83 (s, 3H, R-O-CH_3), 4.01(ddd, 1H, H-5, J = 2.19, 5.12, 7.14 Hz), 4.14 (dd, 1H, H-6, J = 2.01, 12.63 Hz), 4.31 (dd, 1H, H-6', J = 5.03, 12.72 Hz), 5.26 (dd, 1H, H-2, J = 9.33, 10.06 Hz), 5.42 (dd, 1H, H-3, J = 9.33, 9.52 Hz), 5.52 (dd, 1H, H-4, J = 9.24, 9.61 Hz), 5.91 (d, 1H, H-1, J = 9.33 Hz), 6.94–7.76 (m, 4H, Ar –H), 7.91 (s, 1H, Triazole- H).

^{13}C NMR ($CDCl_3$): δ 21.5, 21.8, 21.9, 22.0, 56.5, 62.7, 68.8, 71.2, 73.9, 76.2, 86.8, 115.3, 123.5, 128.2, 160.8, 170.0, 170.3, 170.9, 171.5.

HRMS calculated for $C_{23}H_{28}N_3O_{10}$ (+Na): 528.1594, found 528.1591.

m/z calculated : 505.17 *m/z* found : 506.10 (+ H^+).

R_f = 0.47 (hexanes / ethyl acetate 1:1)

Melting point: 200-205 °C

$[\alpha]_D$ –28.2 (*c*, 0.5, $CHCl_3$)

3-Cyclopentyl-1-propyne derivative 48.

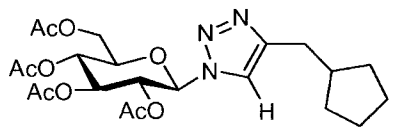

48

^{1}H NMR ($CDCl_3$): δ 1.15-1.89 (m, 9H) 1.85, 2.01, 2.06, 2.07 (4s, 12H total, 4 x $COC\underline{H}_3$), 2.65–2.76 (m, 2H), 3.97 (ddd, 1H, H-5, J = 2.19, 4.94, 10.06 Hz), 4.13 (dd, 1H, H-6, J = 2.01, 12.63 Hz), 4.29 (dd, 1H, H-6', J = 5.12, 12.63 Hz), 5.22 (dd, 1H, H-2, J = 9.33, 9.88 Hz), 5.37--5.45 (m, 2H, H-3, H-4), 5.84 (d, 1H, H-1, J = 9.15), 7.50 (s, 1H, Triazole- H).

^{13}C NMR ($CDCl_3$): δ 21.4, 21.8, 21.8, 22.0, 26.3, 32.8, 33.5, 41.0, 62.7, 68.9, 71.3, 73.8, 76.1, 86.7, 120.0, 149.7, 169.8, 170.3, 170.8, 171.4.

m/z calculated : 481.206 *m/z* found : 482.1 (+ H^+).

R_f = 0.56 (hexanes / ethyl acetate 1:1)

Melting point: 160-165 °C

$[\alpha]_D$ –53 (*c*, 0.5, $CHCl_3$)

Synthesis of methyl 2,3-*O*-isopropylidene-α-L-rhamnopyranoside (50)

In an oven dried 250 mL round bottom flask L-rhamnose monohydrate (**49**, 25 g, 152.4 mmol) was dissolved in 200 proof ethanol (100 mL) and the solution was evaporated to remove water of hydration. This process was repeated two more times to ensure complete removal of water of hydration. Next, dehydrated L-rhamnose was dissolved in anhydrous methanol (250 mL), which was saturated with HCl gas for five minutes. The reaction was allowed to run for 32 hours under nitrogen atmosphere. After 32 hours, TLC (ethyl acetate) showed the formation of the product (R_f = 0.15). The reaction solution was reduced and the solvent removed. The residue was dissolved in 20 mL DMF, *p*-toluene sulfonic acid (800 mg, 4.2 mmol) and dimethoxypropane (20mL) were added. Reaction was allowed to run for 12 hours under nitrogen atmosphere. After 12 hours, TLC (ethyl acetate) showed the formation of product (R_f = 0.49). The reaction mixture was reduced and washed with water (3 x 20mL) and saturated $NaHCO_3$ (3 x 20 mL) and extracted with ethyl acetate (100 mL). The organic extract was dried over $MgSO_4$, filtered and the solvent removed to afford methyl 2,3-*O*-isopropylidene-α-L-rhamnopyranoside (**50**) as yellow oil in 68% yield.

^{1}H NMR ($CDCl_3$): δ 1.30 (d, 3H, H-6, *J* = 6.2 Hz), 1.32, 1.50 (2s, 6H total, C($C\underline{H}_3$)$_2$), 2.92 (d, 1H, OH, *J* = 4.39 Hz), 3.35 (s, 3H, OCH_3) 3.53-3.62 (m, 2H), 4.09 (d, 1H, H-2, *J* = 5.7 Hz), 4.04 (q, 1H, H-3, *J* = 5.42 Hz), 4.82 (s, 1H, H-1).

^{13}C NMR ($CDCl_3$): δ 18.7, 27.4, 29.2, 56.1, 66.8, 75.5, 76.9, 79.6, 99.1, 110.4.

m/z calculated : 218.24 *m/z* found : 187.1 (-OCH_3)

Synthesis of 51 from methyl 2,3-*O*-isopropylidene-α-L-rhamnopyranoside (50)

Methyl 2,3-*O*-isopropylidene-α-L-rhamnopyranoside (**50**, 4.0 g, 18.3 mmol) and pyridinium chlorochromate (15.0 g, 4 equivalents) were stirred in dichloromethane (300 mL) under nitrogen atmosphere at room temperature. Reaction was allowed to run for 12 hours. Reaction rate was monitored by TLC (ethyl acetate), which showed formation of product (R_f = 0.7). The reaction mixture was mixed with 200 mL ether:hexane (1:1) and was filtered through a short column of dry silica gel. The solvent was then reduced to afford **51** as yellow oil in 64% yield.

^{1}H NMR ($CDCl_3$): δ 1.34, 1.46 (2s, 6H total, $C(C\underline{H}_3)_2$), 1.37 (d, 3H, H-6, J = 6.7 Hz), 3.43 (s, 3H, OCH_3) 4.18–4.27 (m, 3H), 4.38–4.42 (m, 1H), 4.82 (s,1H, H-1).

^{13}C NMR ($CDCl_3$): δ 17.0, 26.7, 27.9, 56.9, 65.0, 70.7, 76.9, 99.1, 112.3, 205.3.

Synthesis of alcohol 52 from ketone 51

The product (1 g, 4.62 mmol) from the previous step was dissolved in 20 mL of anhydrous methanol and sodium borohydride (0.174 g, 4.62 mmol) was added and the reaction was allowed to run for 12 hours under nitrogen atmosphere. TLC showed formation of the product (R_f = 0.5, hexane:ethyl acetate, 1:1). The reaction was then washed with water (20 mL) and methylene chloride (2 x 20 mL). The organic extracts were dried over anhydrous $MgSO_4$, filtered and reduced to afford **52** as yellow oil in 83% yield.

^{1}H NMR ($CDCl_3$): δ 1.30 (d, 3H, H-6, J = 6.59 Hz), 1.34, 1.55 (2s, 6H total, $C(C\underline{H}_3)_2$), 2.21 (d, 1H, OH, J = 6.77 Hz), 3.37 (s, 1H, OCH_3) 3.45–3.58 (m, 1H), 3.79 (q, 1H, H-3, J = 6.52 Hz), 3.99 (d,1H, H-3, J = 6.40 Hz), 4.15–4.18 (m,1H), 4.9 (s, 1H, H-1).

^{13}C NMR ($CDCl_3$): δ 17.5, 26.2, 27.0, 55.9, 68.0, 71.7, 73.7, 99.5, 110.2, 170.1.

m/z calculated : 218.24 *m/z* found : 187.1 (-OCH_3).

References:

1. Boons, G-J., "Carbohydrate Chemistry." Blackie Academic & Professional, London, **1998**.
2. Varki, A.; Cummings, R.; Esko J.; Freeze, H.; Hart, G.; Mart, J., "Essentials of Glycobiology", Cold Spring Harbor Press, New York, **1999**, 8-12.
3. http://www.nobel.se/chemistry/laureates/1902/fischer-bio.html
4. Collins, P., Ferrier., "Monosaccharides: Their Chemistry and Their Roles in Natural Products." Wiley: New York, New York, **1995**.
5. Finch, P., "Carbohydrates-Structures, syntheses and dynamics" Kluwer Academic Publishers, Netherlands, **1999**.
6. Das, J.; Schmidt, R. R., "Convenient Glycoside Synthesis of Amino Sugars: Michael-Type Addition to 2-Nitro-D-galactal," *Eur. J. Org. Chem.* **1998**, 1609-1613.
7. Osborn, H. M. I., "Carbohydrates" Academic Press, Boston, **2003**.
8. Baisch, G., Ohrlein, R., "Enzymatic Fucosylations of Non-Natural Accceptors with Non-Natural Donor-Sugars," *Bioorganic & Medicinal Chemistry Letters*, **1997**, *7*, 2431-2434.
9. Ikan, R., "Naturally Occurring Glycosides", John Wiley & Sons, New York, **1999**.
10. Nicolaou, K.C.; Duggan, M.E.; Hwang, C. K.; Somers, P.K.; "Activation of 6-*endo* over 5-*exo* epoxide openings. ring selective formation of tetrahydropyran systems and stereo controlled synthesis of the ABC ring framework of brevetoxin B," *J. Chem. Soc., Chem. Commun.*, **1985**, 1359-1362.
11. Lancelin, J-M.; Morin-Allory, L.; Sinay, P., "Simple Generation of a Reactive Glycosyl-lithium Derivative," *J. Chem. Soc, Chem. Commun.*, **1984**, 355-356.

12. Kren, V.; Martinkova, L., "Glycosides in Medicine: The role of glycosidic residue in biological activity" *Current Medicinal Chemistry*, **2001**, *8*, 1313-1338.

13. Root, Y.R.; Bailor, M.H.; Norris, P., "Synthesis of glucopyranosyl amides using polymer-supported reagents," *Synth. Commun.* **2004**, *34*, 2499-250.

14. Winterfeld, G. A.; Das, J.; Schmidt, R. R., "Convenient Synthesis of Nucleosides of 2-Deoxy-2-nitro-D-galactose and *N*-Acetyl-D-galactosamine," *Eur. J.Org. Chem.* **2000**, 3047-3050.

15. Hemming, K.; Bevan, M.J.; Loukou, C.; Patel, S.D.; Renaudeau, D., "A One- Pot Aza-Wittig Based Solution and Polymer Supported Route to Amines," *Synlett,* **2000**, *11*, 1565-1568.

16. O'Neil, I.A.; Thompson, S.; Murray, C.L.; Kalindjian, S.B., "DPPE: A Convenient Replacement for Triphenylphosphine in the Staudinger and Mitsunobu Reactions," *Tetrahedron Letters*, **1998**, *38*, 7787-7790.

17. Kolb, H.C.; Sharpless, K.B., "The growing impact of click chemistry on drug discovery," *Drug Discovery Today*, **2003**, *24*, 1128-1137.

18. Freeze, S.; Norris, P., "Synthesis of carbohydrate-derived 1,2,3-triazoles using 1,3-dipolar cycloaddition on a soluble polymer support," *Heterocycles,* **1999**, *51*, 1807-1817.

19. Katritzky, A.R.; Zhang, Y.; Singh, S.K.; Steel, P.J., "1,3-dipolar cycloaddition of organic azides to ester or benzotriazolylcarbonyl activated acetylenic amides," Arkivoc, **2003**, *15,* 47-64.

20. Tripathi, S.; Singha, K.; Achari, B.; Mandal, S.B., "In situ 1,3-dipolar azide cycloaddition reactions: synthesis of functionalized D-glucose based chiral piperidine and oxazepine analogues," *Tetrahedron*, **2004**, *60*, 4959-4965.

21. Rostovtsev, V.V.; Green, L.G.; Fokin, V.V.; Sharpless, K.B., "A Stepwise Huisgen Cycloadditon Process: Copper(I)-Catalyzed Regioselective "Ligation" of Azides and Terminal Alkynes," *Angew. Chem. Int. Ed.*, **2002**, *41*, 2596-2598.

22. Tornoe, C.W.; Christensen C.; Meldal, M., "Peptidotriazoles on Solid Phase: [1,2,3]-Triazoles by Regiospecific Copper(I)-Catalyzed 1,3-Dipolar Cycloadditions of Terminal Alkynes to Azides," *J.Org.Chem*, **2002**, *67*, 3057-3064.

23. Li, Z.; Seo, T.S.; Ju, J., "1,3-Dipolar Cycloadditions of Azides with electron-deficient alkynes under mild condition in water," *Tetrahedron letters*, **2004**, *45*, 3143-3146.

24. O'Riordan, K.; Lee, J.C.; " *Staphylococcus aureus* Capsular Polysaccharides," *Clinical Microbiology Reviews*, **2004**, *17*, 218-234.

25. Kneidinger, B.; O'Riordan, K.; Li, J.; Brisson, R. J.; Lee, J.C.; Lam, S., "Three Highly Conserved Proteins Catalyze the Conversion of UDP- *N*-acetyl-D-Glucosamine to Precursors for the Biosynthesis of *O*-Antigen in *Pseudomonas aeruginosa* O11 and Capsule in *Staphylococcus aureus* Type 5," *The Journal of Biological Chemistry*, **2003**, *278*, 3615-3627.

26. http://www.cdc.gov/mmwr/preview/mmwrhtml/mm5126al.htm

27. Kamijo, S.; Jin, T.; Huo, Z.; Yamamoto, Y., "A One-Pot Procedure for the Regio Controlled Synthesis of Allyltriazoles via the Pd-Cu Bimetallic Catalyzed Three-Component Coupling Reaction of Nonactivated Terminal Alkynes, Allyl carbonate, and Trimethylsilyl Azide," *J. Org.Chem.*, **2004**, *69*, 2386-2393.

28. Root, Y.Y., "Synthesis of derivatives of D-ManAcA: Aminosugar Component of *S. aureus* Capsular Polysaccharides," **2003**, M.S. thesis, Youngstown State University.

29. Breinbauer, R.; Kohn, M., "Azide-Alkyne Coupling: A Powerful Reaction for Bioconjugate Chemistry," *ChemBioChem.*, **2003**, *4*,1147-1149.

30. Akula, R.A.; Temelkoff, D.P.; Artis, N.D.; Norris, P., "Rapid access to glucopyranosyl-1,2,3-triazoles *via* Cu(I)-catalyzed reactions in water," **2004**, *Heterocycles.*

Appendix

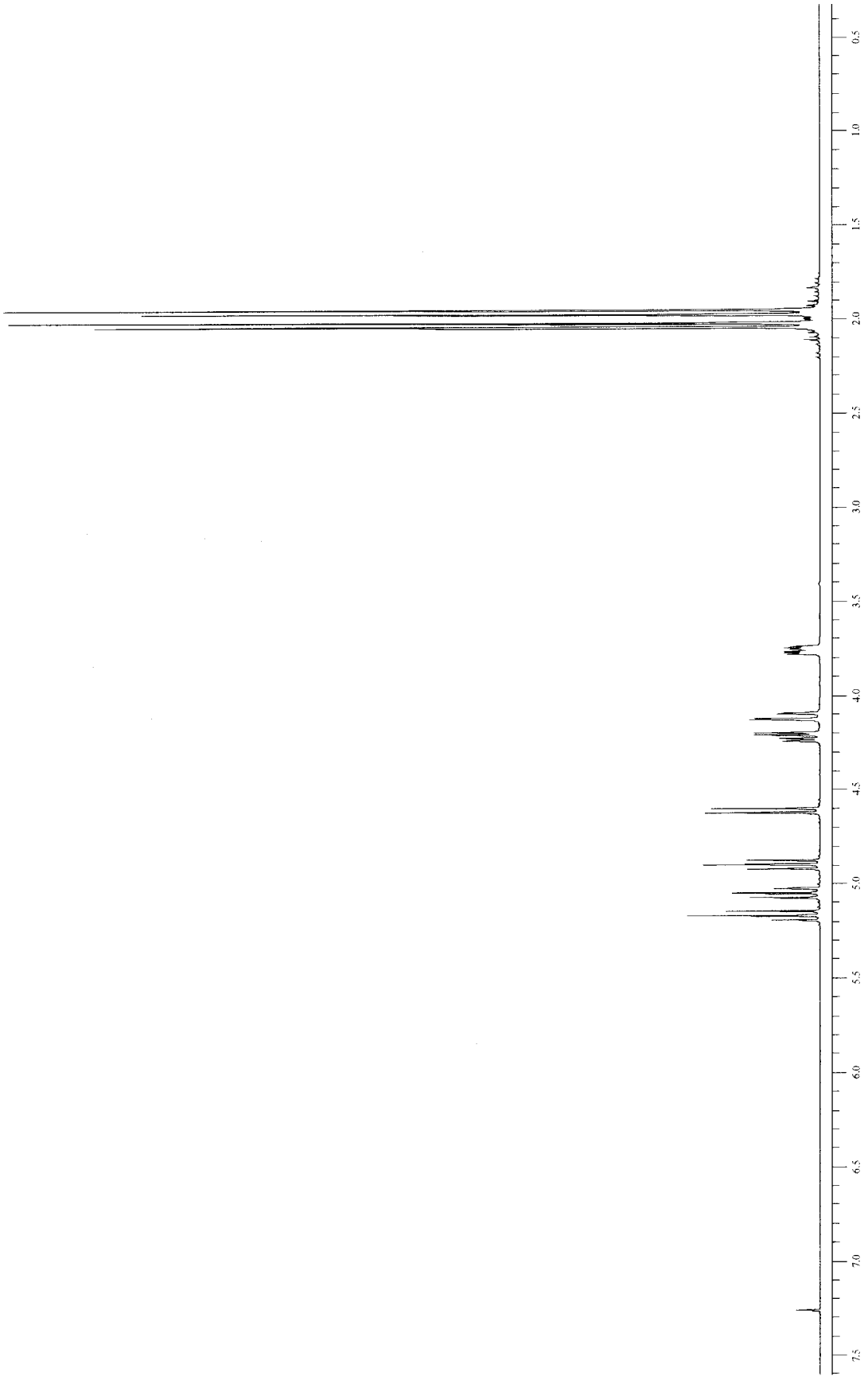

Figure 11: 400 MHz ^{1}H NMR spectrum of azide product **25**

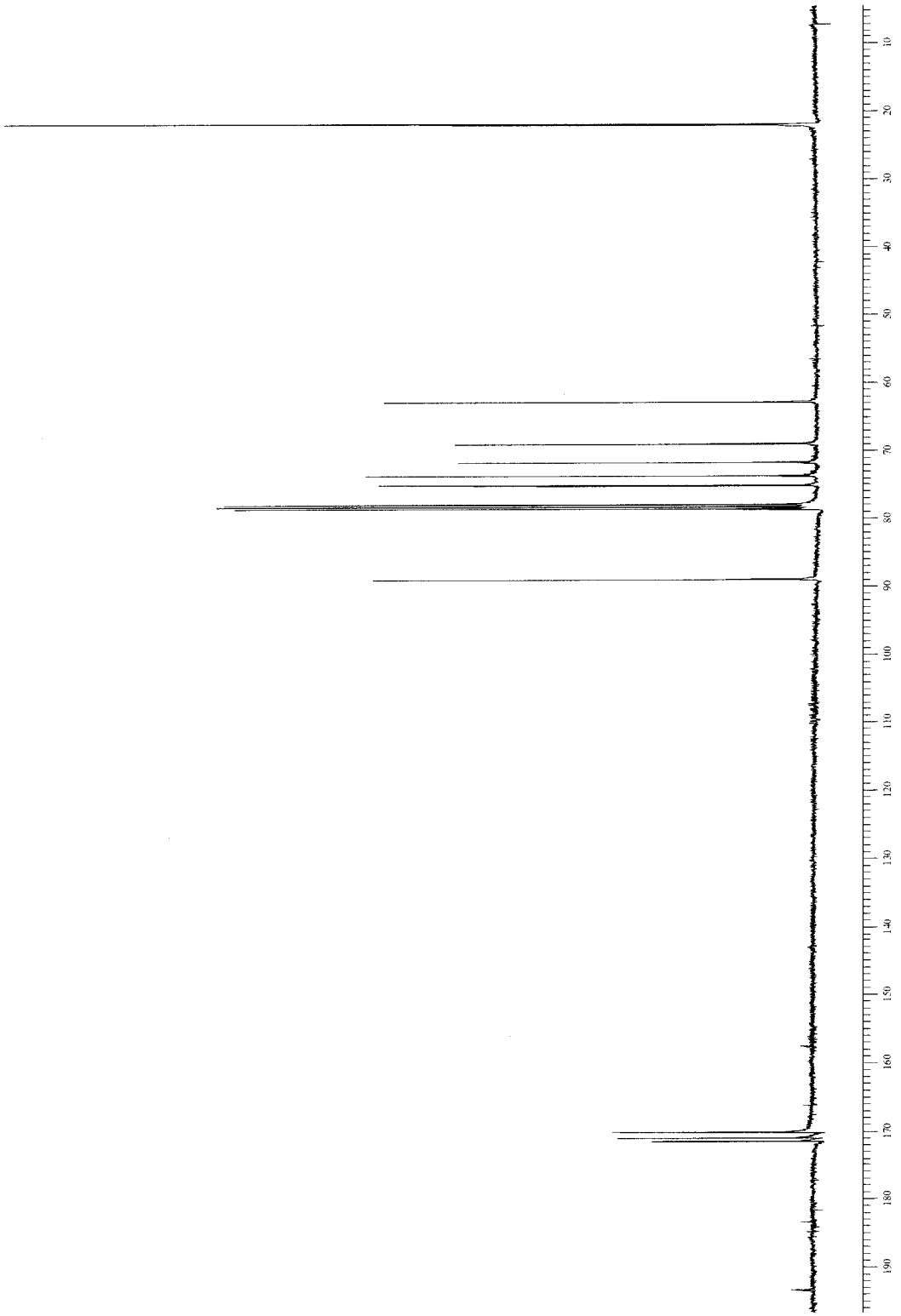

Figure 12: 100 MHz ^{13}C NMR spectrum of azide product **25**

Display Report

Analysis Info:

File: D:\DATA\RAKESH\AZIDE1.D — Printed: Fri Oct 08 14:30:52 2004
Date acquired:
Instrument: — Operator :
Task :
Method : — Sample :

Acquisition Parameter:

Source : — Polarity :
Mode :
CapExit : — Skim 1 :
Scan Range: — Trap Drive:
Accum.time: — Summation :
MS/MS :

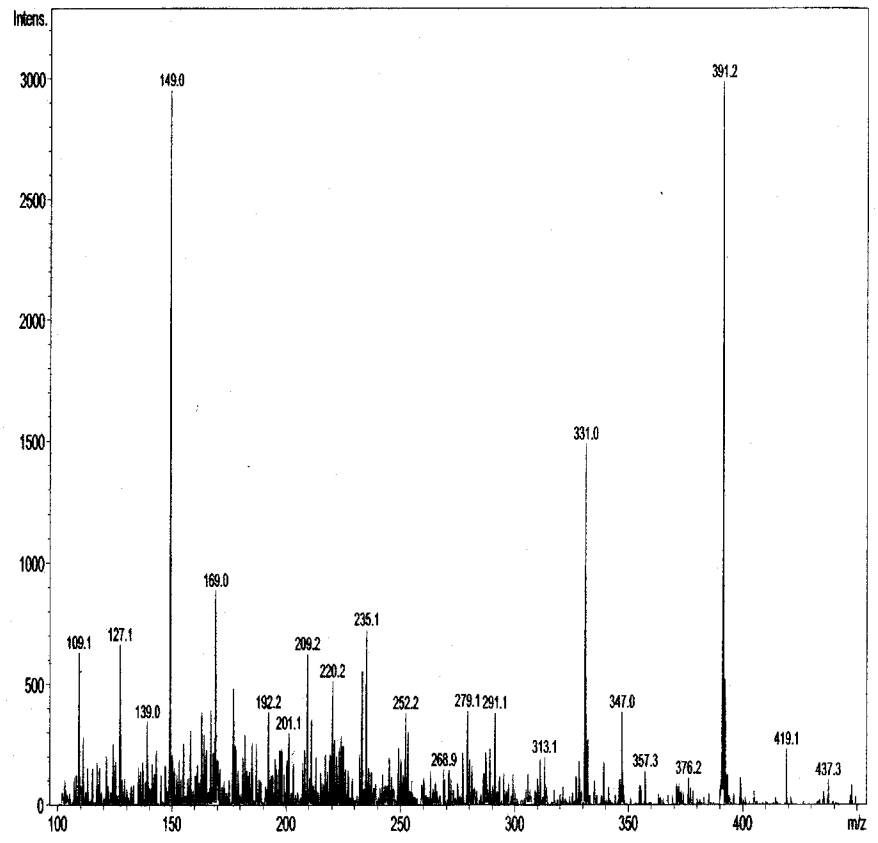

Bruker DataAnalysis Esquire-LC 1.6m, © Bruker Daltonik GmbH
Licensed to BQ_135, Uni. of Ohio

- 1 -

Figure 13: Mass spectrum of azide product **25**

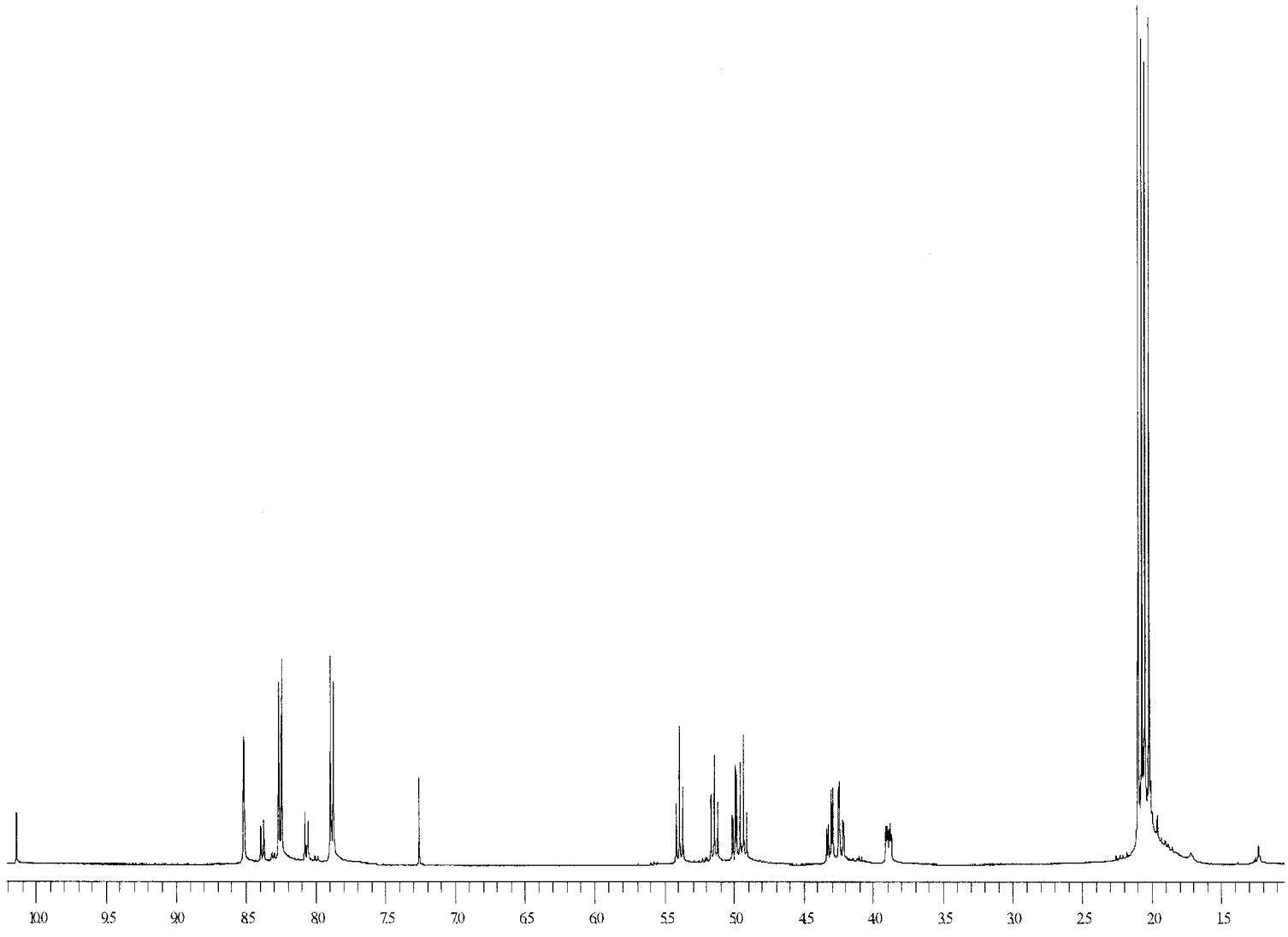

Figure 14: 400 MHz ^{1}H NMR spectrum of imine product **29**

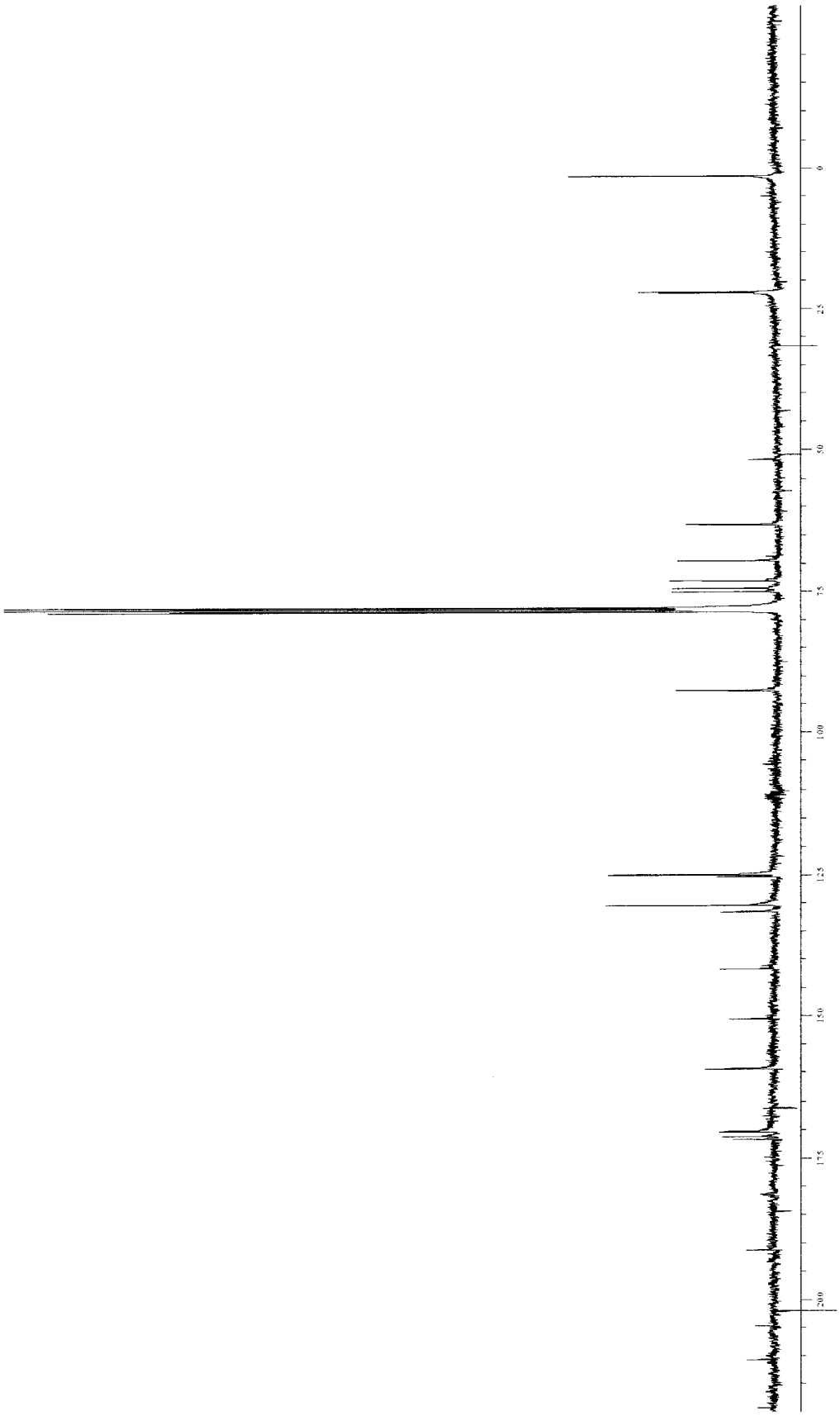

Figure 15: 100 MHz ^{13}C NMR spectrum of imine product **29**

Display Report

Analysis Info:

File: D:\DATA\RAKESH\PNB2.D — Printed: Sat Oct 02 12:30:40 2004
Date acquired:
Instrument: — Operator :
Task :
Method : — Sample :

Acquisition Parameter:

Source : — Polarity :
Mode :
CapExit : — Skim 1 :
Scan Range: — Trap Drive:
Accum.time: — Summation :
MS/MS :

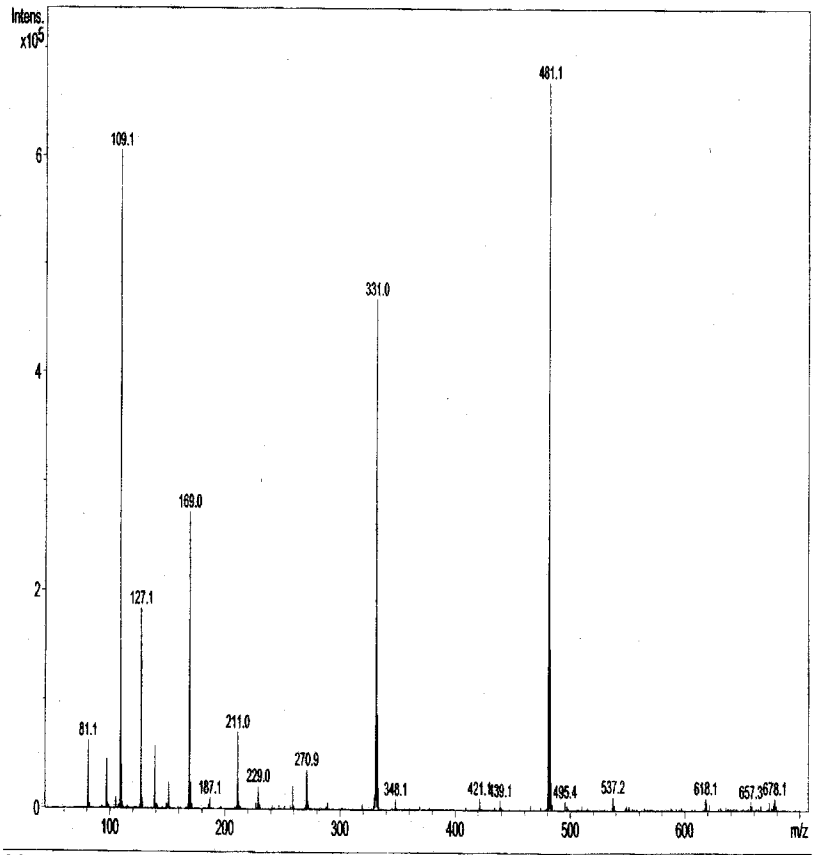

Bruker DataAnalysis Esquire-LC 1.6m, © Bruker Daltonik GmbH
Licensed to HQ_135, Uni. of Ohio

Figure 16: Mass spectrum of imine product **29**

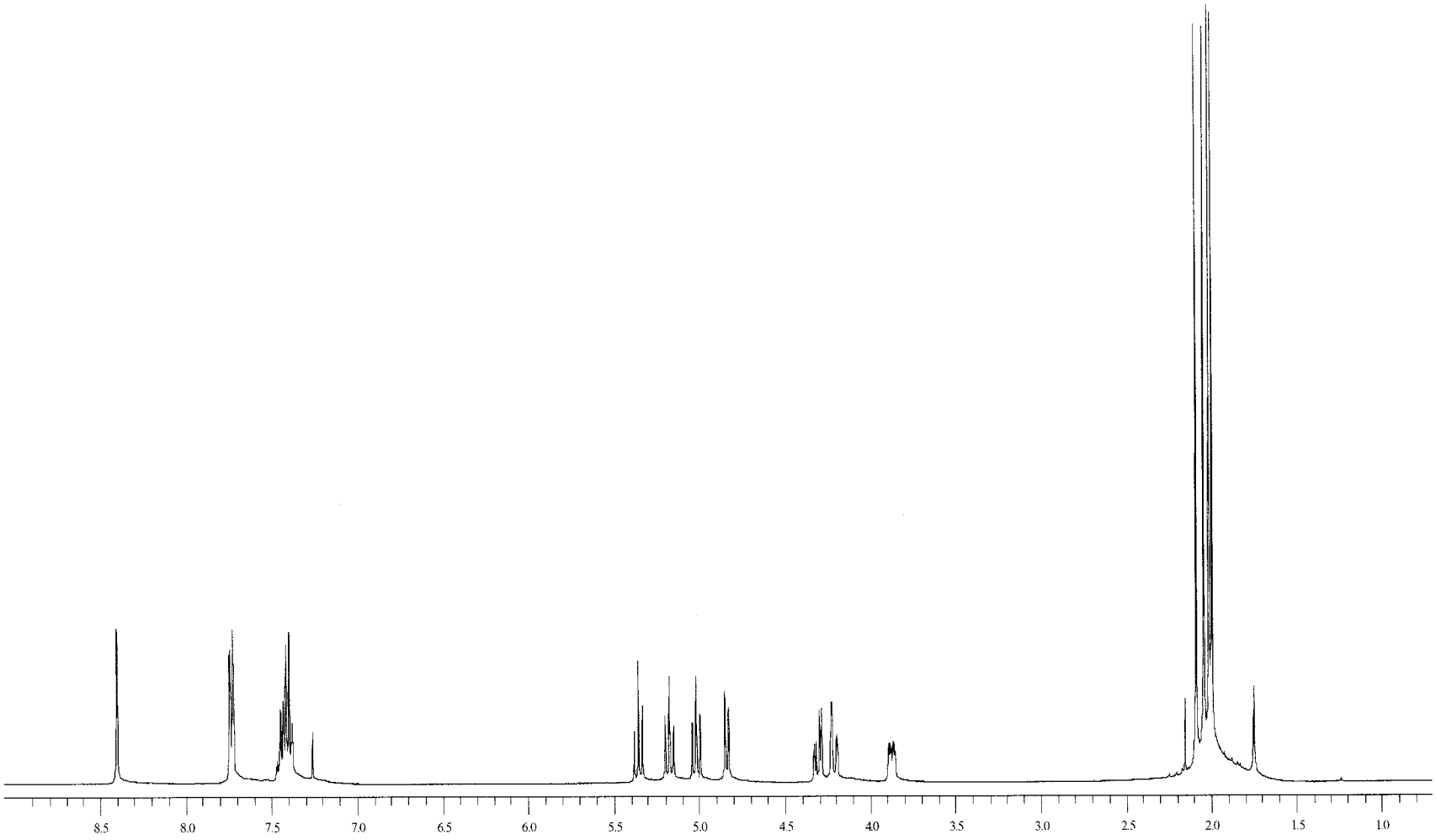

Figure 17: 400 MHz ^{1}H NMR spectrum of imine product **30**

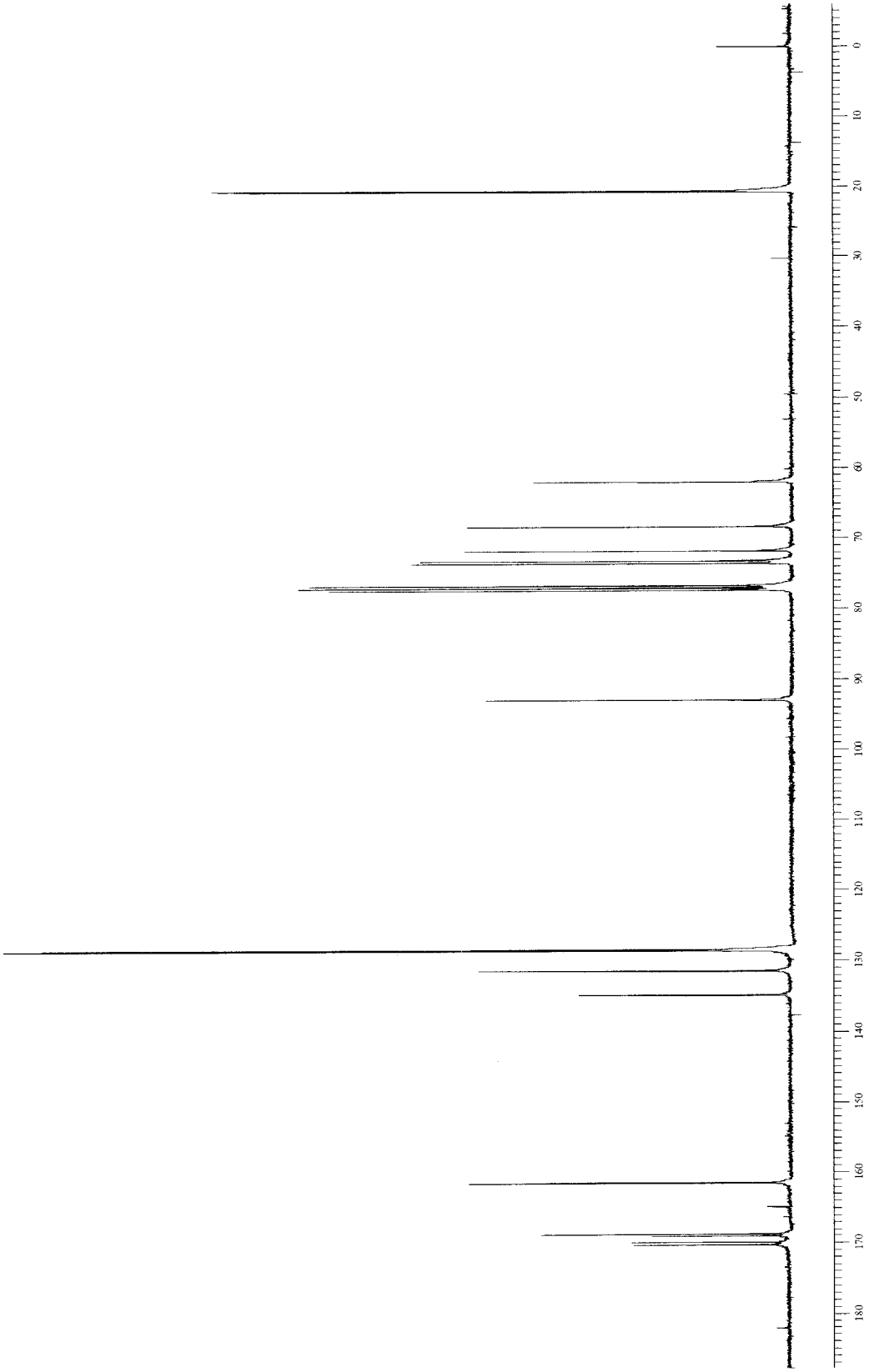

Figure 18: 100 MHz ^{13}C NMR spectrum of imine product **30**

Display Report

Analysis Info:

File: D:\DATA\RAKESH\BENZ.D
Printed: Sat Oct 02 15:53:38 2004
Date acquired:
Instrument:
Operator :
Task :
Method :
Sample :

Acquisition Parameter:

Source :
Polarity :
Mode :
CapExit :
Skim 1 :
Scan Range:
Trap Drive:
Accum.time:
Summation :
MS/MS :

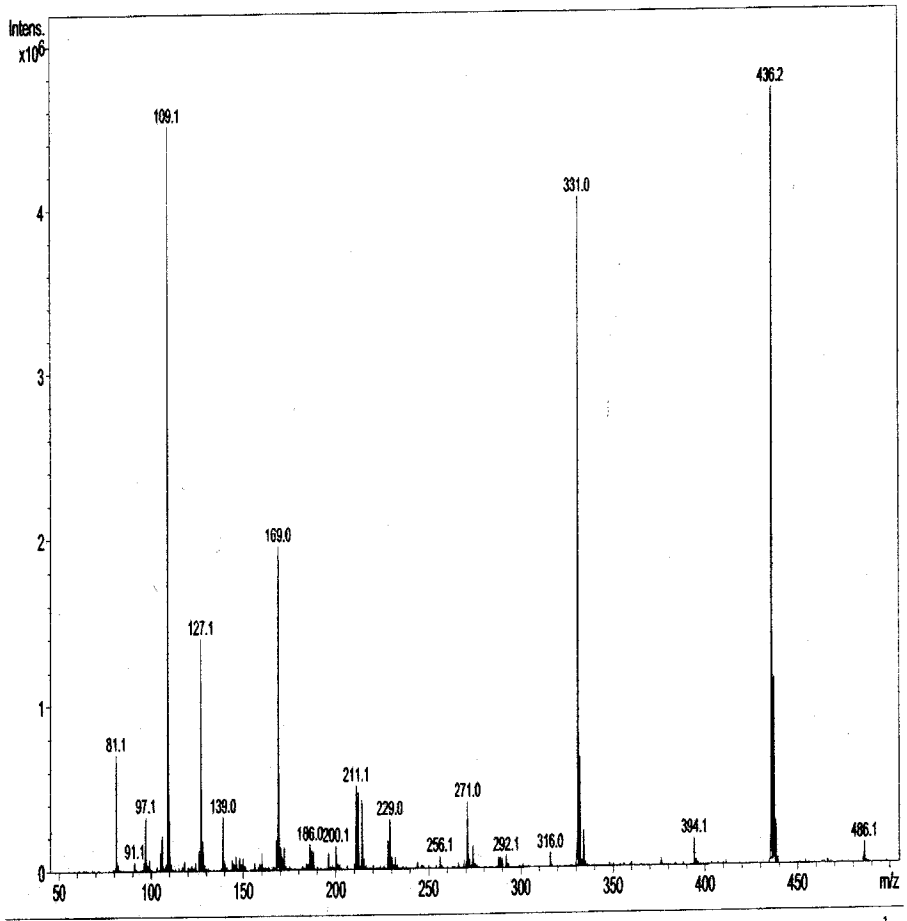

Bruker DataAnalysis Esquire-LC 1.6m, © Bruker Daltonik GmbH
Licensed to BQ_135, Uni. of Ohio

- 1 -

Figure 19: Mass spectrum of imine product **30**

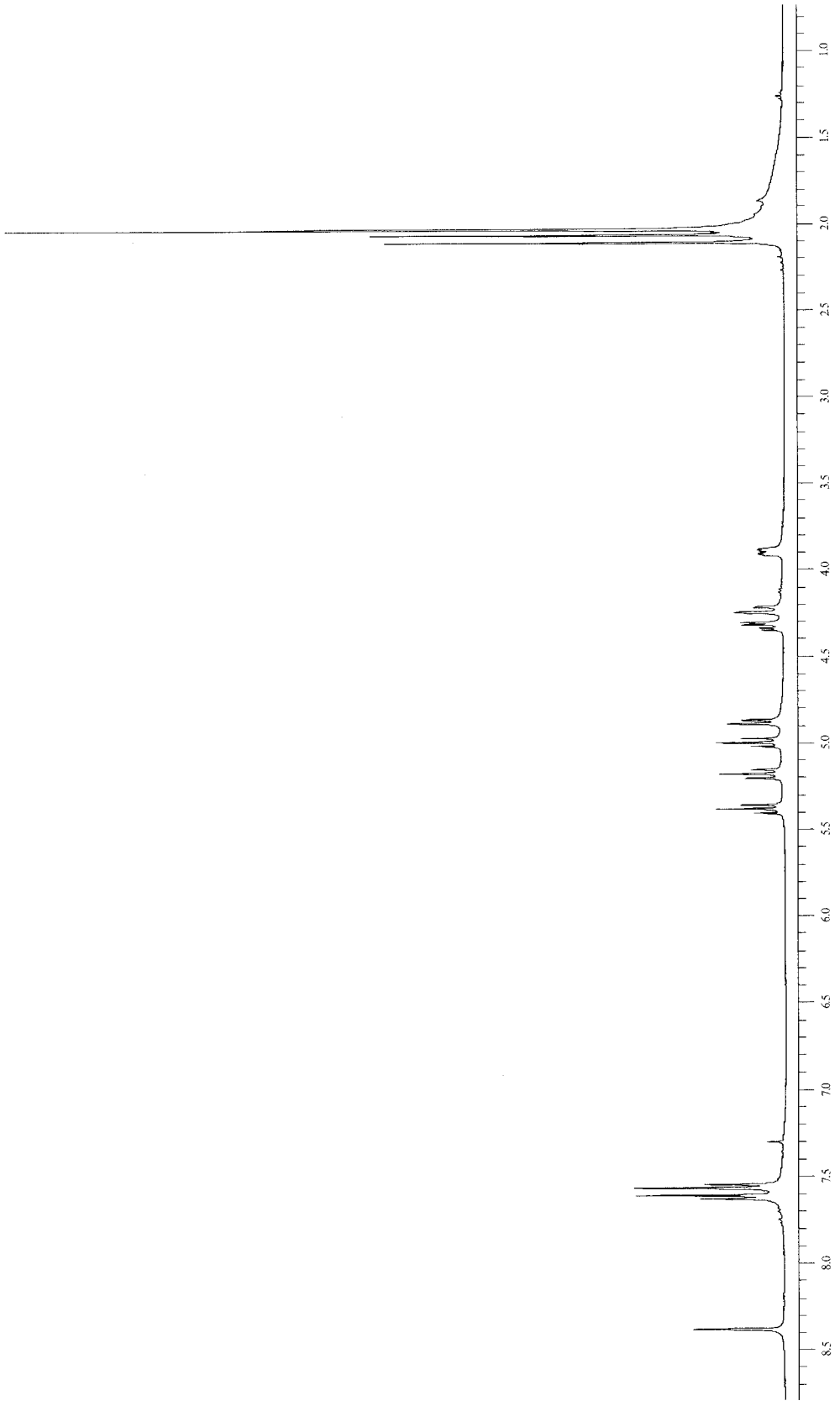

Figure 20: 400 MHz ^{1}H NMR spectrum of imine product **31**

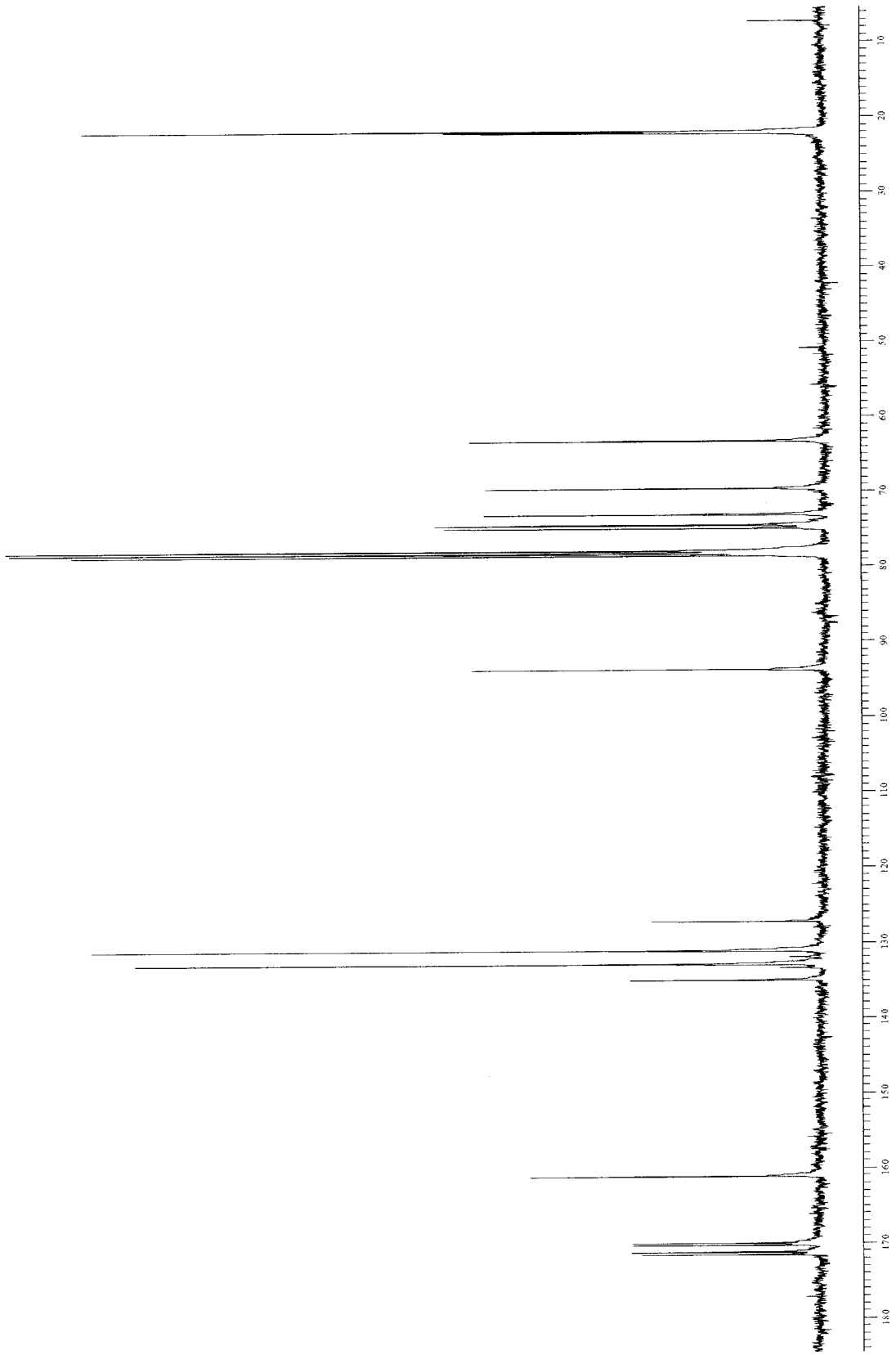

Figure 21: 100 MHz ^{13}C NMR spectrum of imine product **31**

Display Report

Analysis Info:

File: D:\DATA\RAKESH\4BB2.D — Printed: Sat Oct 02 13:18:29 2004
Date acquired:
Instrument: — Operator :
Task :
Method : — Sample :

Acquisition Parameter:

Source : — Polarity :
Mode :
CapExit : — Skim 1 :
Scan Range: — Trap Drive:
Accum.time: — Summation :
MS/MS :

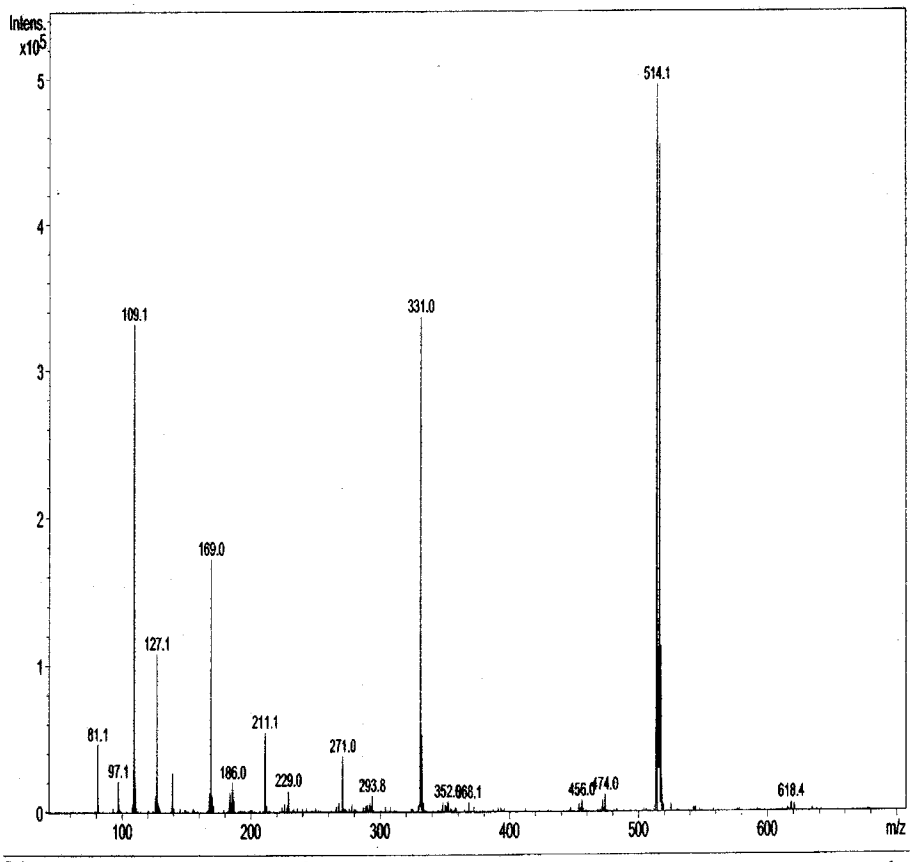

Bruker DataAnalysis Esquire-LC 1.6m, © Bruker Daltonik GmbH
Licensed to BQ_135, Uni. of Ohio

- 1 -

Figure 22: Mass spectrum of imine product **31**

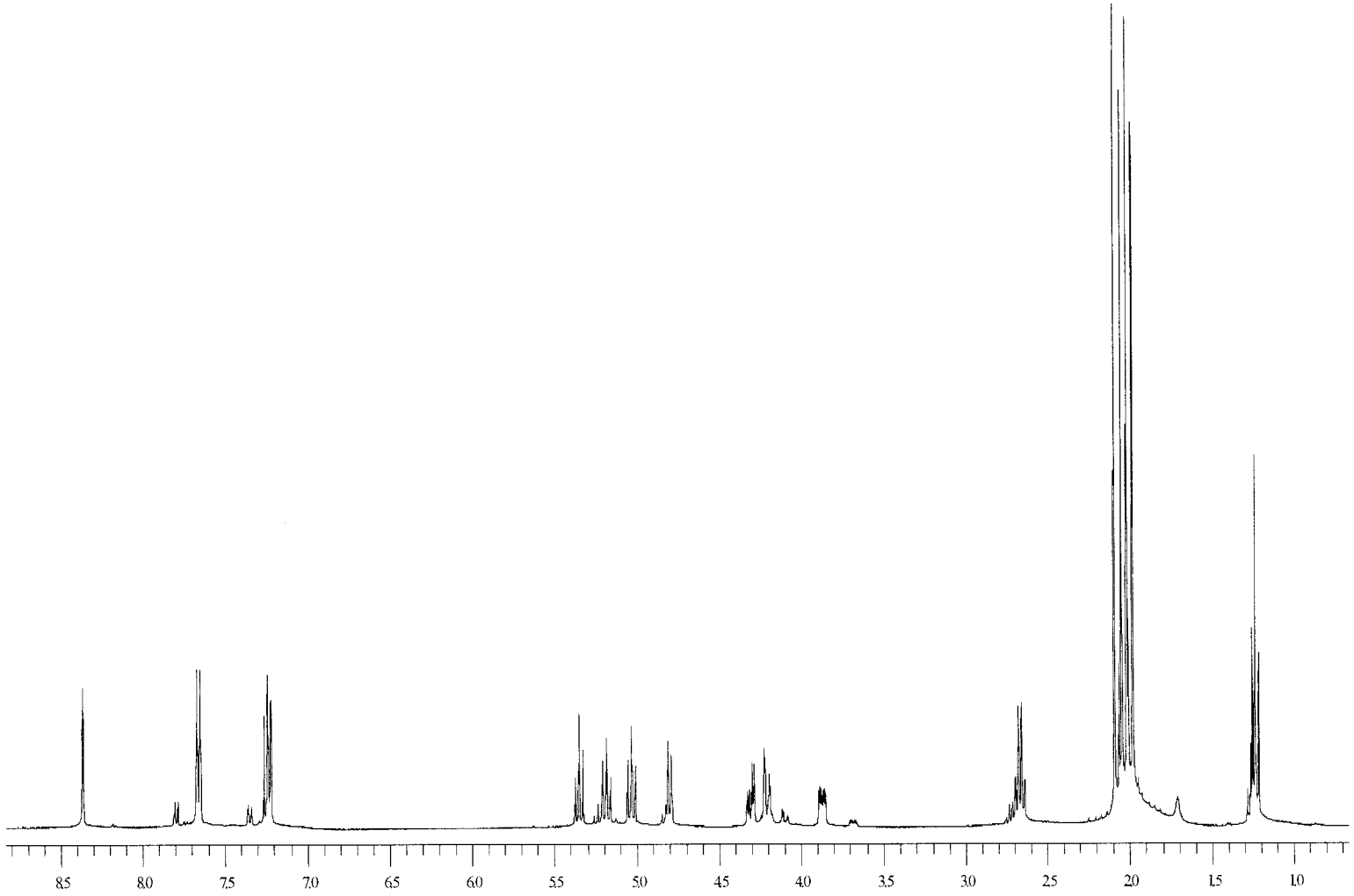

Figure 23: 400 MHz ^{1}H NMR spectrum of imine product **32**

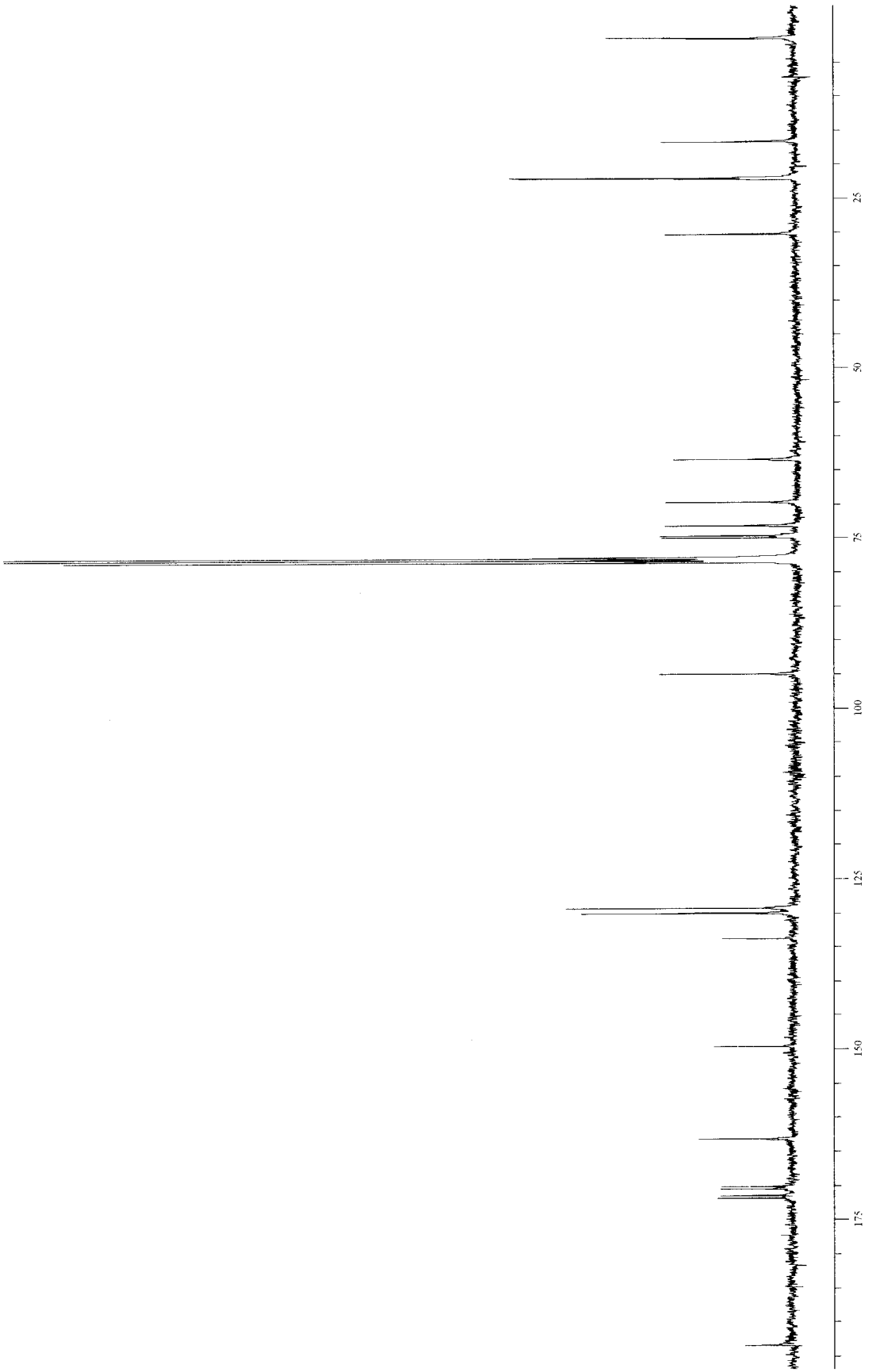

Figure 24: 100 MHz ^{13}C NMR spectrum of imine product **32**

Display Report

Analysis Info:

File: D:\DATA\RAKESH\4EB.D
Printed: Sat Oct 02 14:28:17 2004
Date acquired:
Instrument:
Operator :
Task :
Method :
Sample :

Acquisition Parameter:

Source :
Polarity :
Mode :
CapExit :
Skim 1 :
Scan Range:
Trap Drive:
Accum.time:
Summation :
MS/MS :

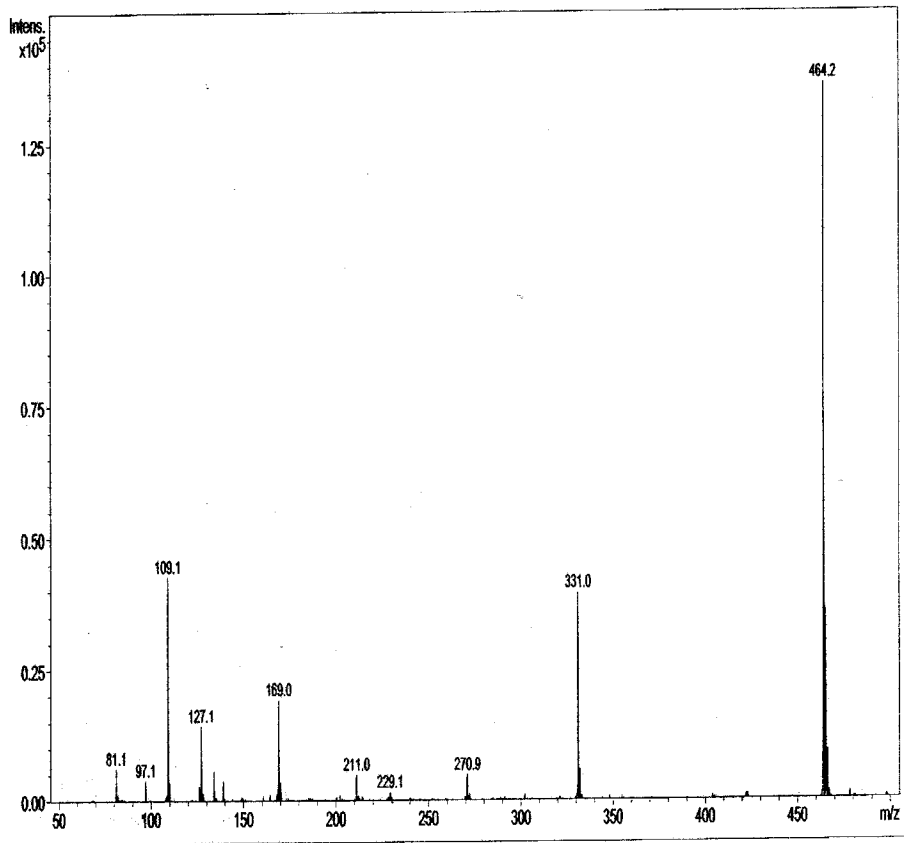

Bruker DataAnalysis Esquire-LC 1.6m, © Bruker Daltonik GmbH
Licensed to BQ_135, Uni. of Ohio

- 1 -

Figure 25: Mass spectrum of imine product **32**

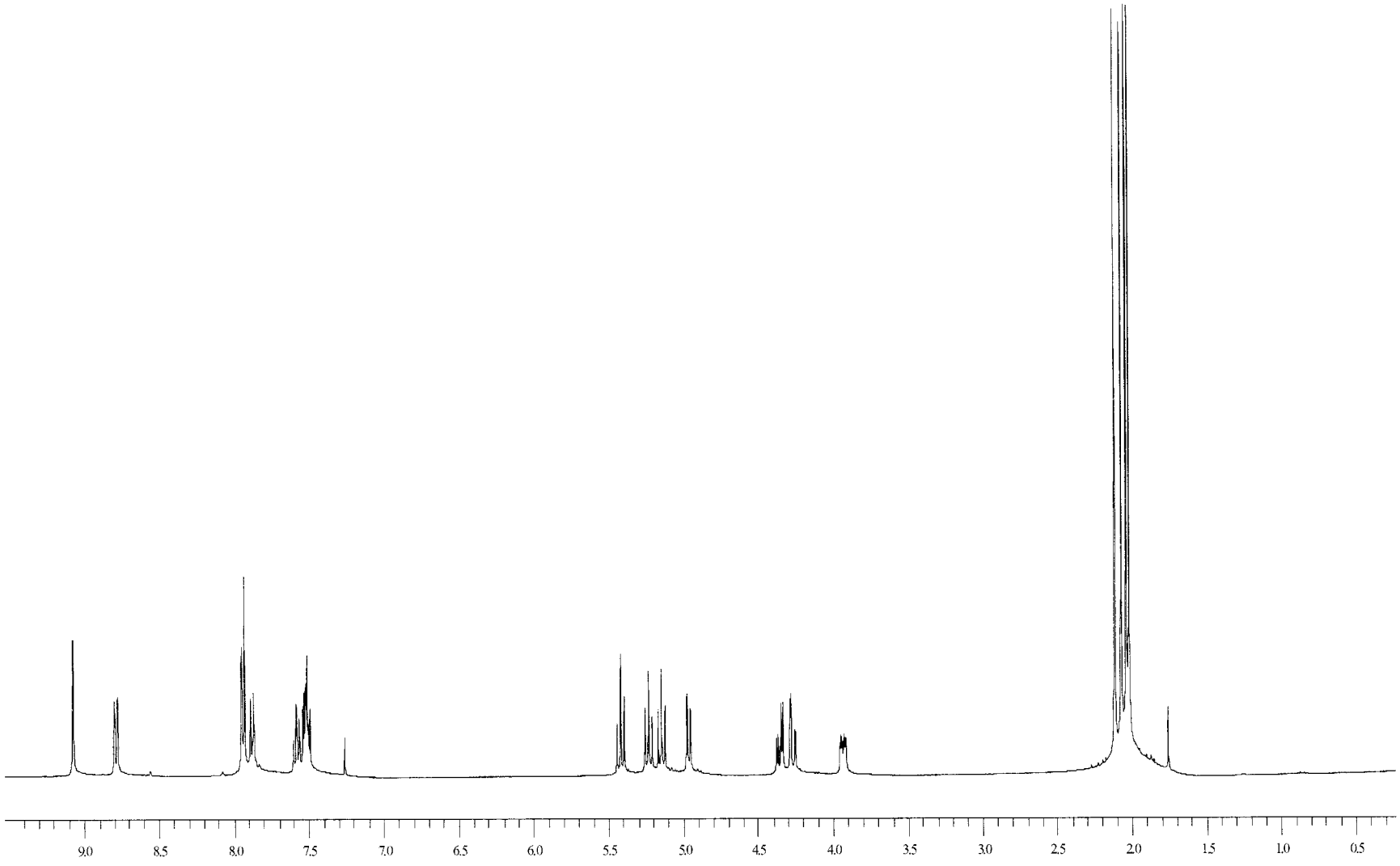

Figure 26: 400 MHz ^{1}H NMR spectrum of imine product **33**

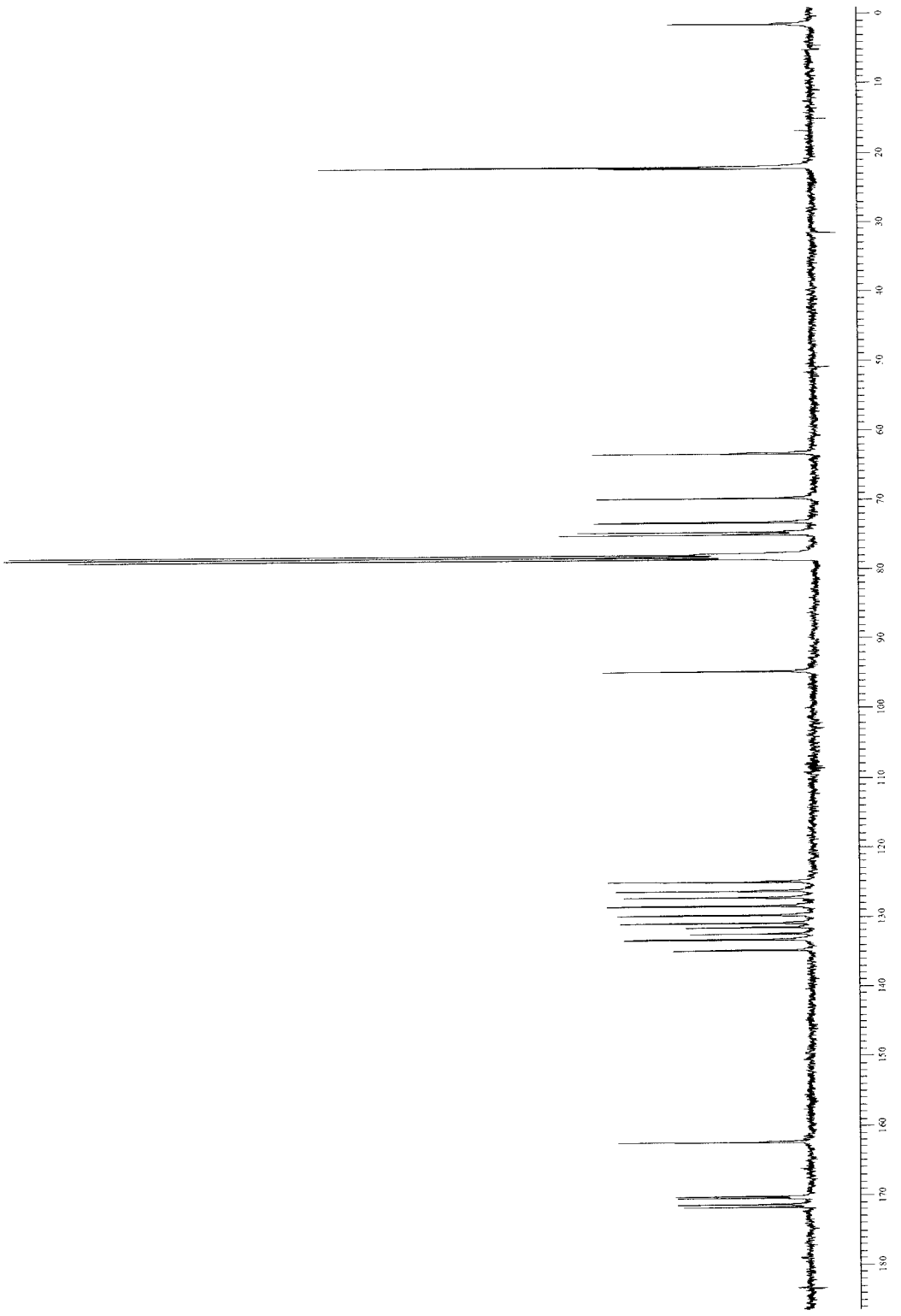

Figure 27: 100 MHz ^{13}C NMR spectrum of imine product **33**

Display Report

Analysis Info:

File: D:\DATA\RAKESH\NAP.D — Printed: Sat Oct 02 15:15:02 2004
Date acquired:
Instrument: — Operator :
Task :
Method : — Sample :

Acquisition Parameter:

Source : — Polarity :
Mode :
CapExit : — Skim 1 :
Scan Range: — Trap Drive:
Accum.time: — Summation :
MS/MS :

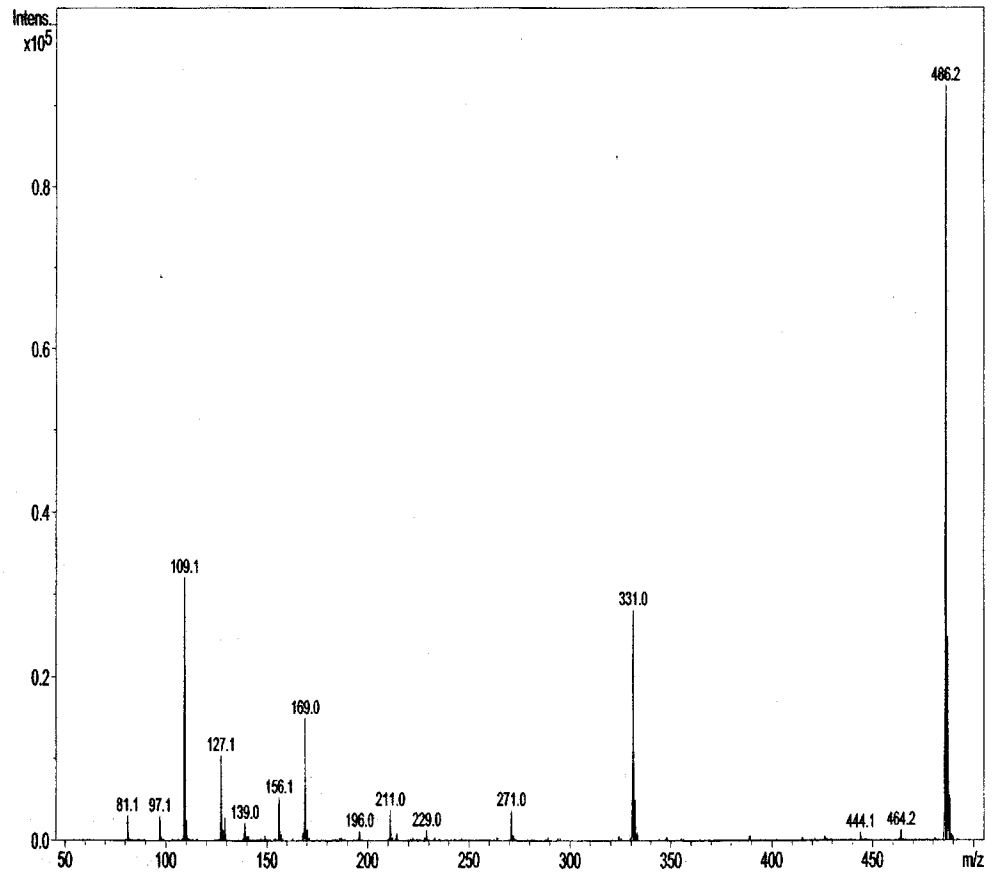

Bruker DataAnalysis Esquire-LC 1.6m, © Bruker Daltonik GmbH — - 1 -
Licensed to EQ_135, Uni. of Ohio

Figure 28: Mass spectrum of imine product **33**

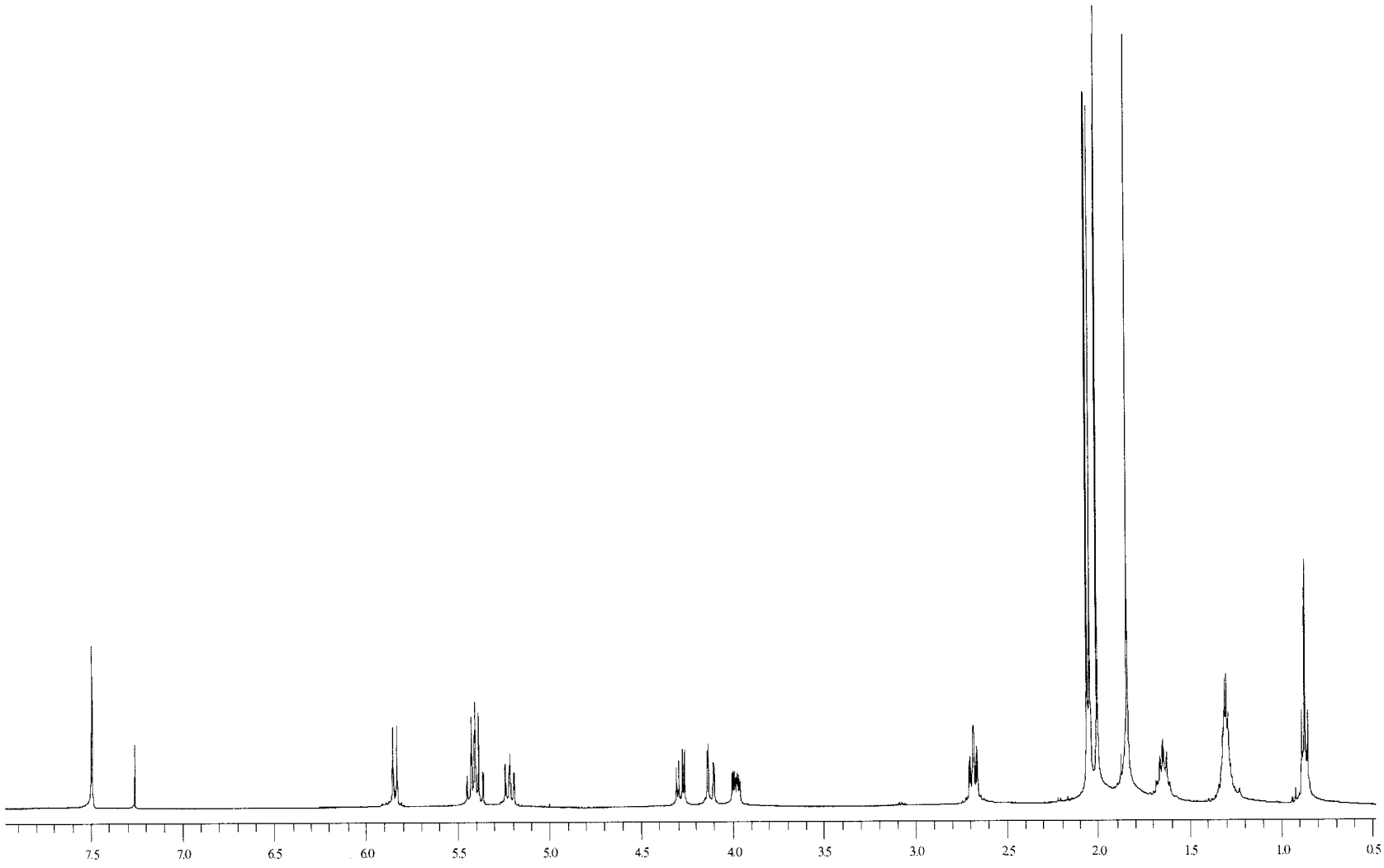

Figure 29: 400 MHz ^{1}H NMR spectrum of triazole product **38**

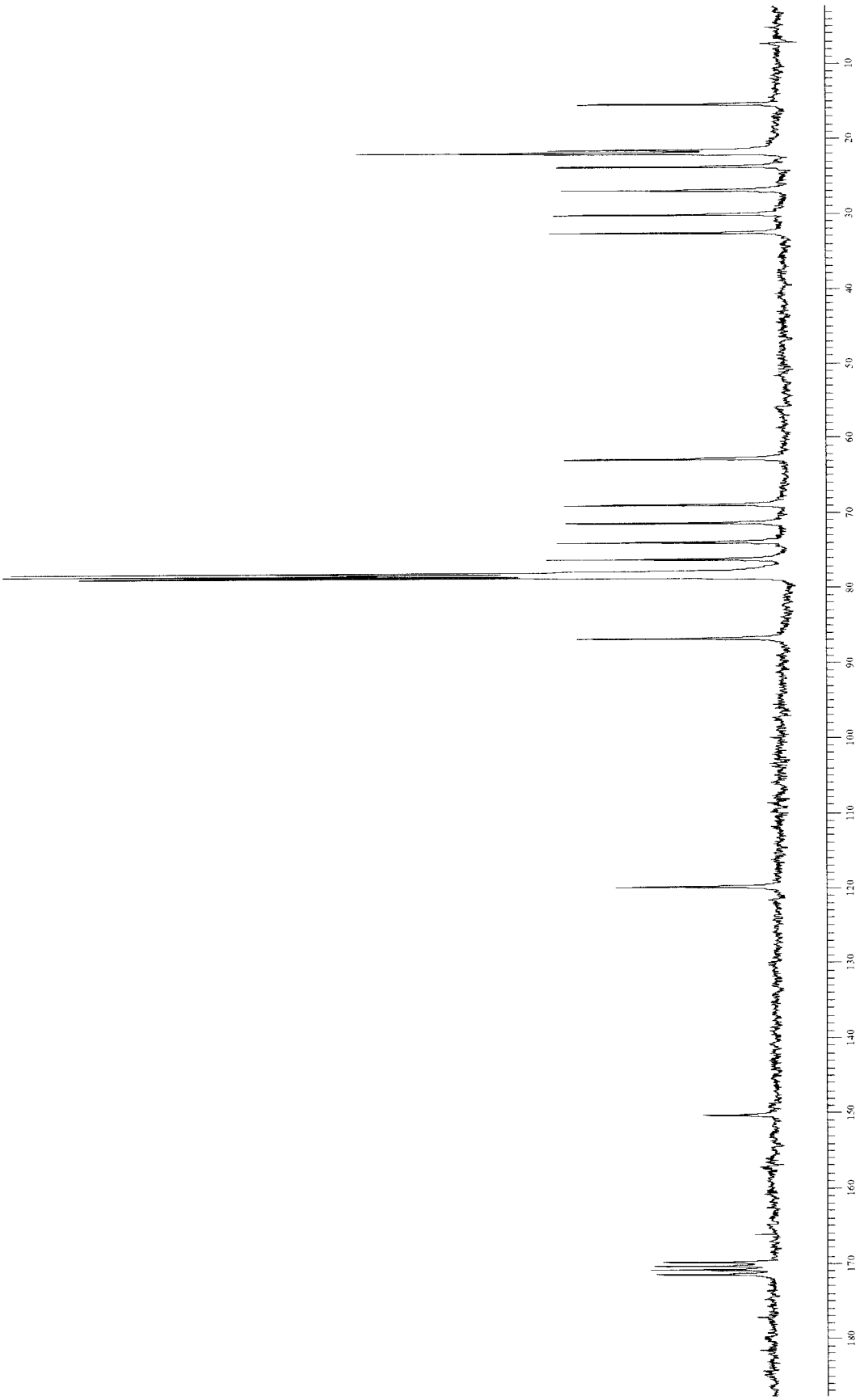

Figure 30: 100 MHz ^{13}C NMR spectrum of triazole product **38**

Display Report

Analysis Info:

File: D:\DATA\RAKESH\HEPTYNE1.D
Printed: Sun Oct 03 11:40:41 2004
Date acquired:
Instrument:
Operator :
Task :
Method :
Sample :

Acquisition Parameter:

Source :
Polarity :
Mode :
CapExit :
Skim 1 :
Scan Range:
Trap Drive:
Accum.time:
Summation :
MS/MS :

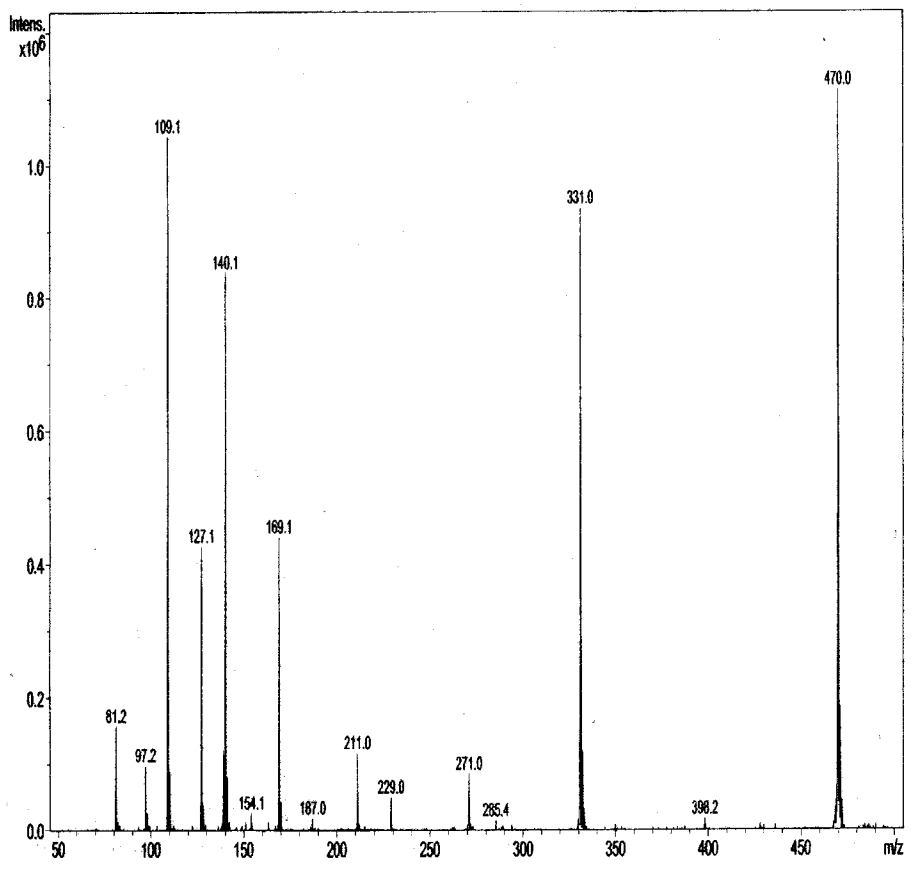

Bruker DataAnalysis Esquire-LC 1.6m, © Bruker Daltonik GmbH
Licensed to BQ_135, Uni. of Ohio

- 1 -

Figure 31: Mass spectrum of triazole product **38**

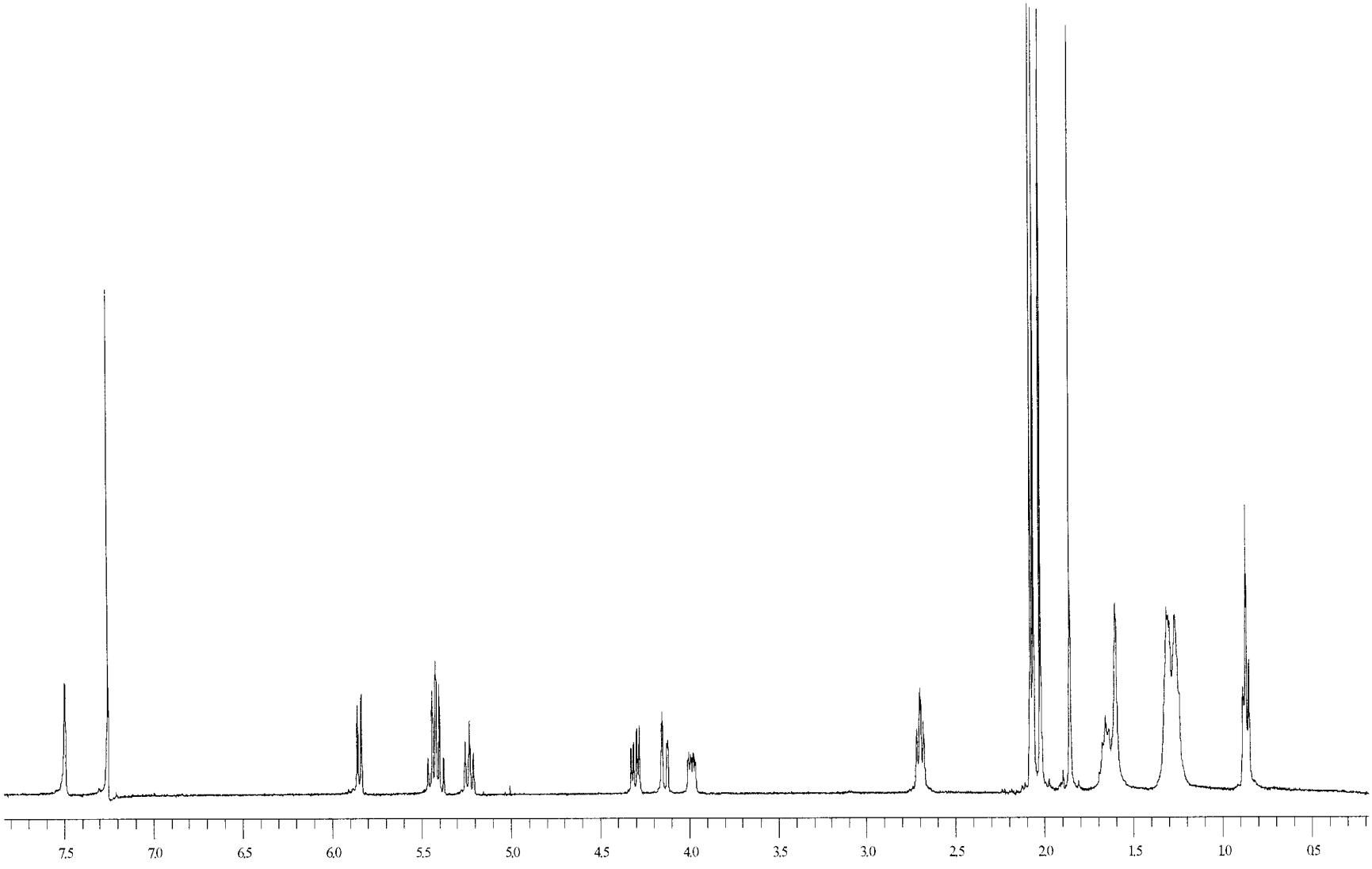

Figure 32: 400 MHz ^{1}H NMR spectrum of triazole product **39**

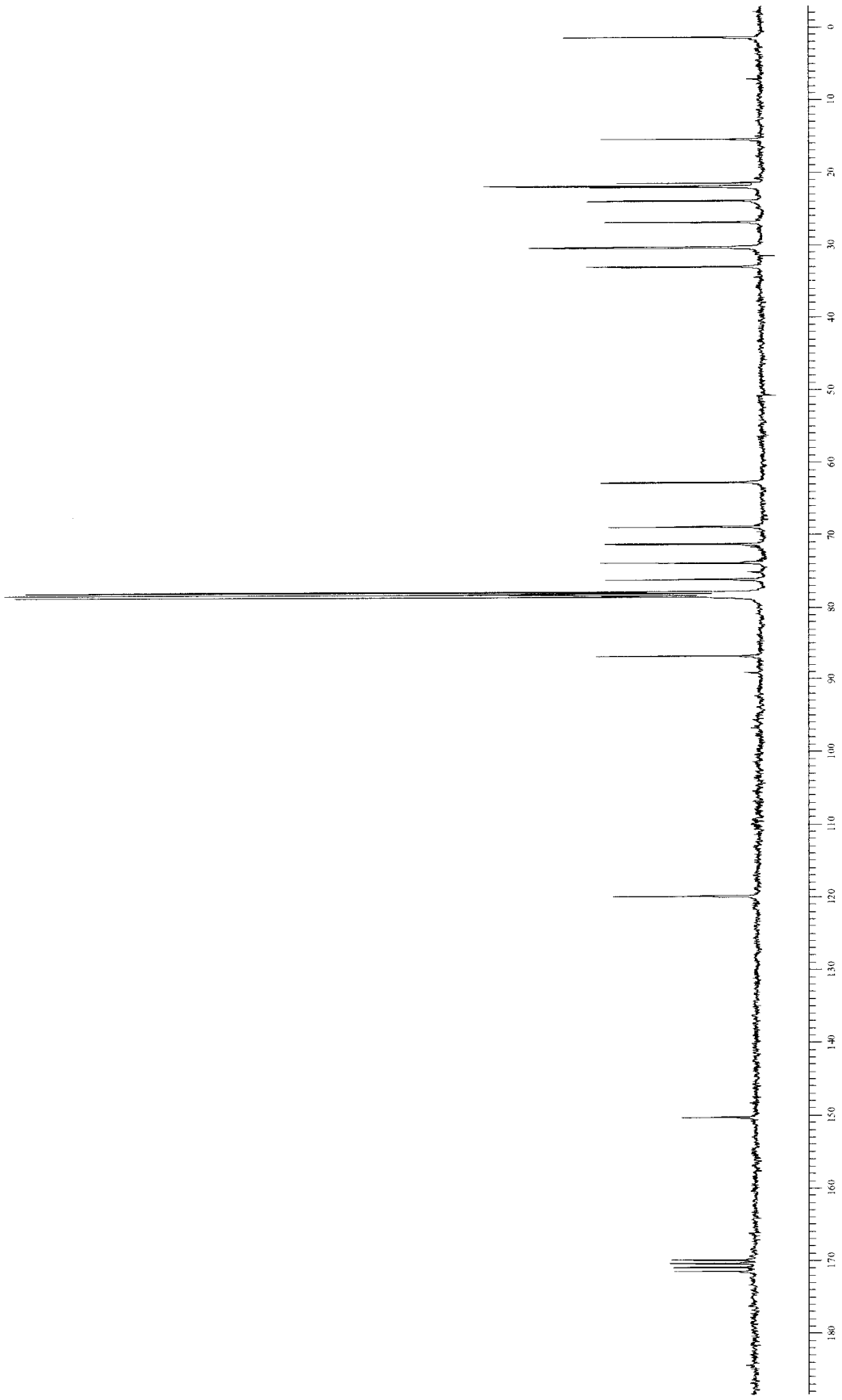

Figure 33: 100 MHz ^{13}C NMR spectrum of triazole product **39**

Display Report

Analysis Info:

File: D:\DATA\RAKESH\NONYNE2.D
Printed: Sun Oct 03 12:03:07 2004
Date acquired:
Instrument:
Operator :
Task :
Method :
Sample :

Acquisition Parameter:

Source :
Polarity :
Mode :
CapExit :
Skim 1 :
Scan Range:
Trap Drive:
Accum.time:
Summation :
MS/MS :

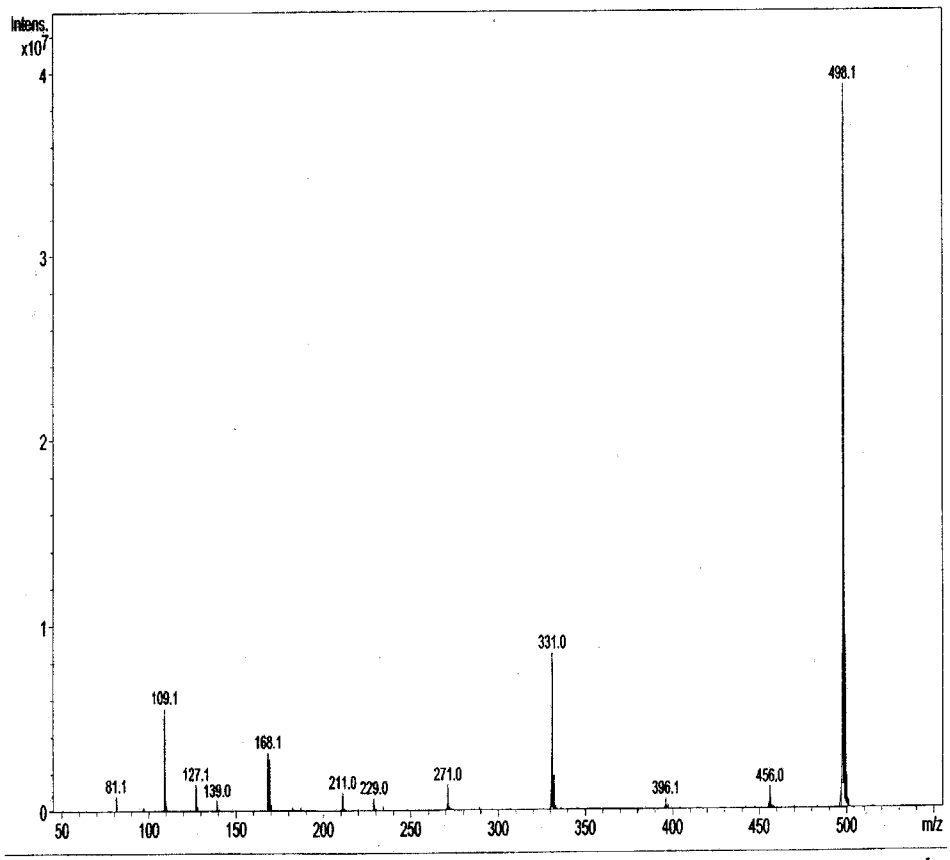

Bruker DataAnalysis Esquire-LC 1.6m, © Bruker Daltonik GmbH
Licensed to EQ_135, Uni. of Ohio

1 -

Figure 34: Mass spectrum of triazole product **39**

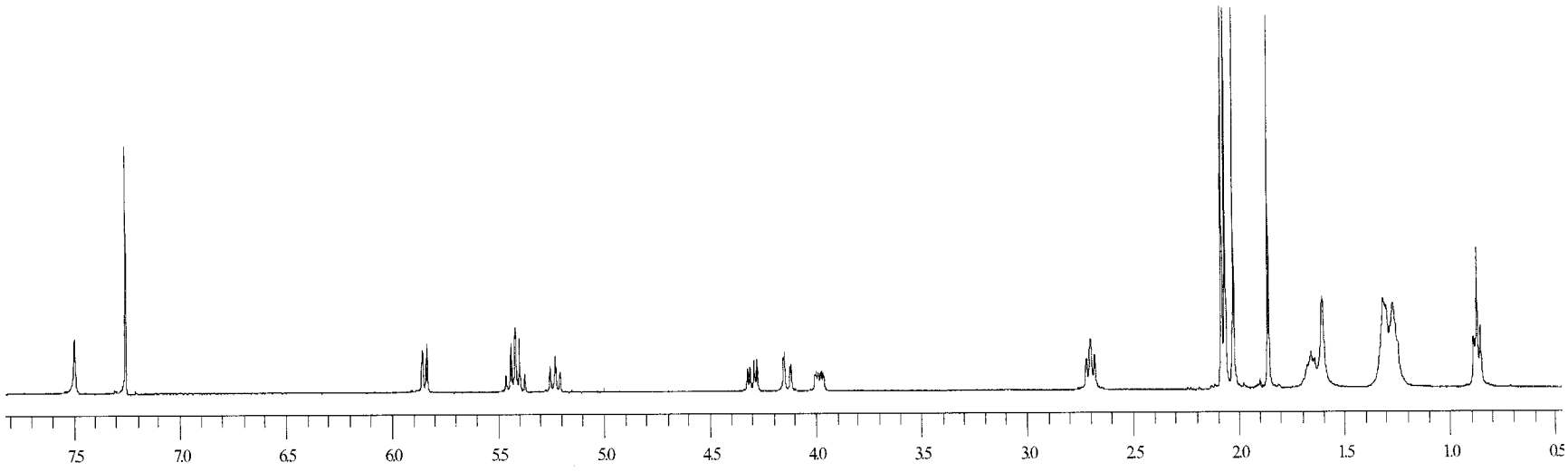

Figure 35: 400 MHz ^{1}H NMR spectrum of triazole product **40**

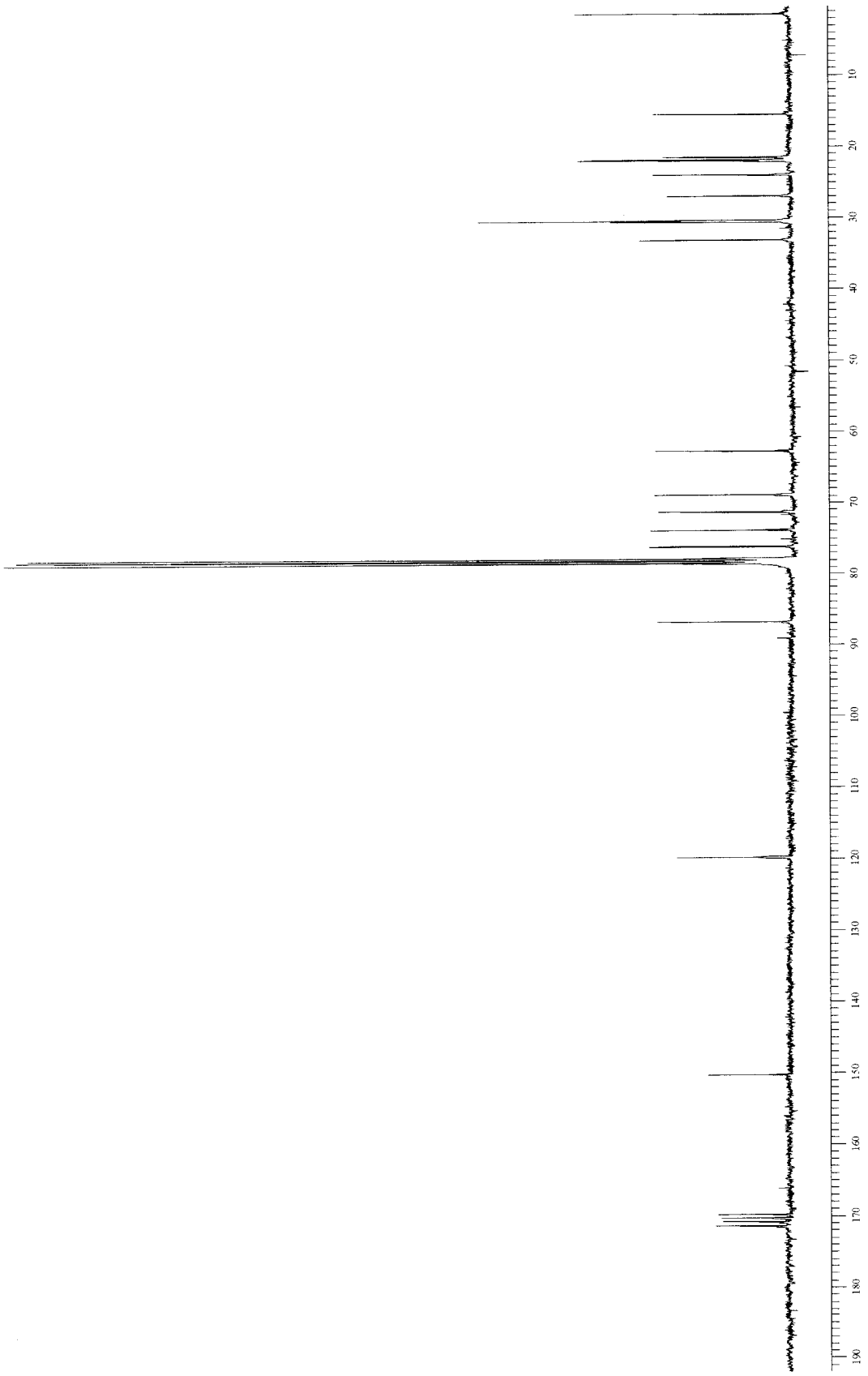

Figure 36: 100 MHz ^{13}C NMR spectrum of triazole product **40**

Display Report

Analysis Info:

File: D:\DATA\RAKESH\DECYNE.D
Printed: Sun Oct 03 13:50:33 2004
Date acquired:
Instrument:
Operator :
Task :
Method :
Sample :

Acquisition Parameter:

Source :
Polarity :
Mode :
CapExit :
Skim 1 :
Scan Range:
Trap Drive:
Accum.time:
Summation :
MS/MS :

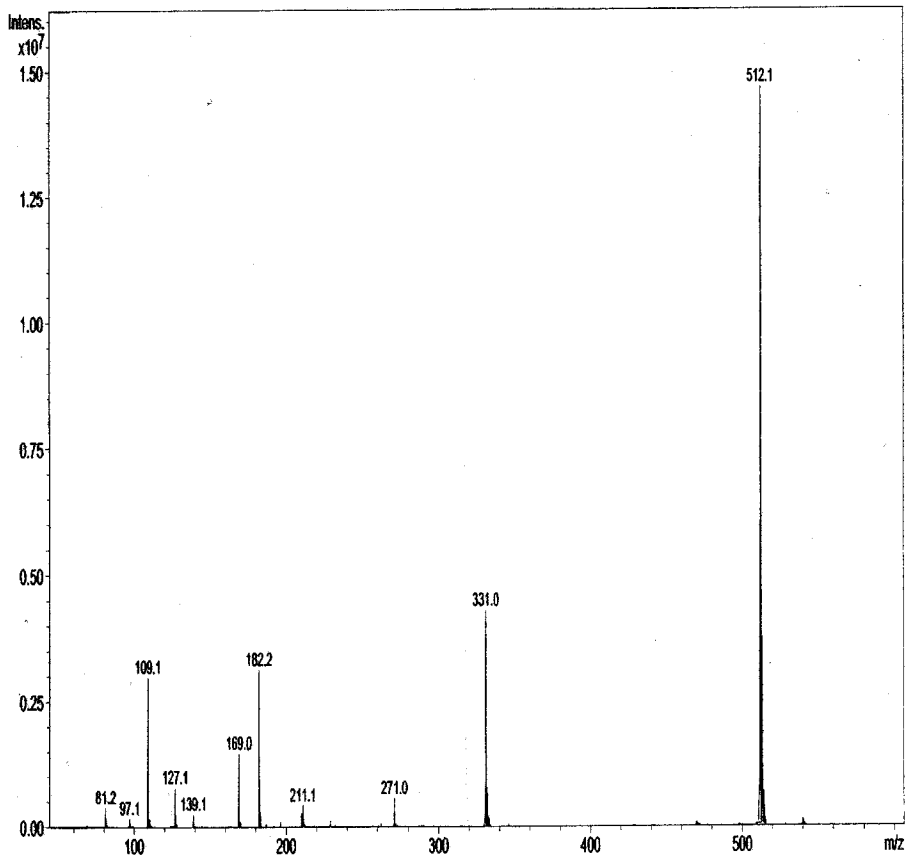

Bruker DataAnalysis Esquire-LC 1.6m, © Bruker Daltonik GmbH
Licensed to EQ_135, Uni. of Ohio

- 1 -

Figure 37: Mass spectrum of triazole product **40**

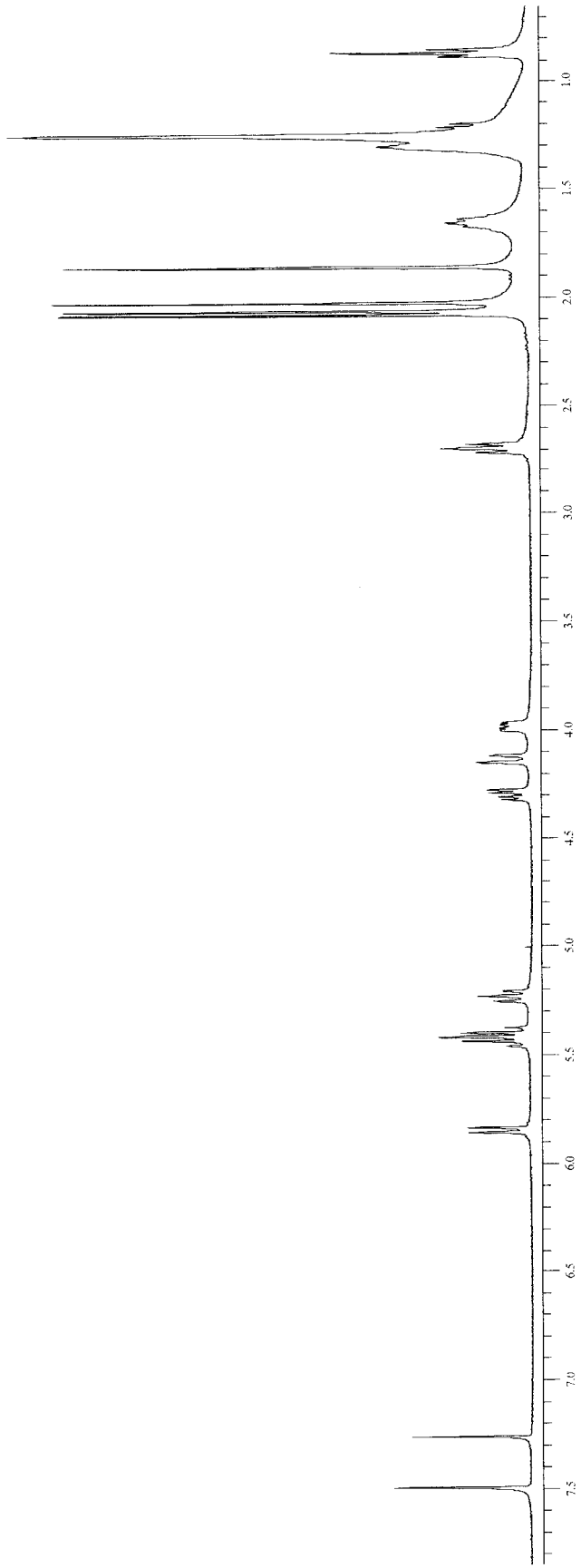

Figure 38: 400 MHz ^{1}H NMR spectrum of triazole product **41**

Figure 39: 100 MHz ^{13}C NMR spectrum of triazole product **41**

Display Report

Analysis Info:

File: D:\DATA\RAKESH\DODECYNE.D
Printed: Sun Oct 03 13:24:17 2004
Date acquired:
Instrument:
Operator :
Task :
Method :
Sample :

Acquisition Parameter:

Source :
Polarity :
Mode :
CapExit :
Skim 1 :
Scan Range:
Trap Drive:
Accum.time:
Summation :
MS/MS :

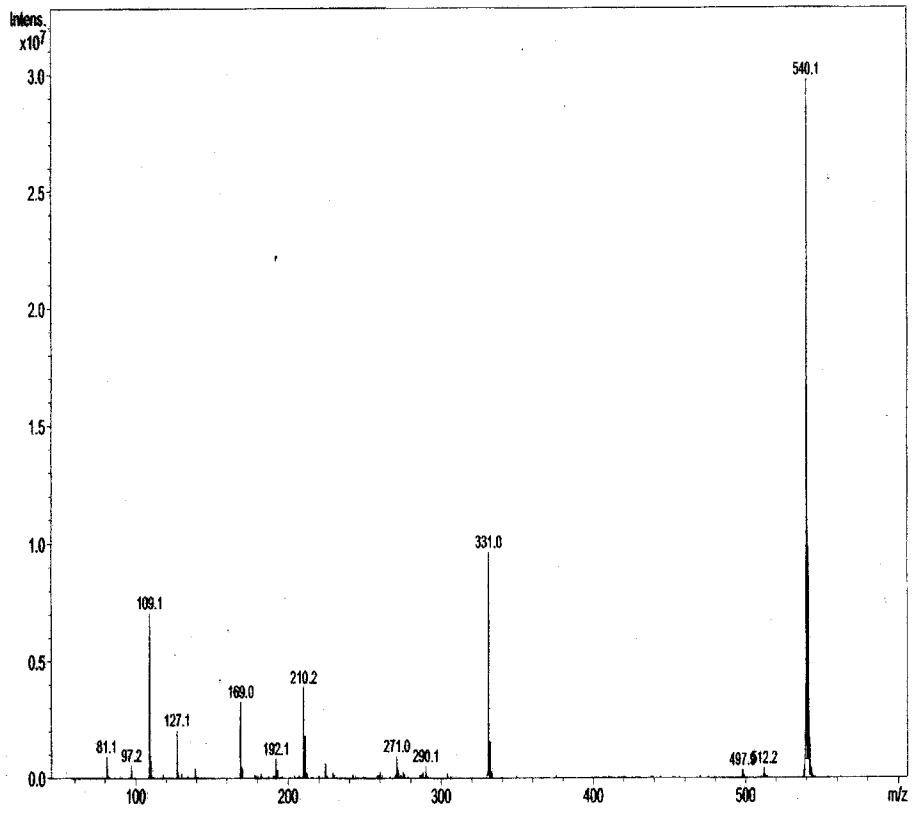

Bruker DataAnalysis Esquire-LC 1.6m, © Bruker Daltonik GmbH
Licensed to BQ_135, Uni. of Ohio

- 1 -

Figure 40: Mass spectrum of triazole product **41**

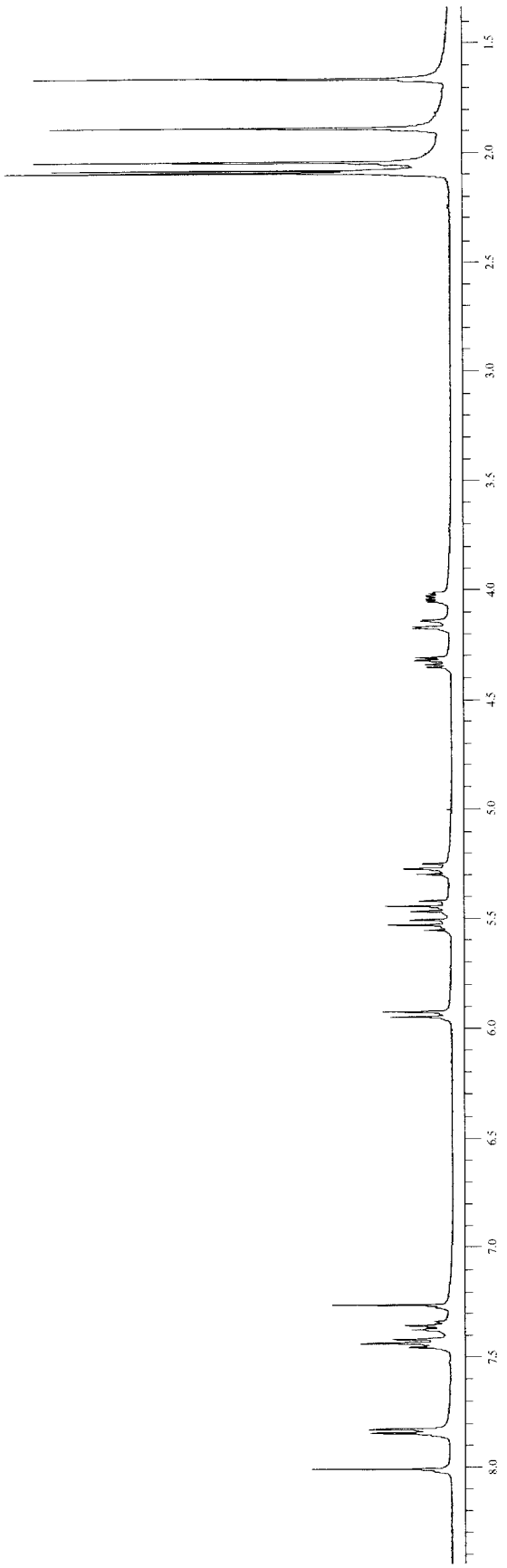

Figure 41: 400 MHz ^{1}H NMR spectrum of triazole product **42**

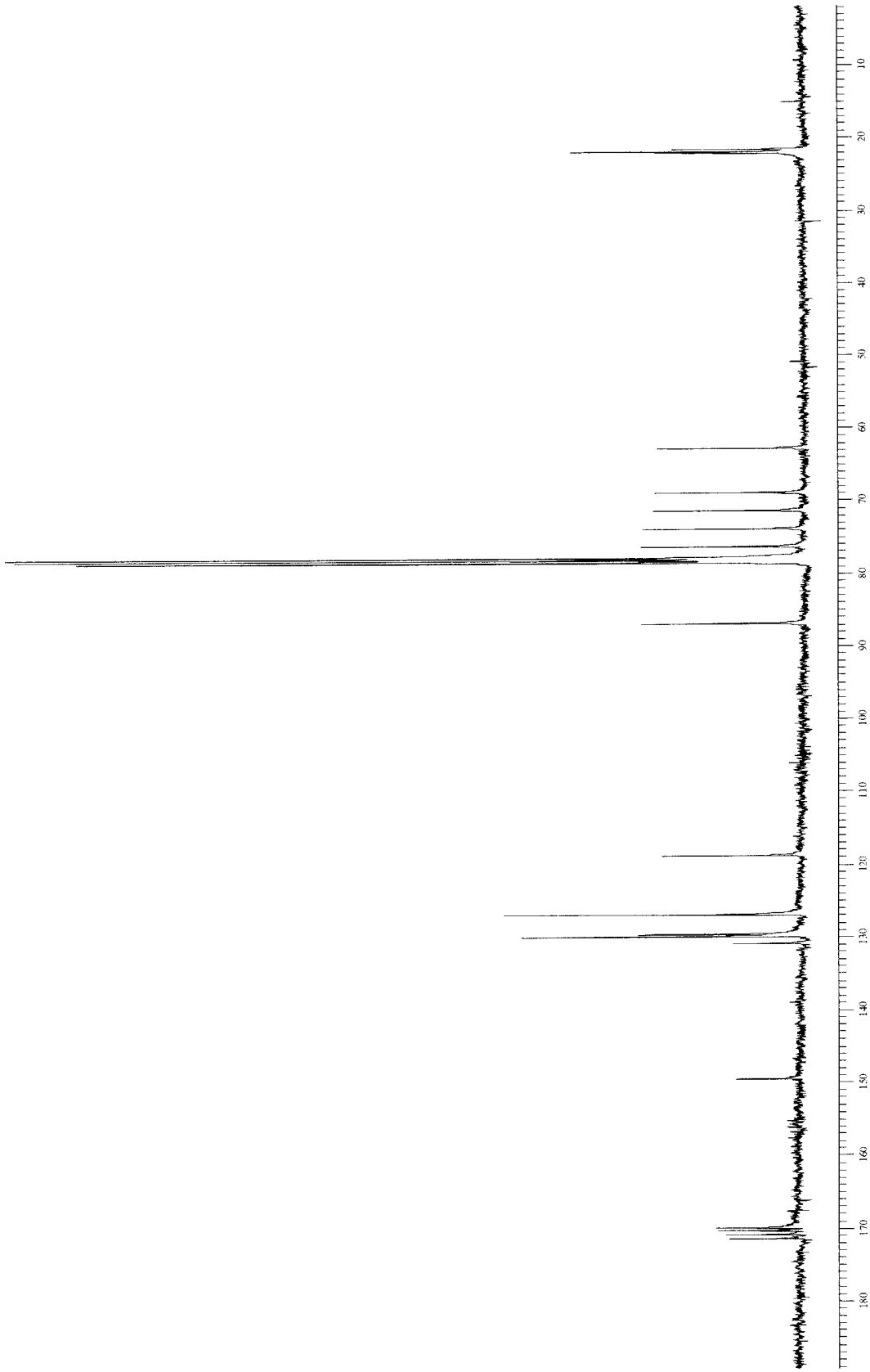

Figure 42: 100 MHz ^{13}C NMR spectrum of triazole product **42**

Display Report

Analysis Info:

File: D:\DATA\RAKESH\RAPHAC01.D — Printed: Fri Jul 09 16:11:35 2004
Date acquired:
Instrument: — Operator :
Task :
Method : — Sample :

Acquisition Parameter:

Source : — Polarity :
Mode :
CapExit : — Skim 1 :
Scan Range: — Trap Drive:
Accum.time: — Summation :
MS/MS :

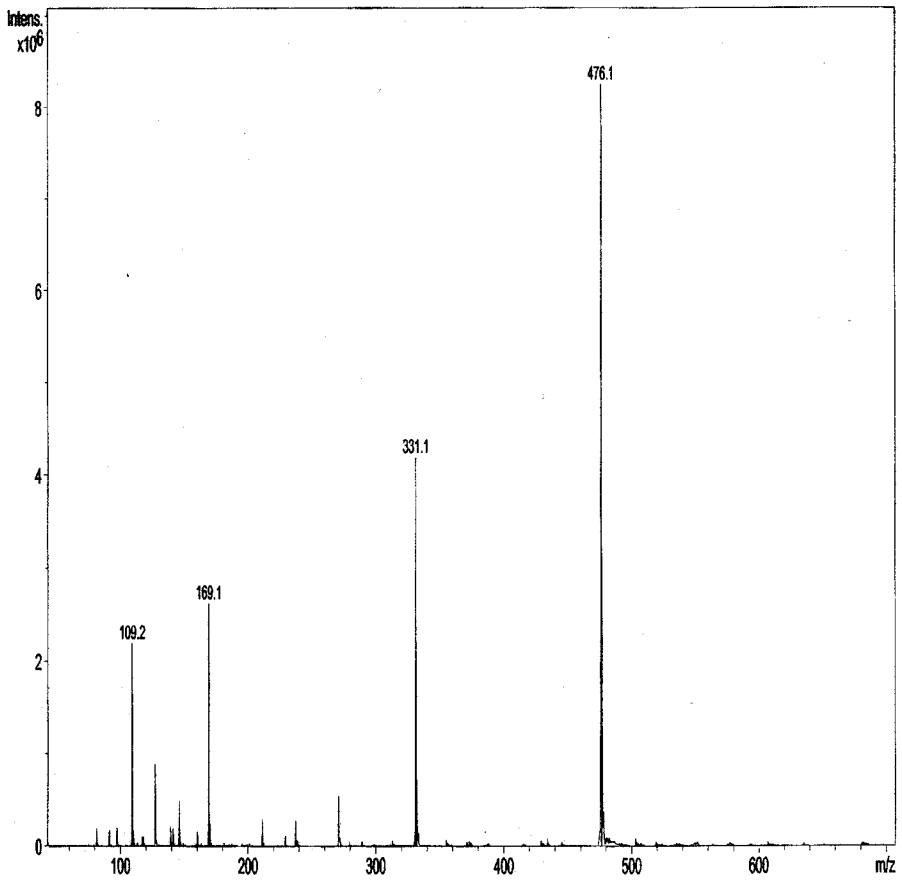

Bruker DataAnalysis Esquire-LC 1.6m, © Bruker Daltonik GmbH
Licensed to EQ_135, Uni. of Ohio

- 1 -

Figure 43: Mass spectrum of triazole product **42**

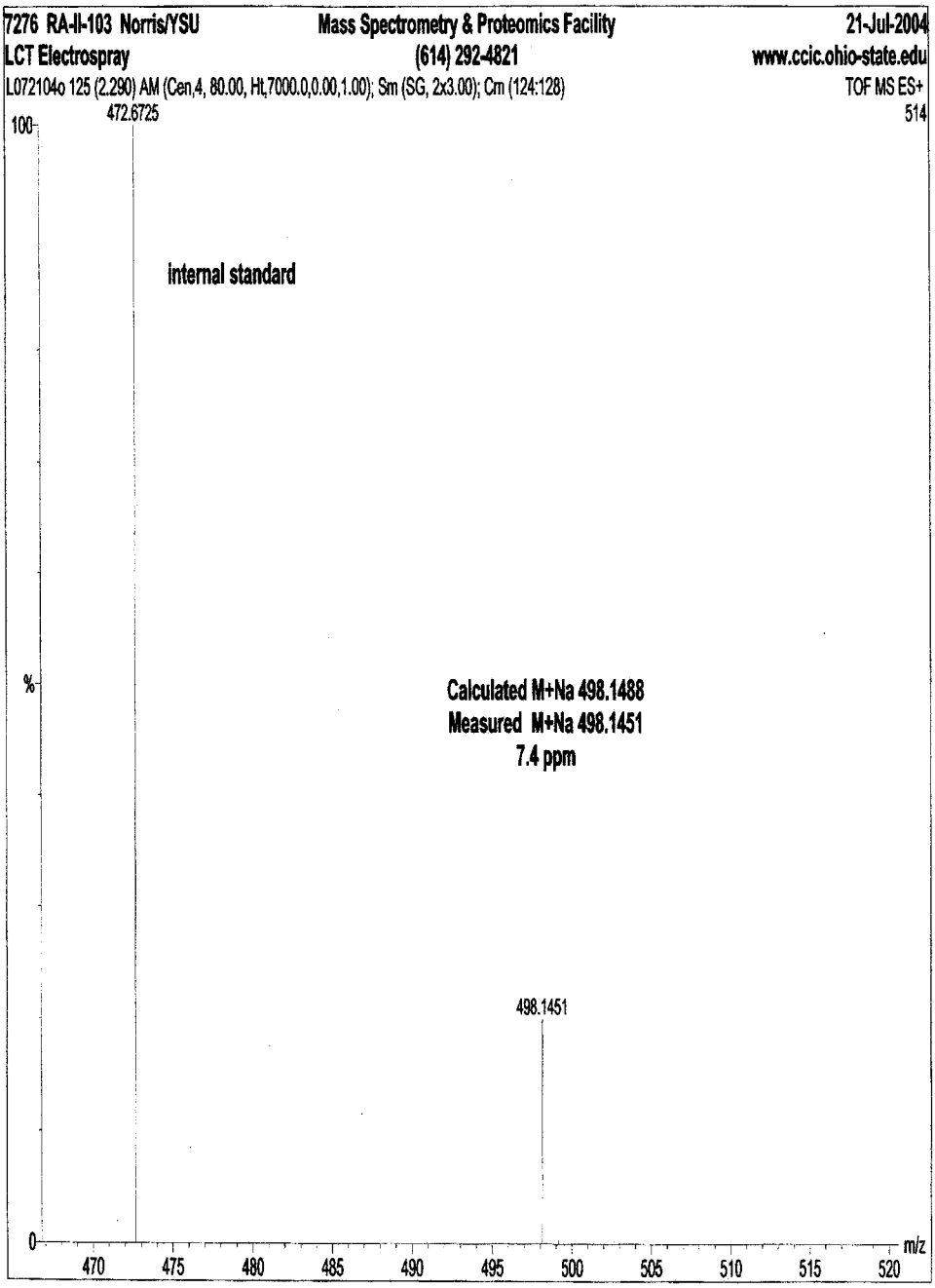

Figure 44: High resolution mass spectrum of triazole product **42**

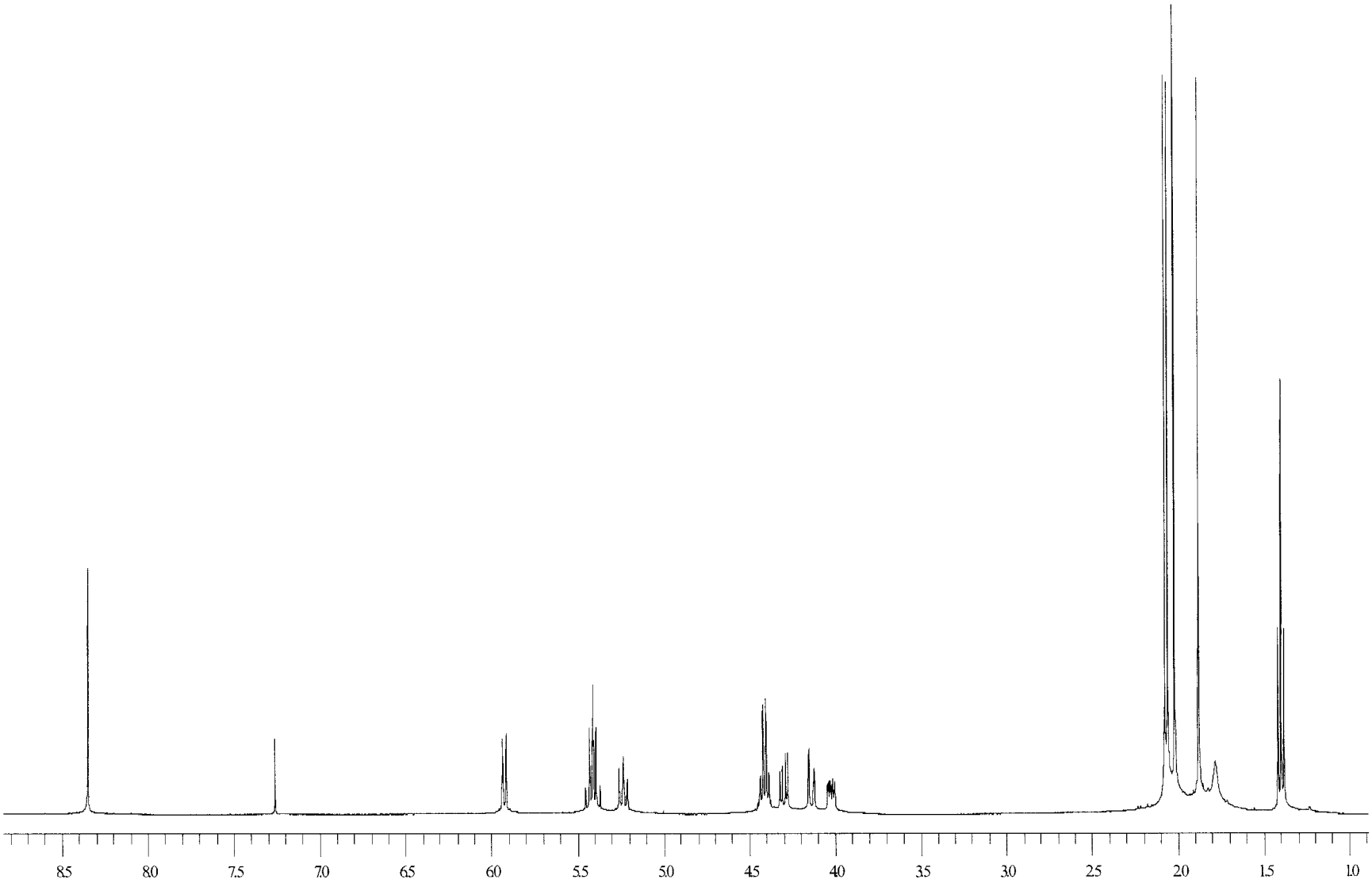

Figure 45: 400 MHz ^{1}H NMR spectrum of triazole product **43**

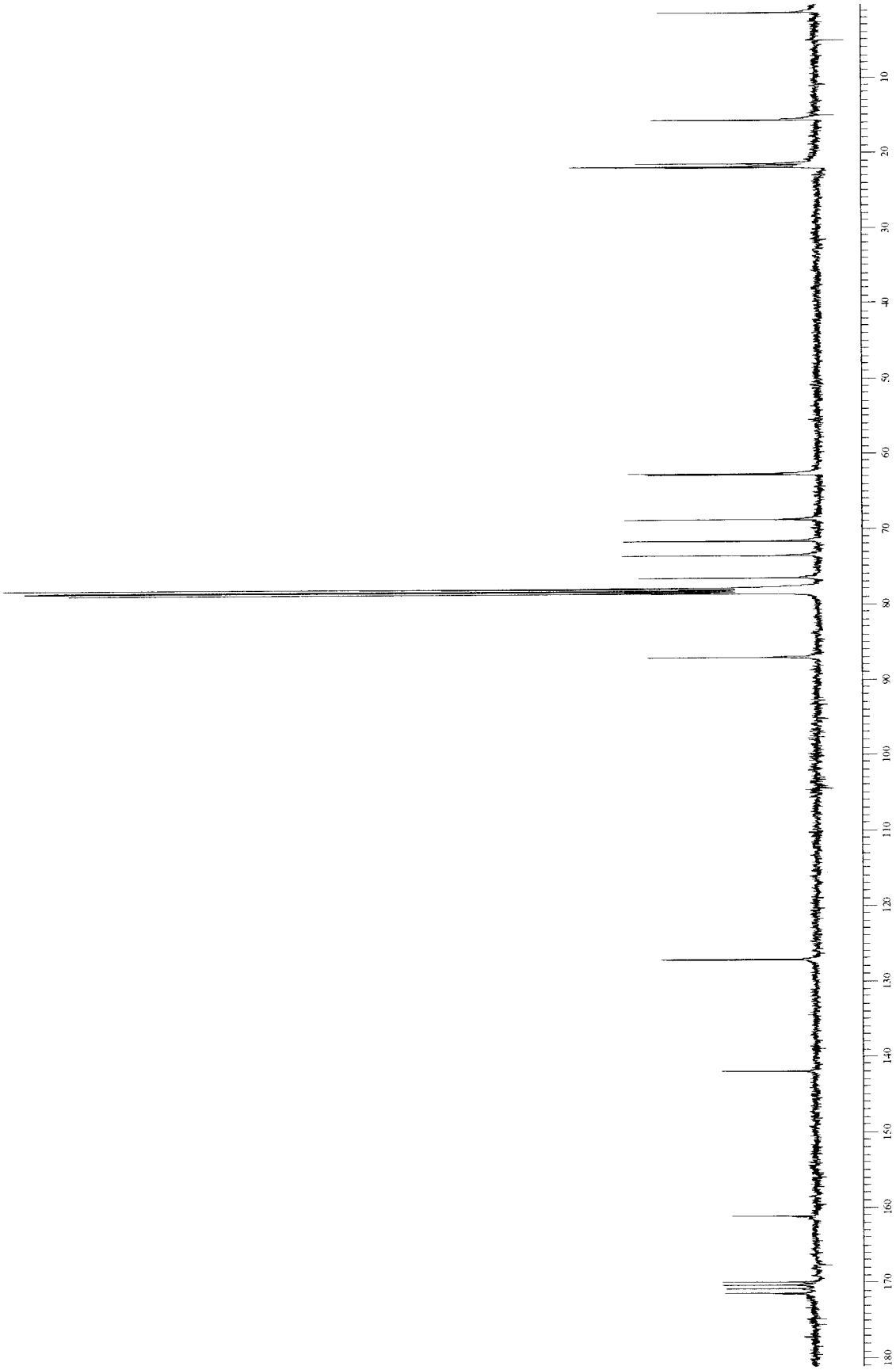

Figure 46: 100 MHz ^{13}C NMR spectrum of triazole product **43**

Display Report

Analysis Info:

File: D:\DATA\RAKESH\EP1.D
Date acquired:
Instrument:
Task :
Method :

Printed: Sun Oct 03 15:25:14 2004

Operator :
Sample :

Acquisition Parameter:

Source :
Mode :
CapExit :
Scan Range:
Accum.time:
MS/MS :

Polarity :
Skim 1 :
Trap Drive:
Summation :

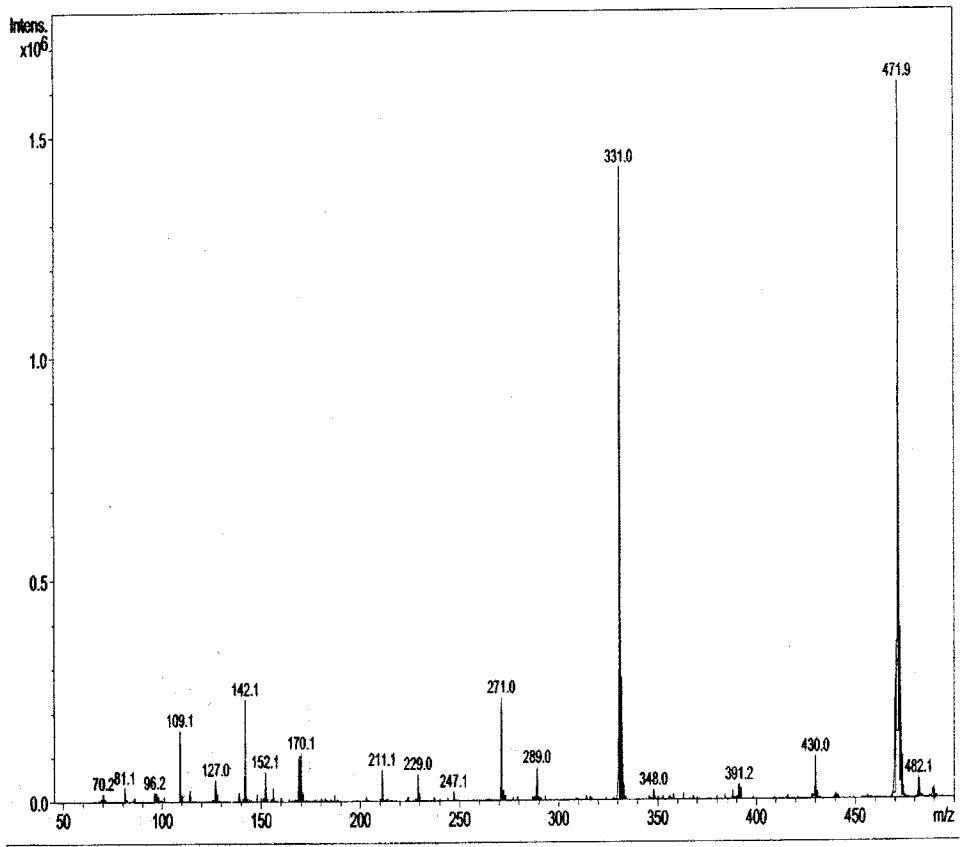

Bruker DataAnalysis Esquire-LC 1.6m, © Bruker Daltonik GmbH
Licensed to EQ_135, Uni. of Ohio

- 1 -

Figure 47: Mass spectrum of triazole product **43**

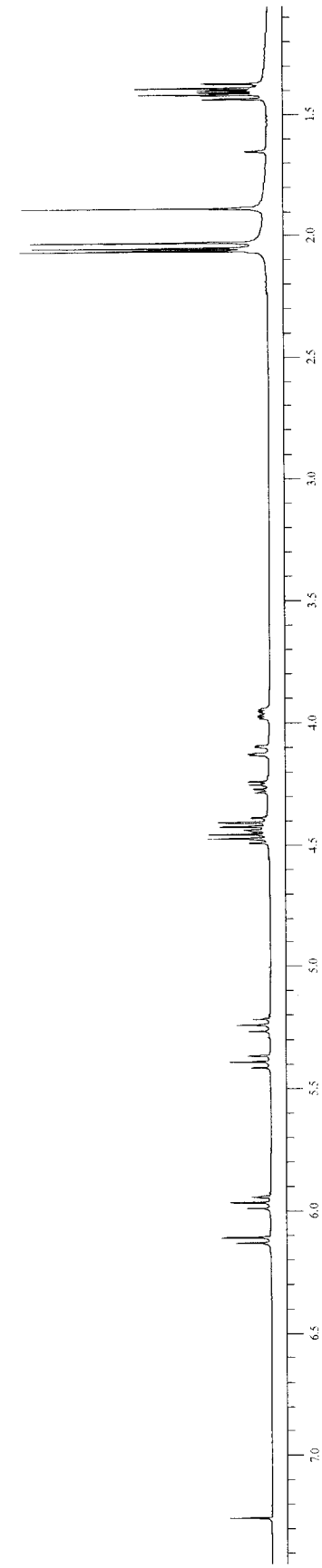

Figure 48: 400 MHz ^{1}H NMR spectrum of triazole product **44**

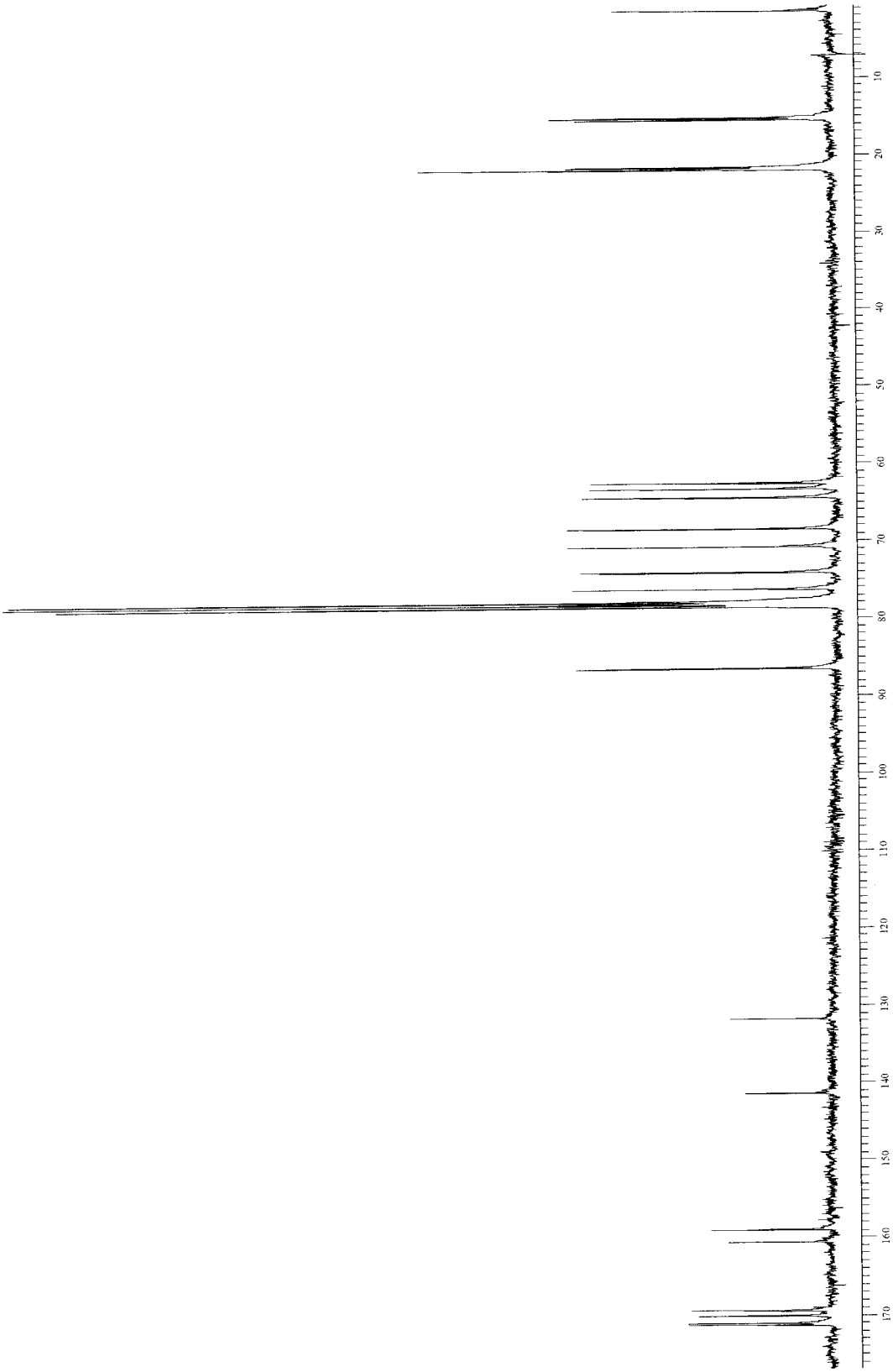

Figure 49: 100 MHz ^{13}C NMR spectrum of triazole product **44**

Display Report

Analysis Info:

File: D:\DATA\RAKESH\DEAD1.D
Printed: Fri Oct 01 15:31:18 2004
Date acquired:
Instrument:
Operator :
Task :
Method :
Sample :

Acquisition Parameter:

Source :
Polarity :
Mode :
CapExit :
Skim 1 :
Scan Range:
Trap Drive:
Accum.time:
Summation :
MS/MS :

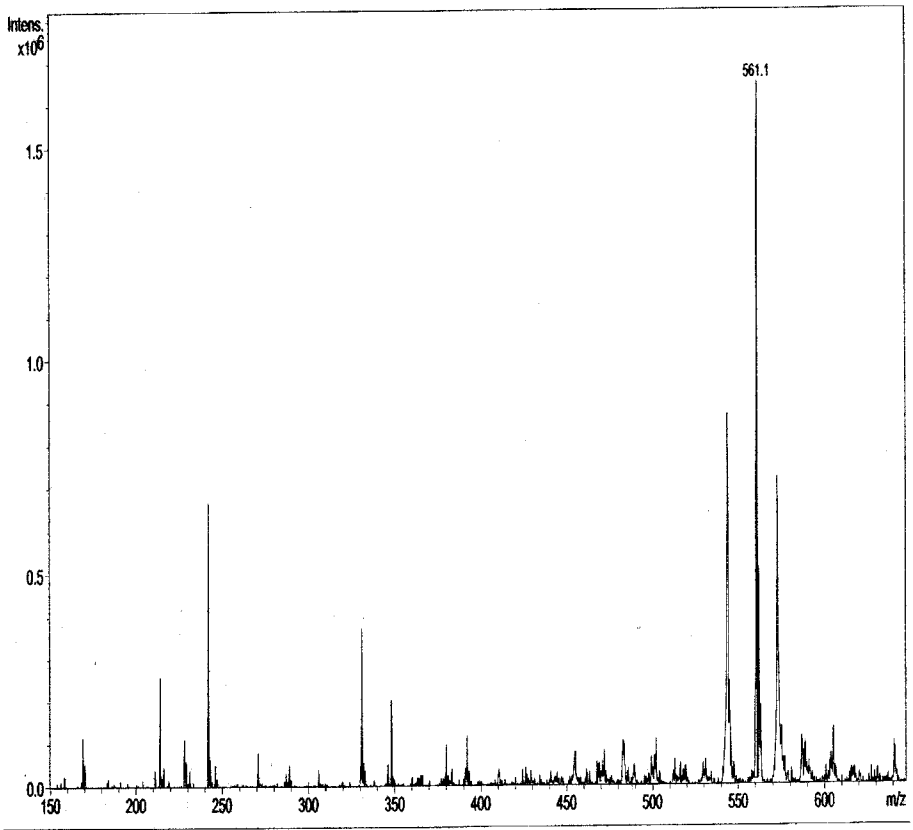

Bruker DataAnalysis Esquire-LC 1.6m, © Bruker Daltonik GmbH
Licensed to BQ_135, Uni. of Ohio

- 1 -

Figure 50: Mass spectrum of triazole product **44**

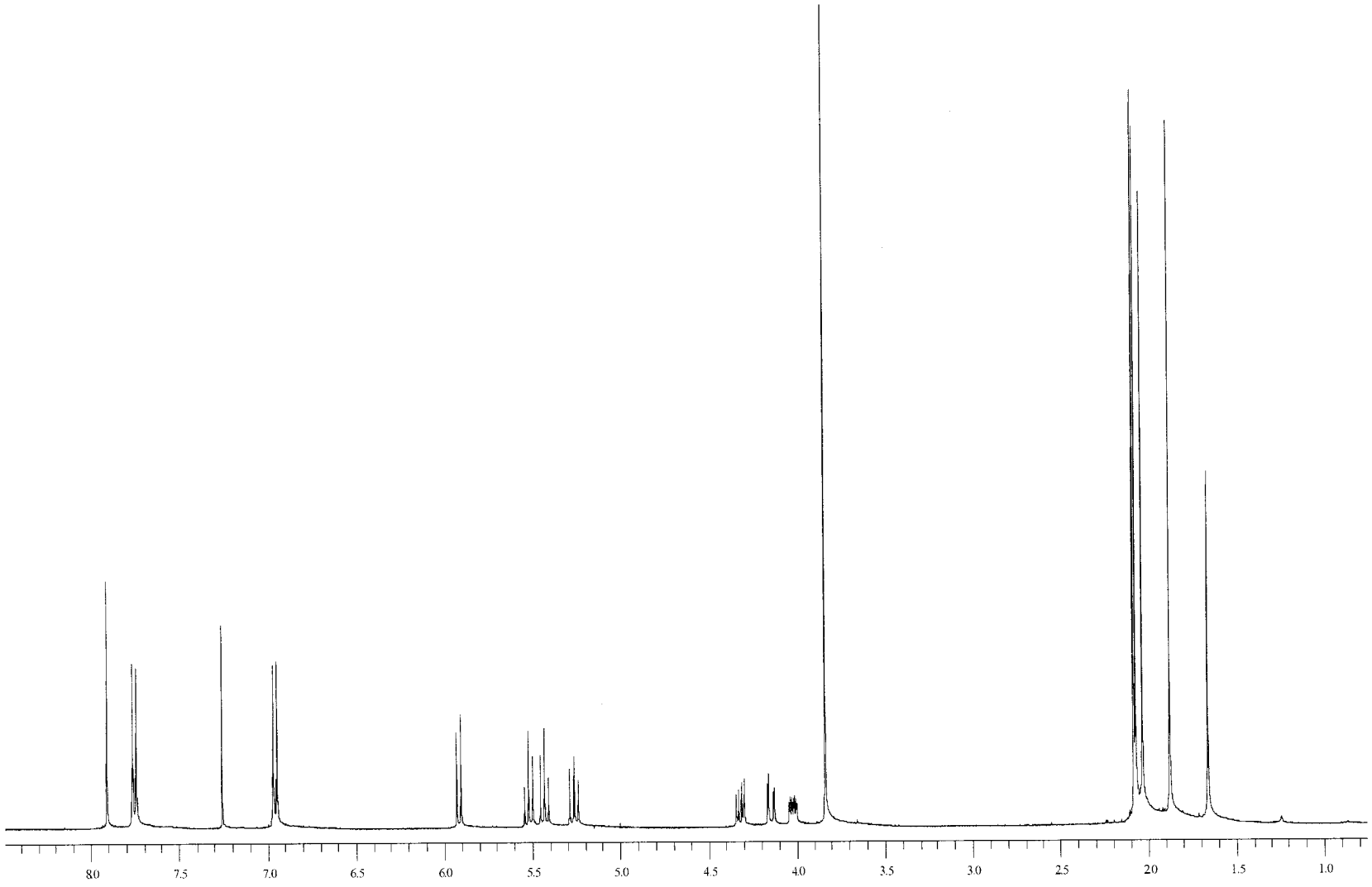

Figure 51: 400 MHz ^{1}H NMR spectrum of triazole product **45**

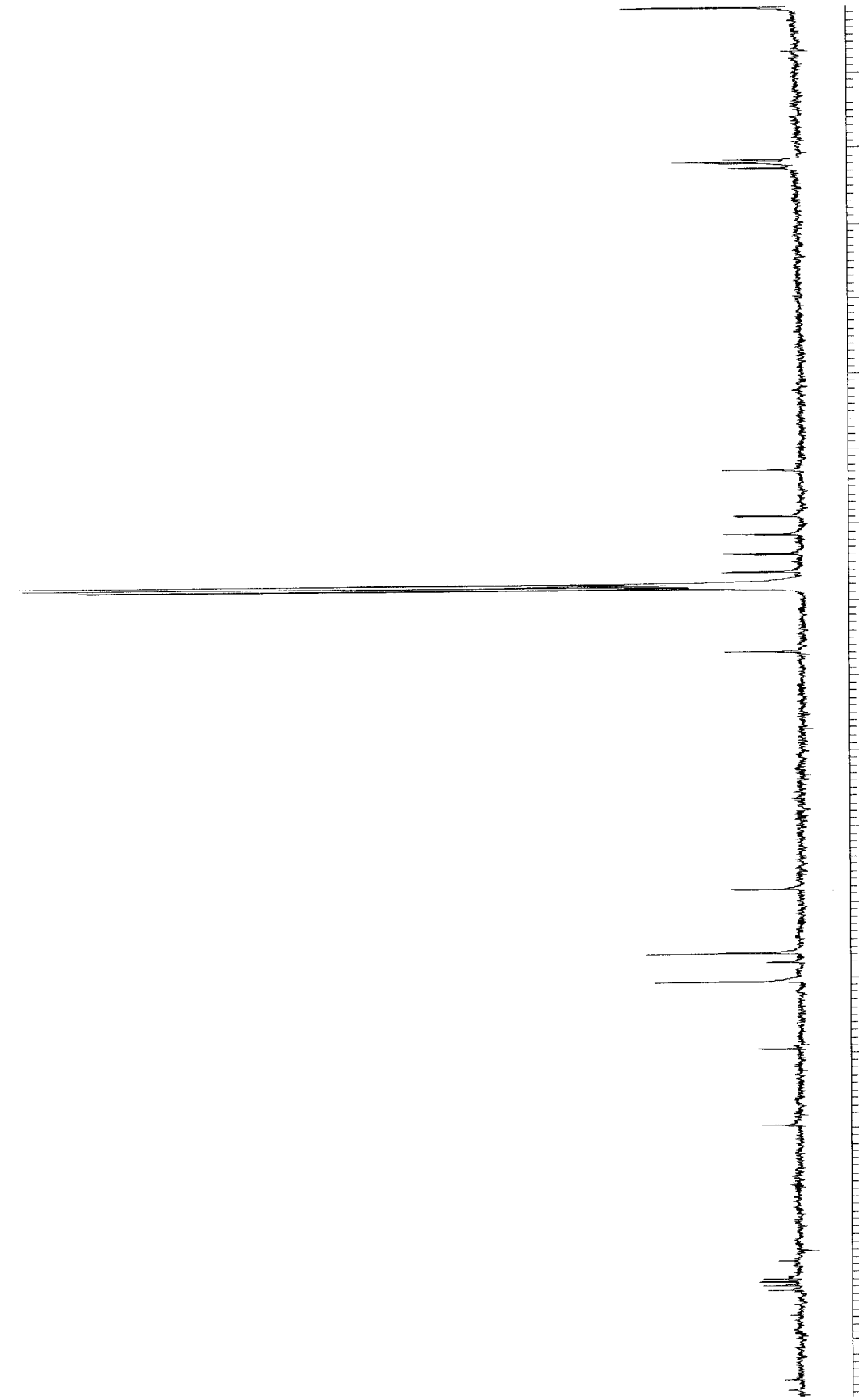

Figure 52: 100 MHz ^{13}C NMR spectrum of triazole product **45**

Display Report

Analysis Info:

File: D:\DATA\RAKESH\4ET1.D
Date acquired:
Instrument:
Task :
Method :

Printed: Sun Oct 03 14:21:17 2004

Operator :
Sample :

Acquisition Parameter:

Source :
Mode :
CapExit :
Scan Range:
Accum.time:
MS/MS :

Polarity :
Skim 1 :
Trap Drive:
Summation :

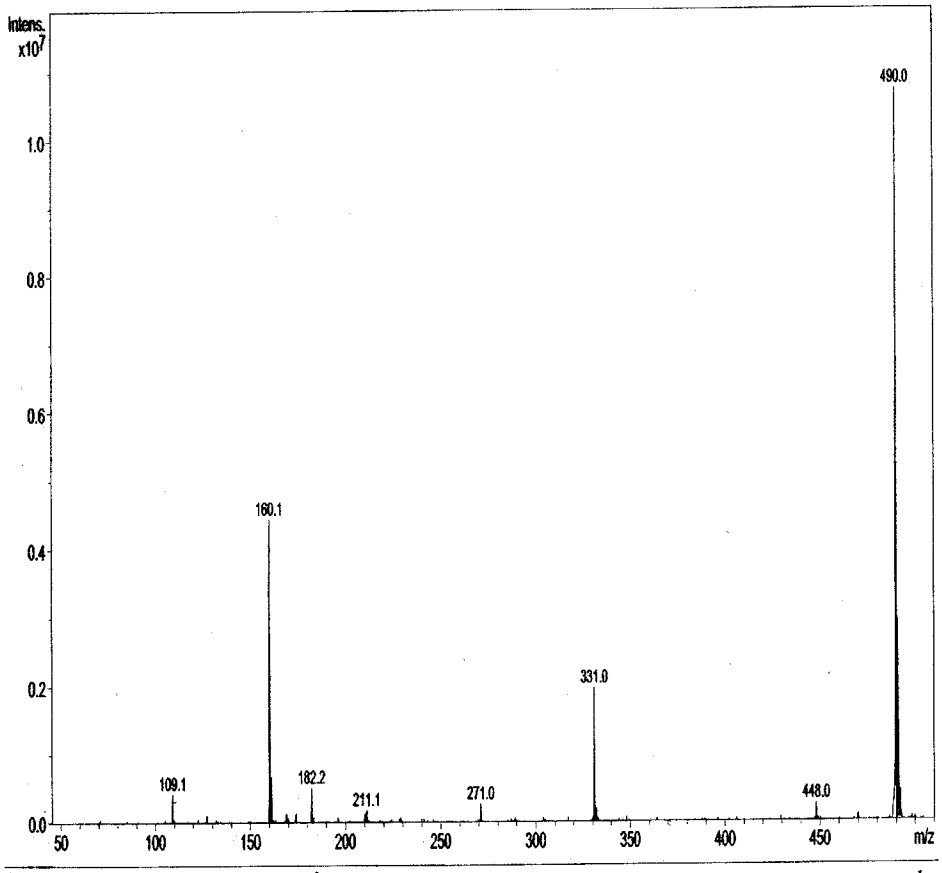

Bruker DataAnalysis Esquire-LC 1.6m, © Bruker Daltonik GmbH
Licensed to EQ_135, Uni. of Ohio

- 1 -

Figure 53: Mass spectrum of triazole product **45**

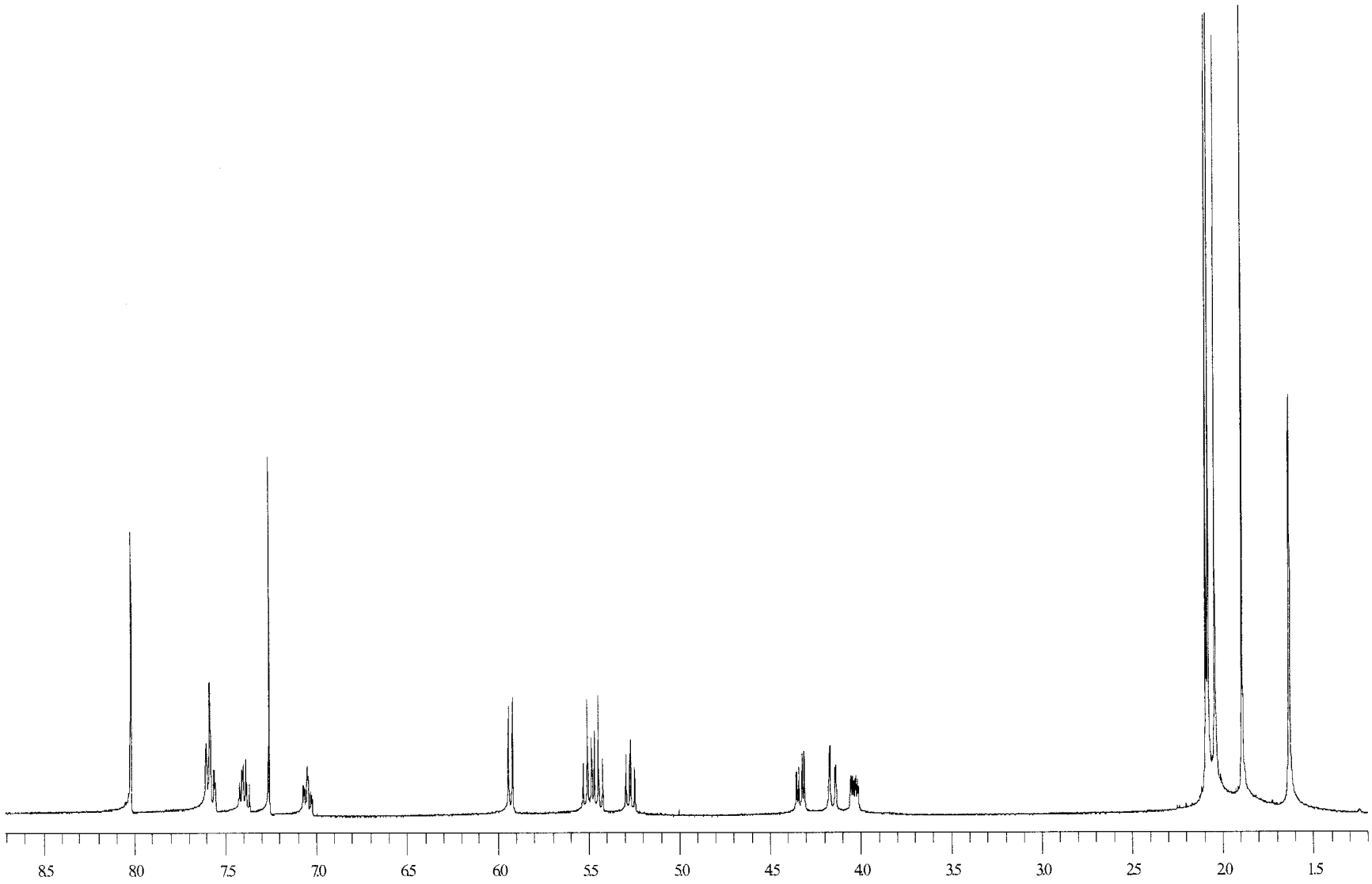

Figure 54: 400 MHz ^{1}H NMR spectrum of triazole product **46**

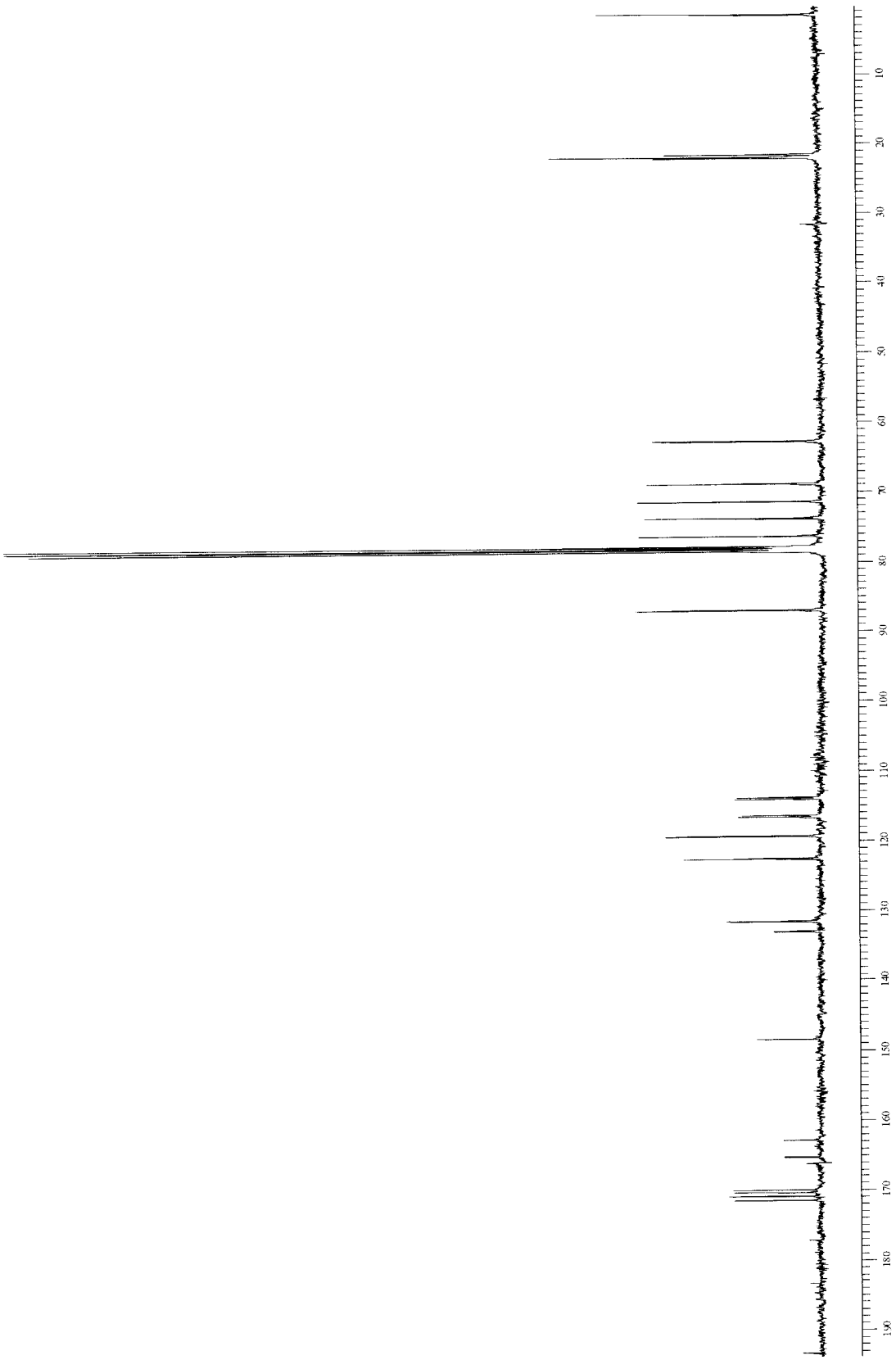

Figure 55: 100 MHz ^{13}C NMR spectrum of triazole product **46**

Display Report

Analysis Info:

File: D:\DATA\RAKESH\RA3-2502.D
Date acquired:
Instrument:
Task :
Method :

Printed: Fri Jul 09 14:21:19 2004

Operator :
Sample :

Acquisition Parameter:

Source :
Mode :
CapExit :
Scan Range:
Accum.time:
MS/MS :

Polarity :
Skim 1 :
Trap Drive:
Summation :

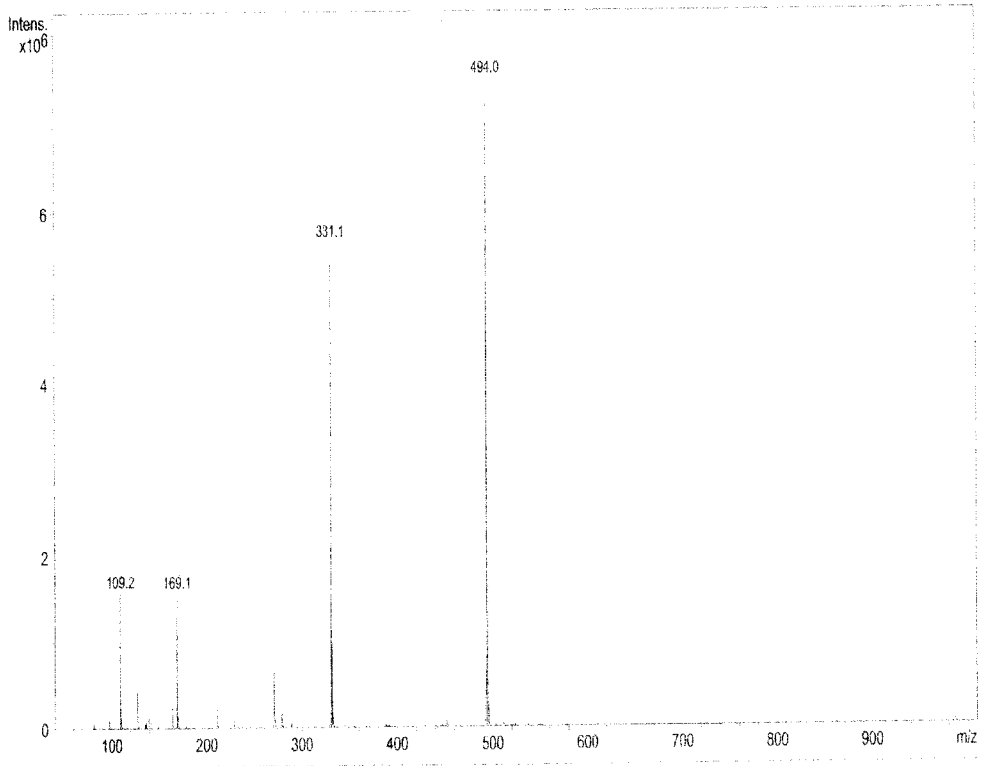

Bruker DataAnalysis Esquire-LC 1.6m, © Bruker Daltonik GmbH
Licensed to BQ_135, Uni. of Ohio

Figure 56: Mass spectrum of triazole product **46**

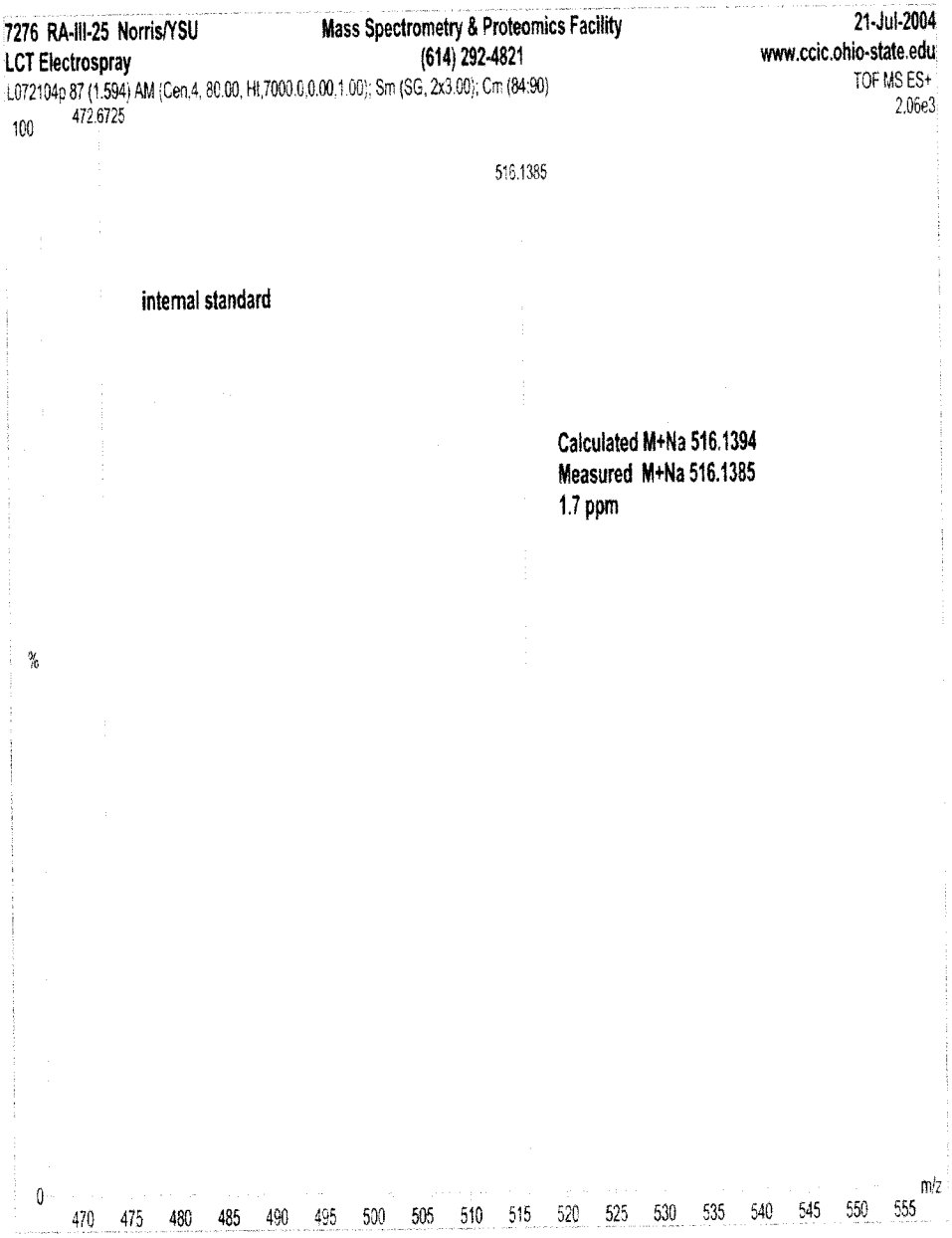

Figure 57: High resolution mass spectrum of triazole product **46**

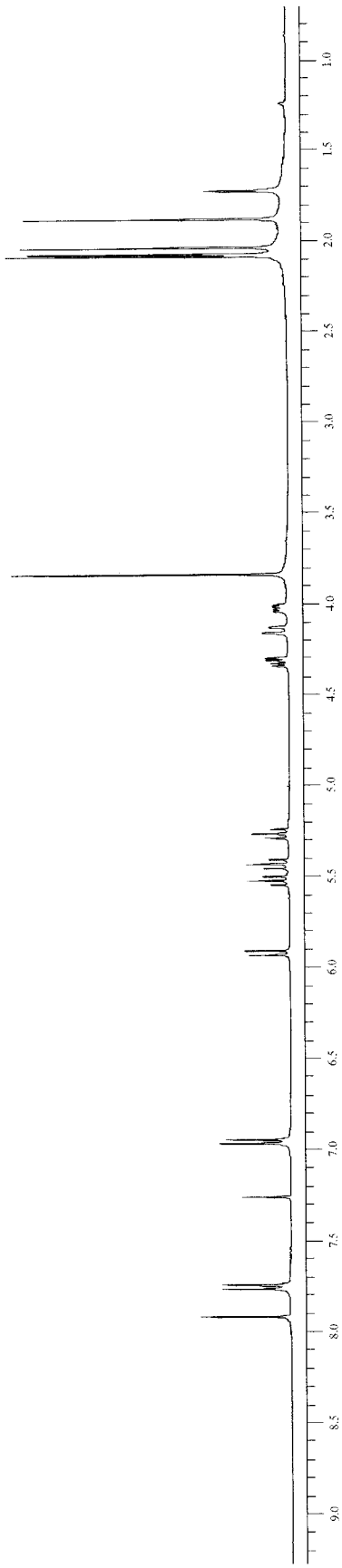

Figure 58: 400 MHz ^{1}H NMR spectrum of triazole product **47**

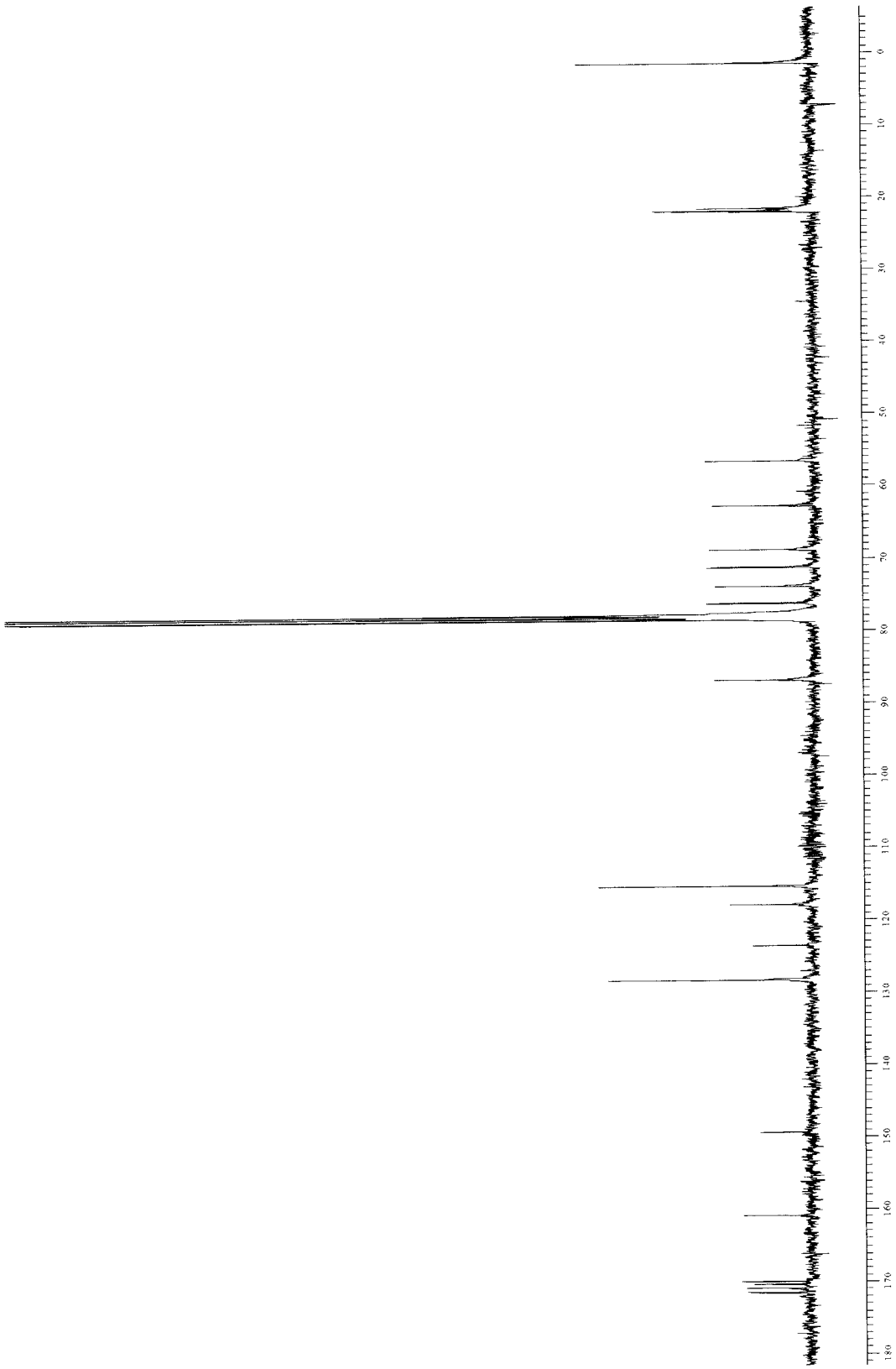

Figure 59: 100 MHz ^{13}C NMR spectrum of triazole product **47**

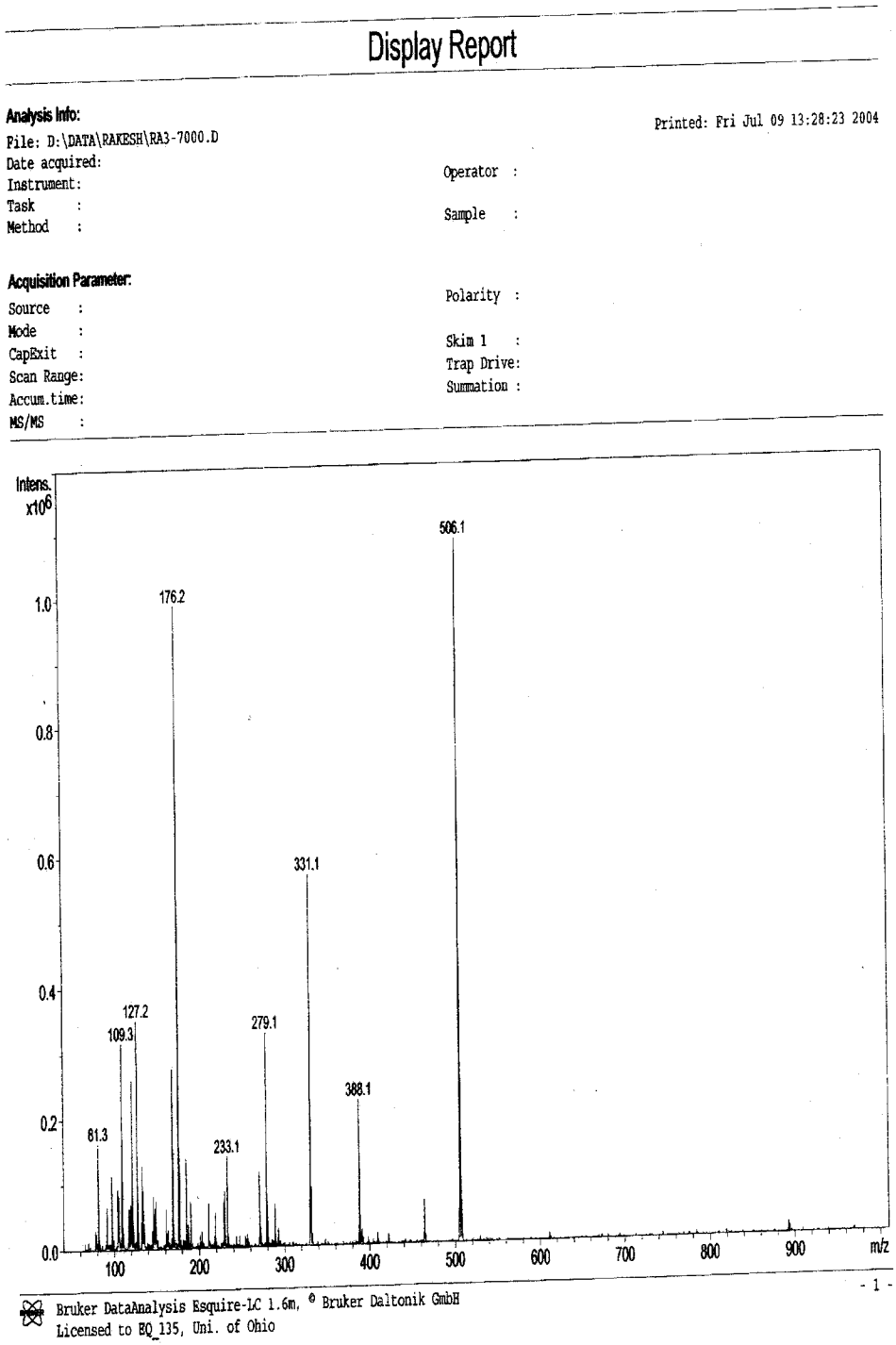

Figure 60: Mass spectrum of triazole product **47**

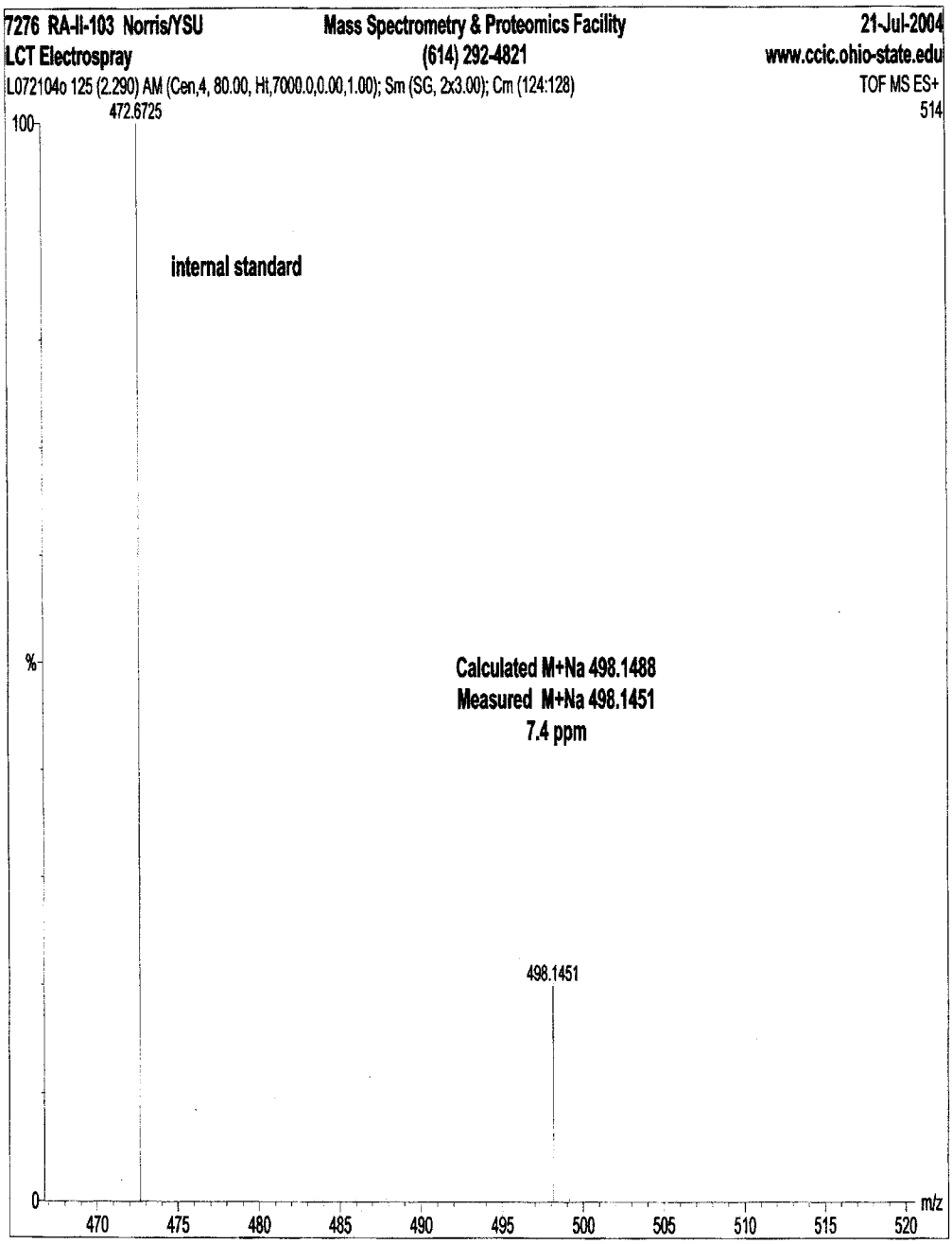

Figure 61: High resolution mass spectrum of triazole product **47**

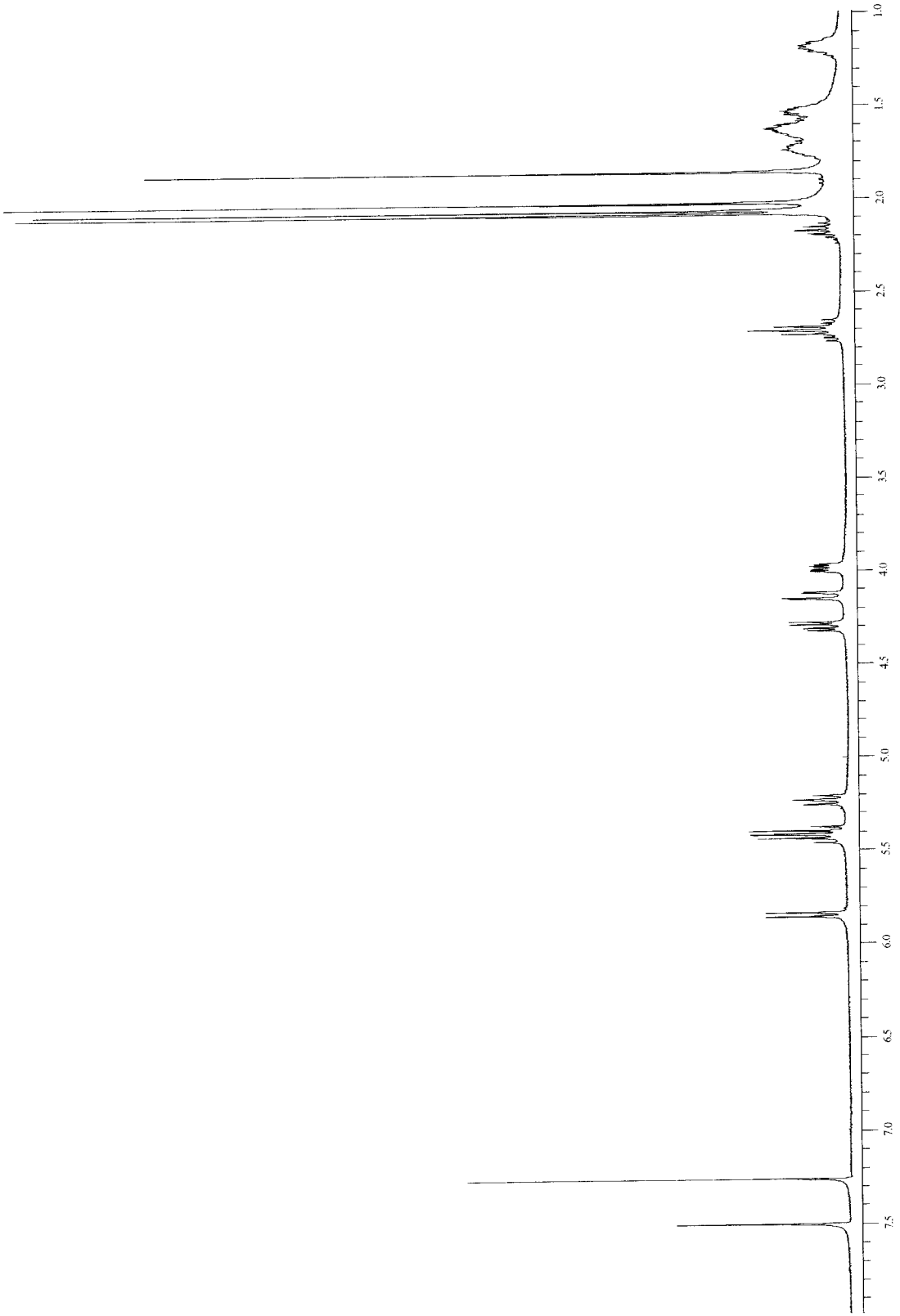

Figure 62: 400 MHz ^{1}H NMR spectrum of triazole product **48**

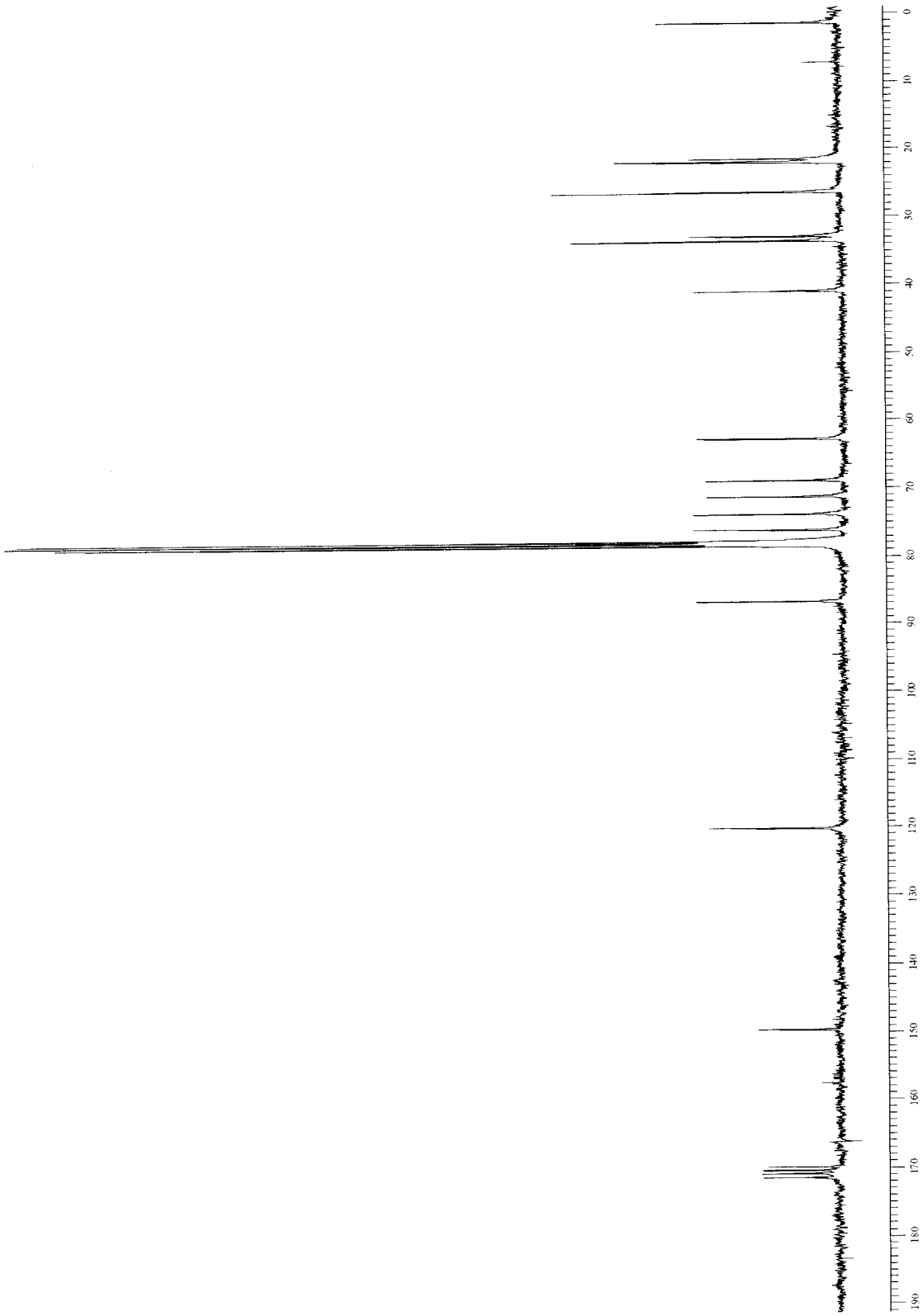

Figure 63: 100 MHz ^{13}C NMR spectrum of triazole product **48**

Display Report

Analysis Info:

File: D:\DATA\RAKESH\3CP.D
Printed: Sun Oct 03 14:47:42 2004
Date acquired:
Instrument:
Operator :
Task :
Method :
Sample :

Acquisition Parameter:

Source :
Polarity :
Mode :
CapExit :
Skim 1 :
Scan Range:
Trap Drive:
Accum.time:
Summation :
MS/MS :

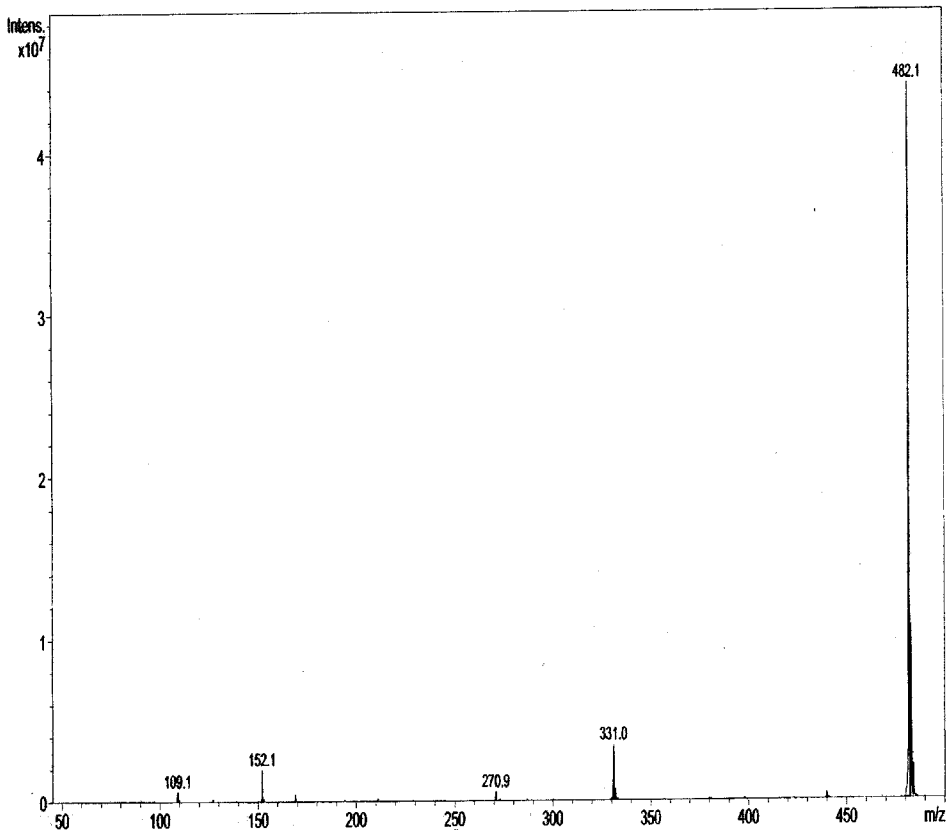

Bruker DataAnalysis Esquire-LC 1.6m, © Bruker Daltonik GmbH
Licensed to EQ_135, Uni. of Ohio

- 1 -

Figure 64: Mass spectrum of triazole product **48**

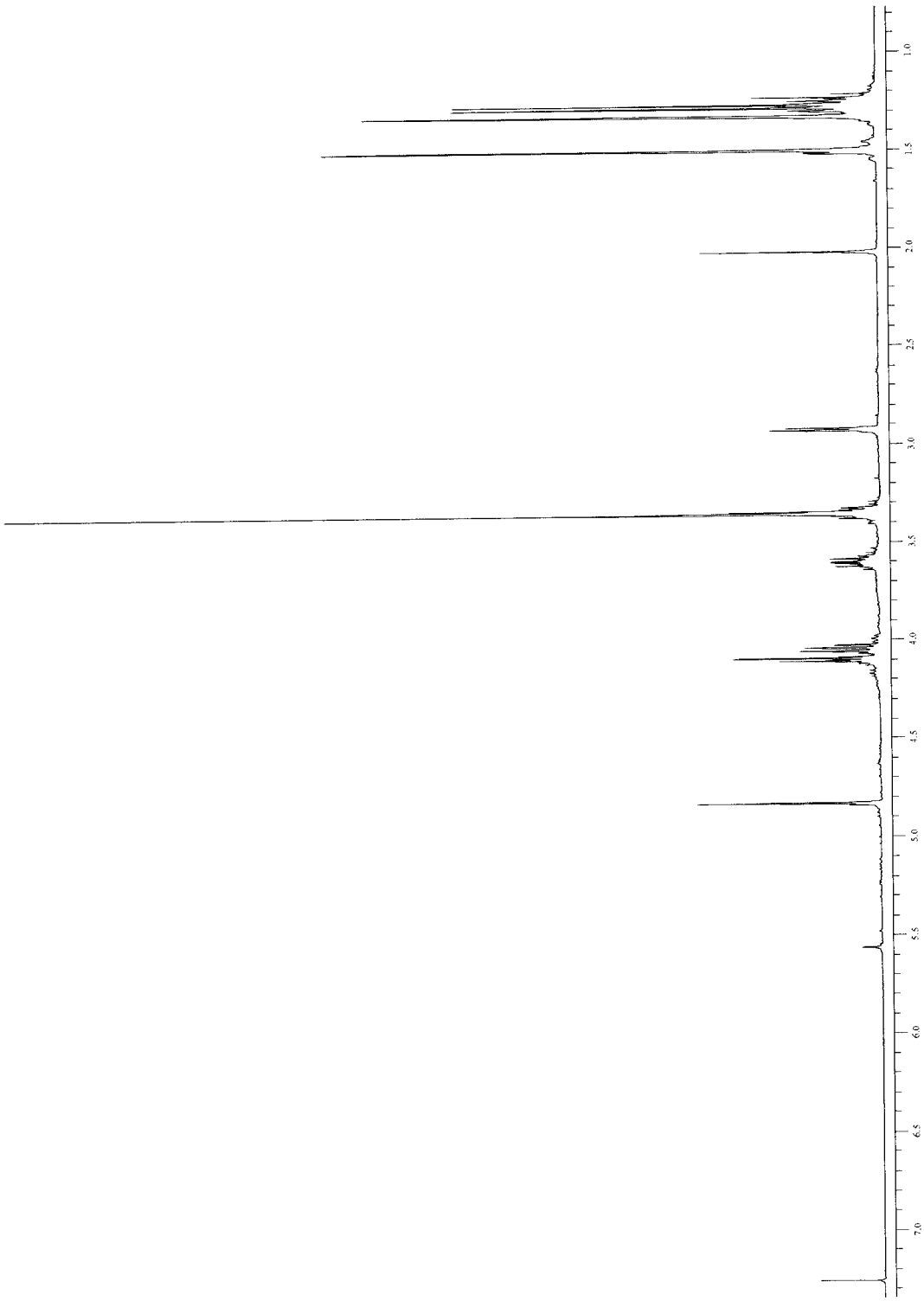

Figure 65: 400 MHz ^{1}H NMR spectrum of product **50**

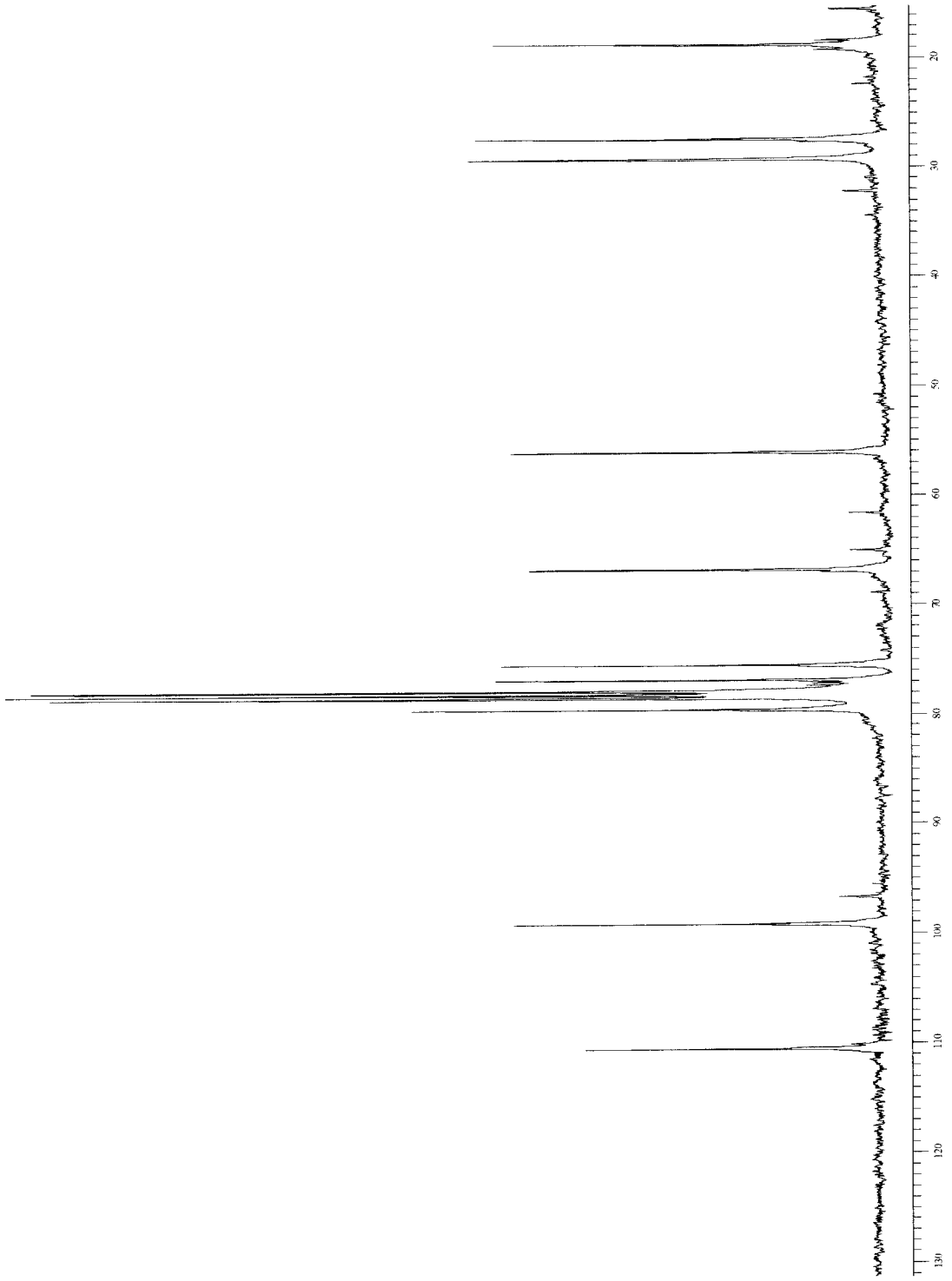

Figure 66: 100 MHz ^{13}C NMR spectrum of product **50**

Display Report

Analysis Info:

File: D:\DATA\RAKESH\PRO-RHAM.D
Date acquired:
Instrument:
Task :
Method :

Printed: Tue Oct 05 14:23:12 2004

Operator :
Sample :

Acquisition Parameter:

Source :
Mode :
CapExit :
Scan Range:
Accum.time:
MS/MS :

Polarity :
Skim 1 :
Trap Drive:
Summation :

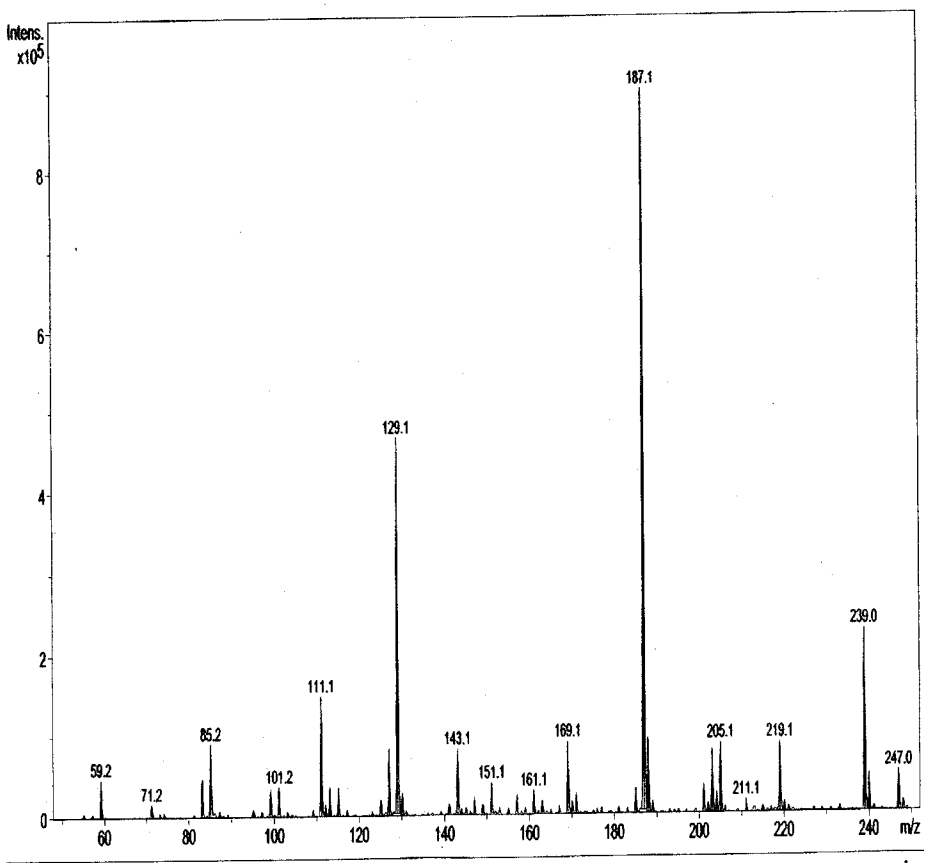

Bruker DataAnalysis Esquire-LC 1.6m, © Bruker Daltonik GmbH
Licensed to EQ_135, Uni. of Ohio

- 1 -

Figure 67: Mass spectrum of product **50**

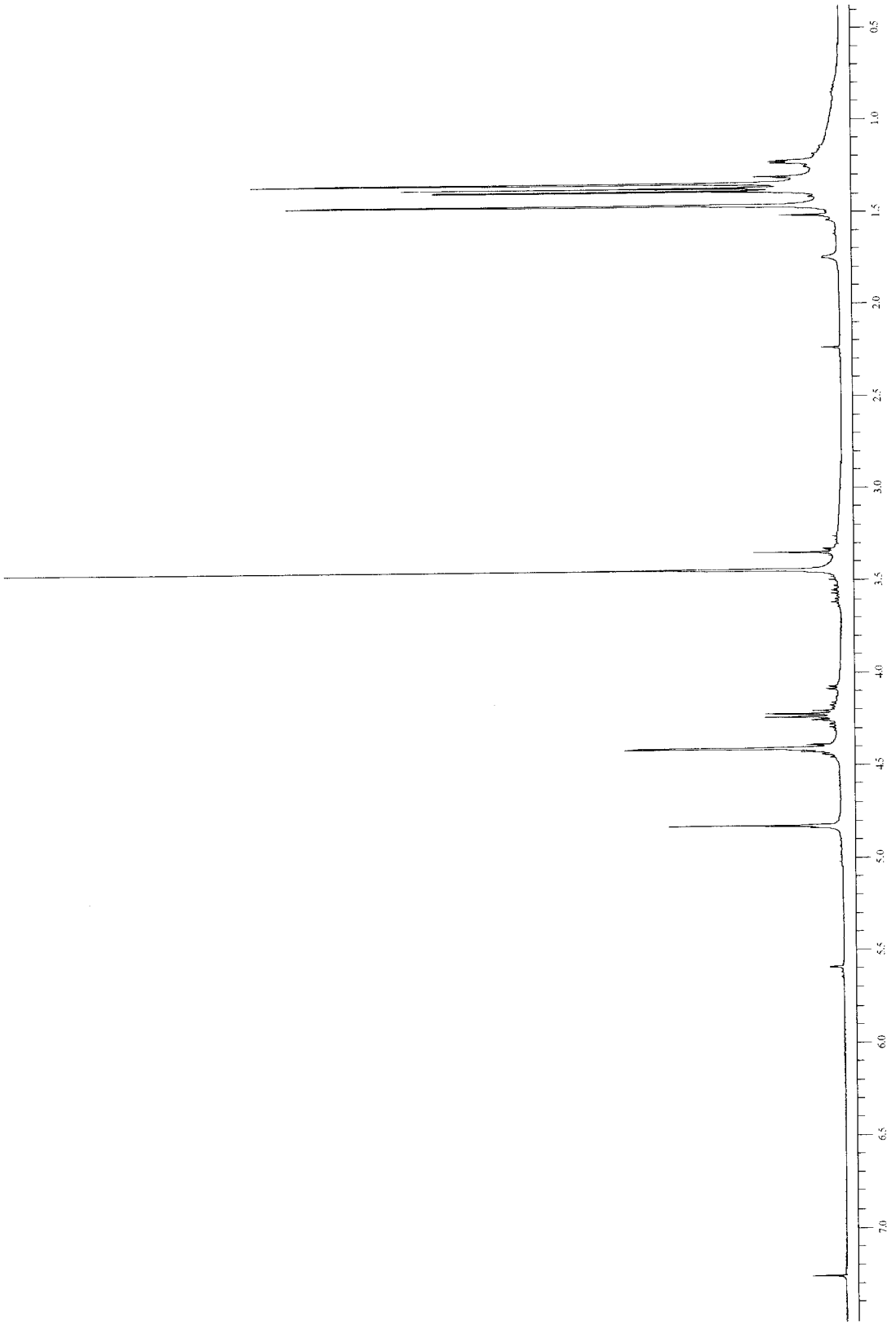

Figure 68: 400 MHz ^{1}H NMR spectrum of product **51**

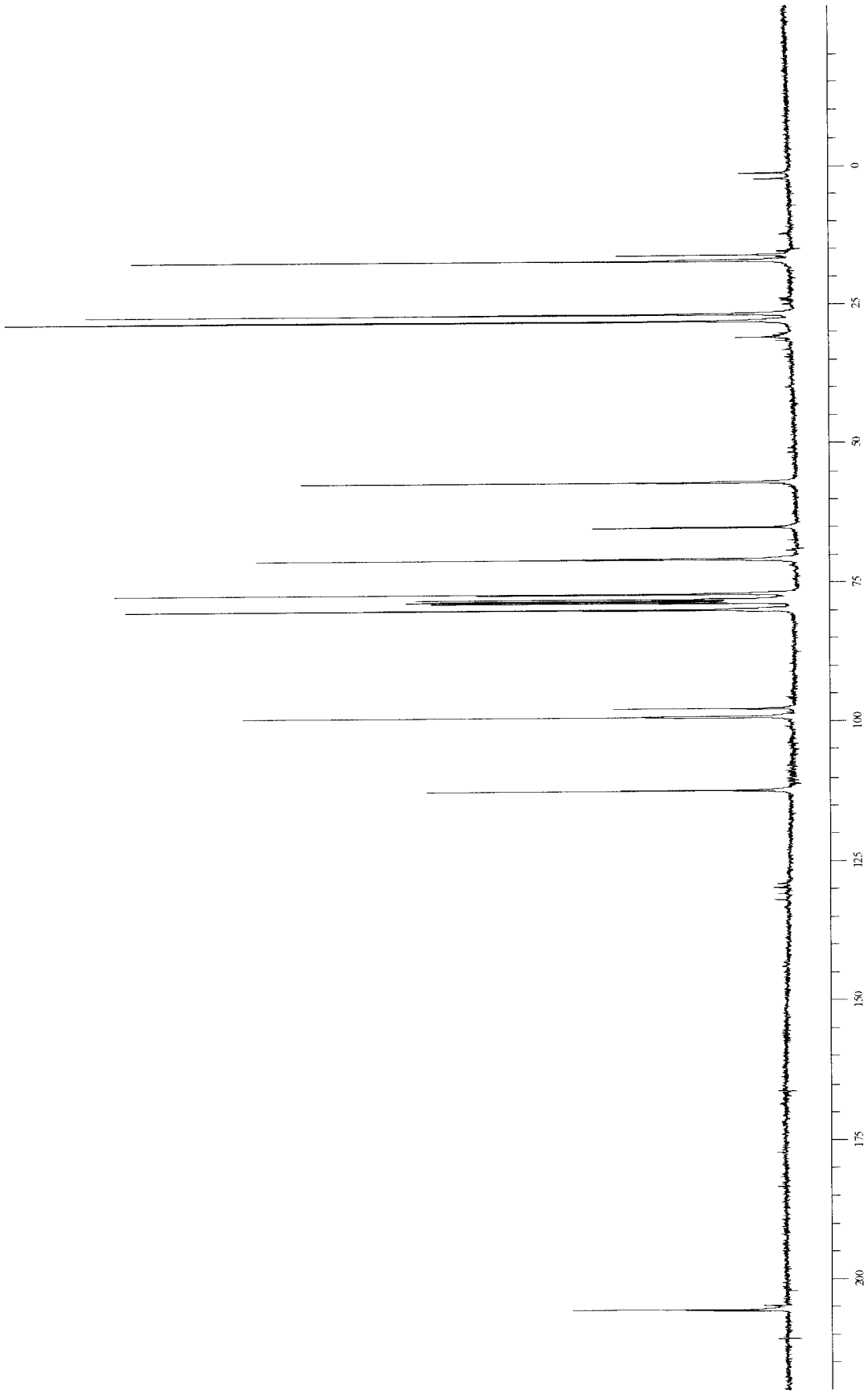

Figure 69: 100 MHz ^{13}C NMR spectrum of product **51**

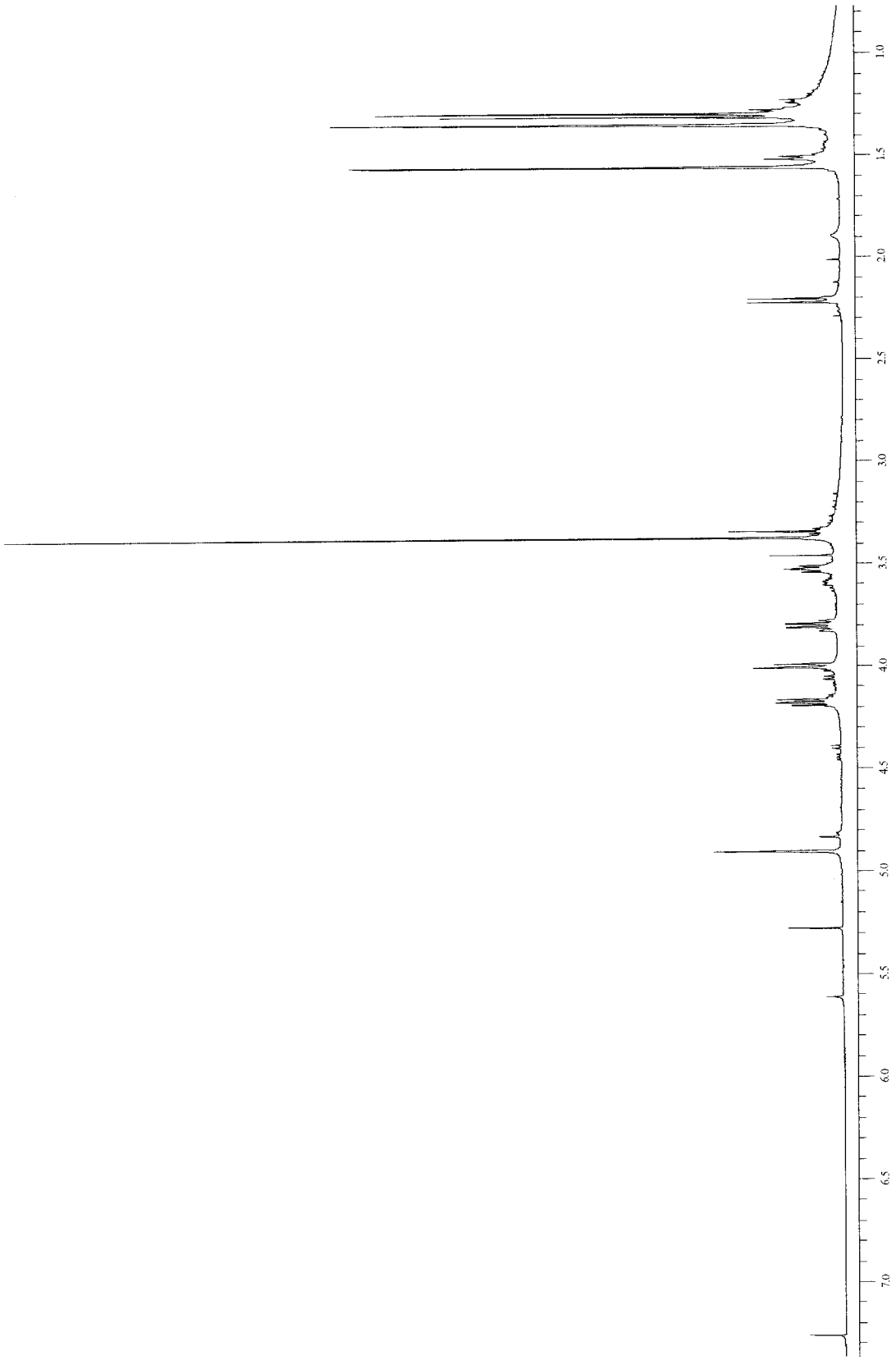

Figure 70: 400 MHz ^{1}H NMR spectrum of product **52**

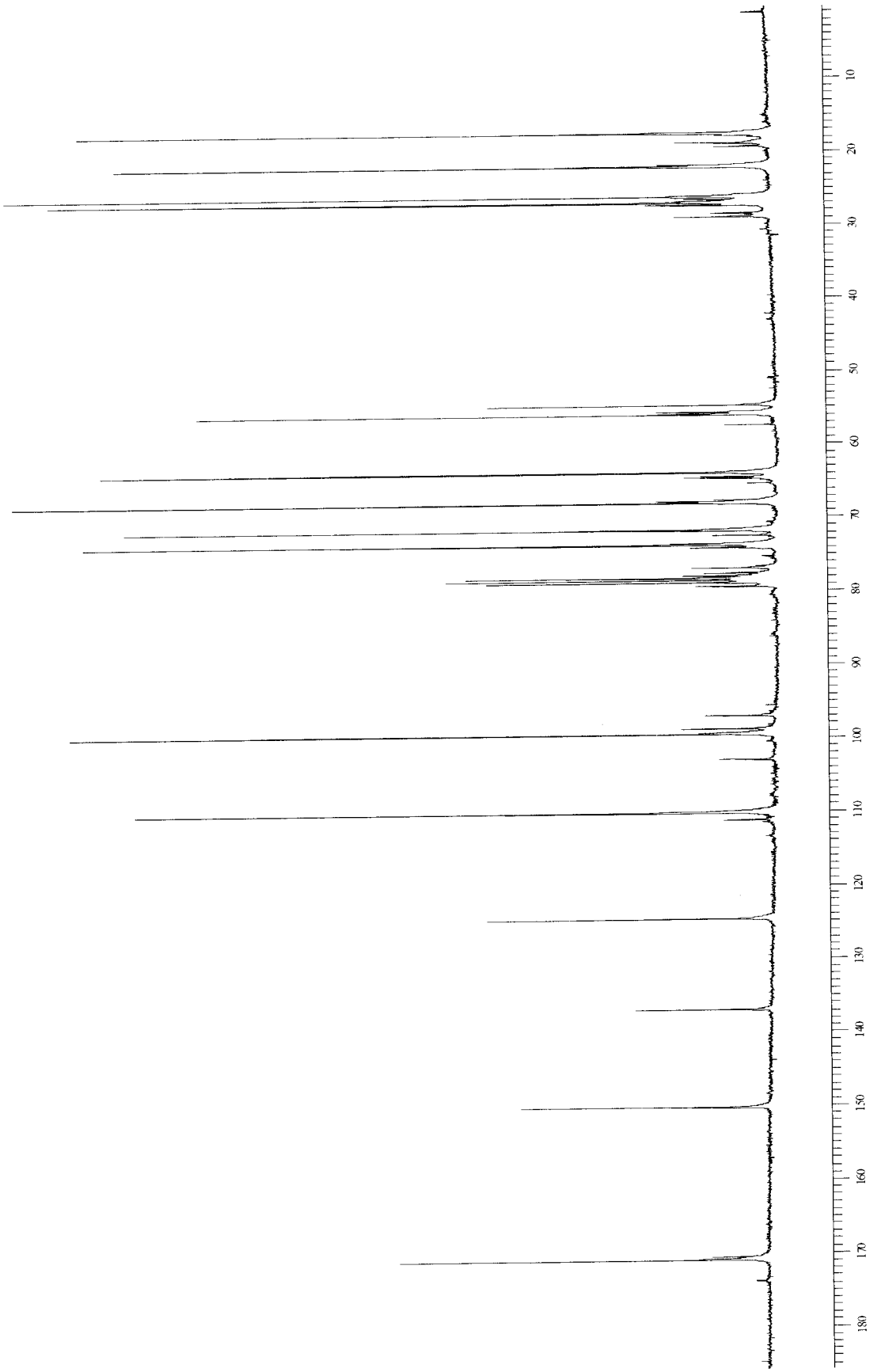

Figure 71: 100 MHz ^{13}C NMR spectrum of product **52**

Display Report

Analysis Info:

File: D:\DATA\RAKESH\ALPHAOH1.D — Printed: Thu Oct 07 15:08:32 2004
Date acquired:
Instrument: — Operator :
Task :
Method : — Sample :

Acquisition Parameter:

Source : — Polarity :
Mode :
CapExit : — Skim 1 :
Scan Range: — Trap Drive:
Accum.time: — Summation :
MS/MS :

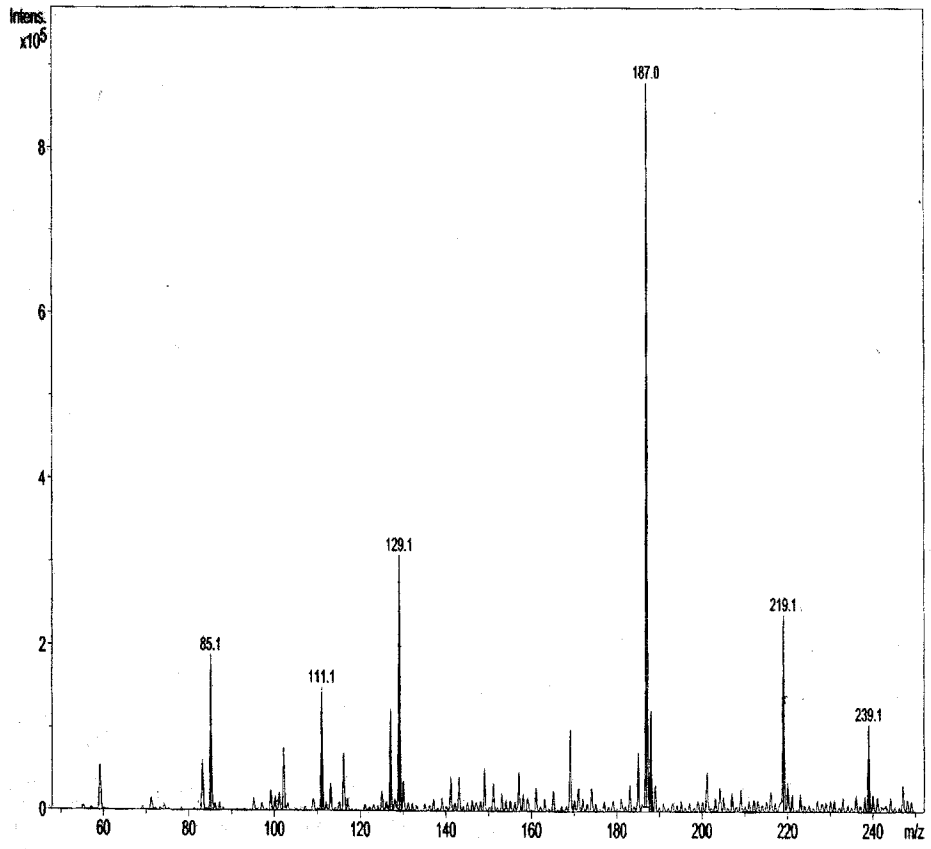

Bruker DataAnalysis Esquire-LC 1.6m, © Bruker Daltonik GmbH
Licensed to EQ_135, Uni. of Ohio

- 1 -

Figure 72: Mass spectrum of product **52**